Nano zero valent iron amended ceramic pot filters for enhanced virus and arsenic removal

Willemijn van Hoorn
December 2015

Department of Water Management
Sanitary Engineering Section

TU Delft

Nano zero valent iron amended ceramic pot filters for enhanced virus and arsenic removal

Master of Science Thesis in Civil Engineering

Sanitary Engineering Section
Department of Water Management
Faculty of Civil Engineering

Delft University of Technology

Willemijn van Hoorn

December 2015

Committee:

Prof. Dr. Ir. L. C. Rietveld	Delft University of Technology Sanitary Engineering Section
Dr. Ir. D. van Halem	Delft University of Technology Sanitary Engineering Section
Dr. Ir. J.C. Diehl	Delft University of Technology Design Engineering Section
Ir. K. C. Friedman	Delft University of Technology Environmental Sciences and Engineering

Acknowledgements

This thesis is the result of my graduation research project for the Sanitary Engineering Section of the Department of Water Management at the Faculty of Civil Engineering and Geosciences at the Delft University of Technology. The objective of this study was to investigate whether it is feasible to extend the capabilities of Ceramic Pot Filters (CPFs) with arsenic removal properties and enhanced virus inactivation by the incorporation of nano Zero Valent Iron (nZVI) before firing.

I would like to thank all people who supported me in my graduation project, especially the members of my graduation committee. First of all, I would like to thank Katie Friedman, not only for her guidance but also for her company. Thank you for all your advices and all those assays you performed. The sometimes long lab-days were much more enjoyable with having you around. And of course I am really glad that I could join you on the trip to the Dominican Republic, it was incredible. I would also like to give a special thanks to Doris van Halem. Your support was indispensable for this thesis. You always had time for my questions, gave me a lot of advice and encouraged me when needed. But most of all it was really fun to work with you. It was great to have such an enthusiastic and motivating supervisor! Furthermore I like to thank Luuk Rietveld for being the chair of my committee. Thank you for your interest and feedback. Jan Carel Diehl I would like to thank for his interest in my research project and being part of my graduation committee.

Most of my work is done in the laboratory of Sanitary Engineering and I would like to thank Armand and Tonny for their assistance. Thank you for showing the way in the lab. Furthermore, I would like to thank Thomas for helping with the filter experiments and performing the tracer-tests. I would also like to thank Jan Kroesbergen for giving me the opportunity to help Katie Friedman with analyzing the samples at Het Waterlaboratorium.

Last but not least, I would like to show much gratitude to my parents who have supported me throughout my education.

Willemijn van Hoorn
November 2015, Delft

Executive summary

Worldwide 748 million people lacked access to improved sources of drinking water in 2014, of this group almost a quarter relies on untreated surface water (World Health Organisation (WHO) & UNICEF, 2014). According to the WHO, simple, socially accepted and low-cost household water treatment systems (HWTS), such as the Ceramic Pot Filter (CPF), can provide a solution for reliable drinking water on the short term. Although CPFs are used worldwide and are generally effective with regard to bacteria removal, they can in most cases not be indicated by the WHO as a "protective" HWTS, since the virus removal is insufficient. Another limitation of the CPF is the incapability of removing arsenic. Prolonged ingestion of water with elevated arsenic levels can lead to severe health issues including dermal lesions and various types of cancers (WHO, 2011b). The objective of this study was therefore to provide reliable experimental data to investigate whether it is feasible to extend the capabilities of CPFs with arsenic removal properties and enhanced virus inactivation by the incorporation of nano Zero Valent Iron (nZVI), which is a well-known arsenic adsorbent and has also potential capabilities for virus reduction. As a basis for the research approach, the following sub-objectives were formulated: (i) study the arsenic adsorption capacities nZVI amended CPFs, (ii) determine the microbiological inactivation efficiency by nZVI amended CPFs, (iii) evaluate the leaching of the incorporated nZVI and (iv) provide knowledge on the effect of incorporating nZVI into CPFs before firing.

In this study, Ceramic Disk Filters (CDFs) were manufactured by combining clay soil with water and sawdust, pressing them in a disk shape and, firing them. Additionally, metals (nZVI, Composite Iron Matrix CIM powder or silver nanoparticles (nAg)) were added to the clay mixture before firing, to obtain an iron content of 0.05%, 0.5% or 5% based on the weight of a dry disk. The manufactured CDFs were tested based on the following established requirements: (i) arsenic must be removed to below the provisional WHO guideline of 10 µg/L, (ii) for bacteria a Log_{10} Reduction Value (LRV) of 2 or greater is required, (ii) for viruses a LRV of 3 or greater is required, (iv) the leached amount of metals must not exceed the WHO guidelines and (v) CDFs should have a flow rate of 0.08-0.24 L/h, which corresponds to 1-3 L/h for a full-size CPF.

The removal of bacteria and viruses was quantified by loading the CDFs with test water with *Escherichia coli* and MS2 bacteriophages, as indicator organisms for bacteria and viruses, respectively. During this filter experiment also the metal leaching from the CDFs was evaluated, an arsenic breakthrough experiment was performed and the flow rates were measured. Furthermore, batch experiments were conducted with ground CDFs, both fired and unfired, to get more insight on

the capabilities of the adsorption and inactivation of MS2 bacteriophages and the removal of arsenic, and to study the consequences of firing nZVI into the CDFs. Moreover, knowledge was obtained on the effect of firing nZVI into ceramic material by means of X-ray diffraction (XRD), ^{57}Fe Mössbauer spectroscopy, optical microscopy and Scanning Electron Microscope – Energy Dispersive X-ray spectroscopy (SEM-EDX).

The main findings, with regard to the requirements for a CPF, were: (i) although this study showed that ZVI on itself is an effective arsenic adsorbent an immediate total arsenic breakthrough of 200 µg/L was observed for the CDFs with 5% nZVI; (ii) all CDFs, except the CDF with 0.05% nZVI, were able to remove *E. coli* sufficiently to meet the requirements for bacteria removal (LRV 0.75-4.28); (iii) MS2 bacteriophages were poorly removed (LRV 0.11-0.24) (iv) there is no health-based guideline of the WHO for iron and the leached silver stayed far below the maximum WHO guideline of 0.1 mg/L; (v) the translated flow rates for CPFs were for all type CDFs higher than the requirement of 1-3 L/h (3.4 – 15.6 L/h), except for the CDF with 0.05% nAg (1.5 L/h).

Overall, it can thus be concluded that it is not recommended to incorporate nZVI in CPFs before firing with the purpose to enhance the removal of arsenic and viruses. Although, ZVI on itself is well capable of removing arsenic, especially at nanoscale, it was found that when it is incorporated into clay it looses effectiveness and when the clay is fired even more. In the batch experiments the unfired crushed CDF with 5% nZVI was able to remove approximately 90% of the initial 200 µg/L arsenite (As(III)) in 30 minutes of contact time, while the fired crushed CDF only removed a few per cent As(III). Part of the faster As(III) removal of the unfired CDF was a result of sorption by the clay, but the nZVI contributed considerably. Although, the LRVs for MS2 bacteriophages by fired CDF material were higher in the batch experiment (LRV 0.42-1.52) than in the filter experiment – probably due more intensive contact - there was also no enhanced MS2 bacteriophage reduction noticed for the fired CDFs with nZVI compared to the fired blank CDF.

There are probably several reactions that caused this loss of performance of nZVI. The results of the filter experiments indicated that there was insufficient surface contact with the nZVI particles; either due to unavailability of nZVI particles on the pore surface or due to too high flow rates. The addition of nZVI particles namely led to a considerable increase of flow rate, probably as a result of successive expansion and shrinking of the nZVI during firing. Furthermore, it is hypothesized that due to the vitrification process, in which the clay bonds together, the nZVI became enclosed in the clay structure. Furthermore, the ^{57}Fe Mössbauer spectra evidenced that during firing all the added nZVI was oxidized into hematite, which probably affects the removal of arsenic. Different ZVI corrosion products have a different ability to adsorb arsenic: ZVI exhibits the greatest arsenic adsorption, secondly magnetite, then hematite and lastly goethite (Mamindy-Pajany et al. (2011)).

This study showed that ZVI has potential for the removal of arsenic in HWTS, but with application in a different setting than by firing it in the CPF. Suggestions were made for potential alternatives: (i) CPFs with an iron coating; (ii) CPF with ZVI pre-treatment in the form of an hang-element or an extra bucket on top of the CPF, like the effective SONO filter for arsenic removal (Neumann et al., 2013); (iii) CPF with inside iron mixed ceramic pellets (Shafiquzzam et al.,2013). When designing a new type of CPF it is important to make sure that the iron (oxides) particles can be reached and that the flow rate is not too high, which ensures that the contact time with the iron (oxides) particles is long

enough. Furthermore, additional research is needed on the enhancement of virus removal and inactivation. It is recommended to study the combination of nZVI and nAg in more detail, since this showed in the batch experiments enhanced virus inactivation compared to CDF with solely nZVI or nAg, and also to look at other combination of metals, such as silver and copper. In order to better understand the adsorption of viruses onto different media it is advised to determine the actual Point of Zero Charge (pH_{PZC}) of the used media. Lastly, for a later stage of future research it is advised to perform experiments with more challenging water and varying parameters such as the turbidity, the pH, competing ions, the ionic strength, influent arsenic concentration and different types of viruses.

Table of contents

Acknowledgements ..... **i**

Executive summary ..... **iii**

1 Introduction **1**
1.1 Ceramic pot filter 1
1.2 Previous research on CPFs and the application of ZVI 3
1.3 Problem description 5
1.4 Objective 5
1.5 Research approach 6
1.6 Outline report 6

2 Theoretical background **7**
2.1 ZVI particles 7
2.2 Arsenic removal mechanisms 8
2.3 Bacteria removal and inactivation 13
2.4 Virus adsorption and inactivation 14
2.5 Processes that take place during firing of CPFs 15

3 Materials and methods **17**
3.1 Chemicals and test waters 17
3.2 CDF synthesis 18
3.3 CDF characterization 20
3.4 Batch experiments 22
3.5 Filter experiments 23
3.6 Analyses 25

4 CDFs characterisation **27**
4.1 XRD analysis 27
4.2 ^{57}Fe mössbauer spectroscopy 30
4.3 Material analysis microscopy 32
4.4 SEM an SEM-EDX 33
4.5 Flow rates of CDFs 36
4.6 Conservative tracer transport through CDFs 38
4.7 Conclusions CDF characterization 40

5 Batch experiments **43**
5.1 MS2 bacteriophage batch experiments 43
5.2 Arsenic batch experiments 49

6 Filter experiments 59
6.1 Removal and inactivation of *E. coli* and MS2 bacteriophages with CDFs 59
6.2 Removal of arsenic by CDFs 67
7 Conclusions and recommendations 71
7.1 Conclusions 71
7.2 Rcommendations 73
Bibliography 77
List of figures 83
List of tables 85
Appendix I: Materials and methods 87
Appendix II: CDF characterisation 91
Appendix III: Batch experiments 95
Appendix IV: Filter experiments 97

1 Introduction

This introduction firstly elaborates on waterborne threats in developing countries and a short-time solution for this: Household Water Treatment Systems (HWTSs), in particular the Ceramic Pot Filter (CPF). Secondly, relevant literature on CPFs and the application of Zero Valent Iron (ZVI) is summarized. Subsequently, the problem description and the objective of this thesis are outlined. In the penultimate section, the research approach is discussed. And finally, to conclude this chapter an outline of this report is given.

1.1 Ceramic Pot Filter

1.1.1 Waterborne threats in developing countries

The World has met the Millennium Development goal "halving the proportion of people without sustainable access to safe drinking water and basic sanitation by 2015[1]" in terms of drinking water. However, in 2014 still 748 million people worldwide lacked access to improved sources of drinking water, of which almost a quarter relies on untreated surface water according to the World Health Organisation (WHO) & UNICEF (2014). Even when treated water is supplied, it is often re-contaminated during collection, transportation or household storage (Trevett & Carter, 2008). Consumption of this contaminated water leads to waterborne diseases, such as diarrhoea. It was estimated that in 2012 1.5 million people, the majority children, died due to diarrheal diseases (WHO, 2014).

But, microbiological pathogens in drinking water form not the only waterborne threat in developing countries. Groundwater, a common drink water source, can contain high concentrations of arsenic. Prolonged ingestion of water with elevated arsenic levels can lead to adverse health issues including dermal lesions, such as hyperpigmentation and hypo pigmentation, and various cancers, such as skin-, bladder- and lung cancer (WHO, 2011b). It is estimated that in Bangladesh alone, around 45 million people are exposed to arsenic concentrations higher than 10 µg/L, which is the maximum guideline set by the WHO (Flanagan et al., 2012).

1.1.2 Household water treatment

Since it will take additional time before many households in developing countries have access to reliable piped water systems, it is necessary to come up with alternatives. According to UNICEF and the WHO, simple, socially accepted and HWTSs can provide a solution to protect human health

[1] Goal 7, target number 10 of the Millennium Development Goals.

[2] Log_{10} reduction value (LRV) = $\log_{10}$ (pre-treatment concentration) – $\log_{10}$ (post-treatment concentration)

[3] In this study an influent concentration of 200 µg/L is used (see Chapter 3 Materials and methods), but actual source water

because they can rapidly be implemented (WHO & UNICEF, 2009). HWTS treat the raw water at home and when the water the water is safely stored, the recontamination of drinking water can be reduced.

Various HWTS technologies have been developed for developing countries to remove microbial and/or chemical contaminants.
Many of the designed HWTS for arsenic removal are based on the adsorption of arsenic. In the majority of these HWTS, the adsorption media includes some form of iron. Examples are the SONO Filter (Abul Hussam & Munir, 2007) and Kanchan Filter, which contain cast iron and iron nails, respectively, to remove arsenic.
A meta-study by Hunter (2009) points out that in the long term, the low-cost ceramic water filter is the most promising HWTS to decrease the amount of waterborne diseases compared to other interventions, such as chlorination, a Biosand filter and Solar Disinfection. The most widely implemented type of ceramic water filter is the CPF. Estimates suggest that in 2012, approximately 4 million people worldwide used CPFs as a point-of-use water treatment system (Van der Laan et al., 2014).

1.1.3 CPF system

CPFs consist of a flowerpot-shaped ceramic filter element that hangs on its rim in a plastic receptacle (see Figure 1-1). The ceramic filter element is locally manufactured from a mixture of clay, water and burnout material, such as rice husks or sawdust, which is pressed into a pot shape and subsequently fired. The combustion of the burnout material results in a porous filter material. The main mechanisms through which the raw water is purified are physical straining, adsorption, diffusion and sedimentation (Van Halem et al., 2007). Furthermore, the antimicrobial activity of the applied silver solution may also play a role in the water treatment process.

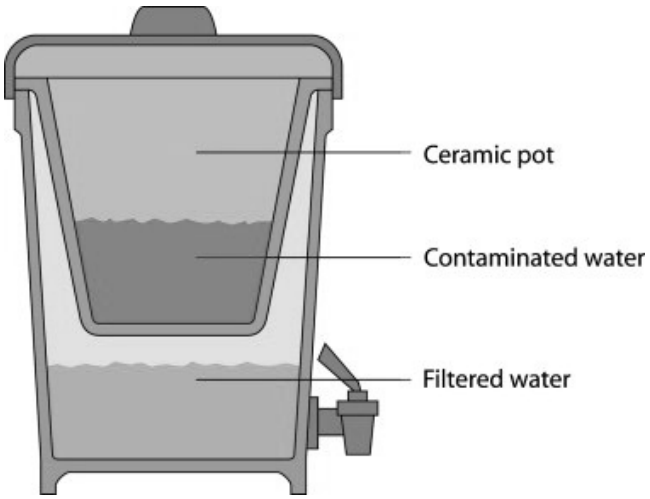

Figure 1–1|CPF system (van Halem et al., 2009).

1.2 Previous research on CPFs and the application of ZVI

1.2.1 CPF research

Removal efficiency of pathogenic microorganisms

The performance of CPFs in terms of microorganism removal, both in the field and in the laboratory, has been reported in several studies, but the variability among them is quite large. According to Van der Laan et al. (2014) the inconsistency of removal performance in literature is due to the use of various materials, different variables in the production process, the way CPFs are used and differences in performance assessments.

An overview of worldwide testing of bacteria and viruses reduction conducted on CPFs in the period of 2000-2010 was published by Simonis & Basson (2011). The listed results of the 15 laboratory- and field studies vary between a $\log_{10}$ reduction value[2] (LRV) for *Escherichia coli,* which is an indicator organism for bacteria, of 0.9 and 6.8. Hence, not all CPFs presented by Simonis & Basson (2011) meet the WHO requirements for bacteria to be indicated as a "protective" HWTS, as can be seen in Table 1-1 (LRV ≥ 2; WHO, 2011). This summary of testing, however, gives on averages a LRV of 2. Hence, generally CPFs can reduce bacteria sufficient to be a "protective" HWTS, when manufactured, used and tested in a correct way.

Table 1-1| Log_{10} reduction requirements for HWTS for the targets "interim", "protective" and "highly protective" established by the WHO (WHO, 2011a).

Target	Log_{10} reduction required: **Bacteria**	Log_{10} reduction required: **Viruses**	Log_{10} reduction required: **Protozoa**
Highly protective	≥ **4**	≥ **5**	≥ **4**
Protective	≥ **2**	≥ **3**	≥ **2**
*Interim**	Achieves "protective" target for two classes of pathogens and results in health gains		

Research to characterize the removal of protozoa by CPF is more limited than for the bacteria removal. Van Halem (2006) reported LRVs for CPFs between 2 and 6 for sulphite reducing *Clostridium* spores, which was used as indicator organism for protozoa. Furthermore, Lantagne (2001) measured LRVs of 4.6 and 4.3 for *Giardia lamblia* and *Cryptosporidium*, respectively. As can be seen in Table 1-1, these measurements indicate that CPFs are a "protective" HWTS in terms of protozoa removal (WHO, 2011).

Virus removal by CPFs is also less frequently evaluated compared to bacteria removal. Brown & Sobsey (2010) reported an average LRV of 1.2 for MS2 bacteriophages, which is an indicator organism for viruses, after 100 L throughput. Van Halem (2006) found LRVs in the range of 0.5-3 for

[2] Log_{10} reduction value (LRV) = $\log_{10}$ (pre-treatment concentration) – $\log_{10}$ (post-treatment concentration)

MS2 bacteriophages, whereas Salsali et al. (2011) observed removal efficiencies for MS2 bacteriophages between 0.21 and 0.42.
HWTSs need to have LRVs for viruses at or greater than 3 in order to be "protective', as indicated in Table 1-1 (WHO, 2011a). Since all reported studies have noticeable lower LRVs, it can be concluded that the minimal virus reduction is an important shortcoming of the CPF.

Enhancing antiviral activity

Several attempts were made to improve the viral effectiveness of CPFs. The role of silver was investigated in several studies. Results of a study with virus-sized microspheres of 0.02 mm indicated that colloidal silver generally enhanced the reduction of viruses (Bielefeldt et al., 2010).
On the other hand, a study by Van Halem (2006) showed higher MS2 bacteriophages LRVs (LRV 0.51-1.44) for CPFs without colloidal silver coating compared to with coating. It was hypothesized that the reason for this higher virus reduction with the absence of silver was clogging of the CPF and build-up of a biofilm. But, Van der Laan et al. (2014), who tested this hypothesis, could not confirm it. However, it might be that in study by Van der Laan the formation of biofilm was restrained by the low water temperatures, which are not representative for the often tropical circumstances where CPFs are used.

Another attempt to enhance the inactivation of viruses was the incorporation of iron oxides to the clay before firing (Brown & Sobsey, 2009). The modified ceramic material showed increased adsorption and inactivation capacities of viruses compared to the ceramic material without iron oxides.

Enhancing arsenic removal capacities

The poor virus removal is not the only disadvantage of CPFs. As discussed previously, arsenic is often present in raw ground water sources. Not much research has been done on the removal of arsenic by CPFs.
In an unpublished study by Robbins (2011), the arsenic removal efficiency of CPFs coated with ferric-iron was tested. For this purpose experiments were carried out with micro-columns with the same thickness and properties as a CPF. An arsenic reduction from 250 µg/L to below 10 µg/L, which is the maximum guideline set by the WHO, was observed for over 365 filter runs.

Shafiquzzam et al. (2013) developed another ceramic application for the removal of arsenic: porous, solid-phase iron mixed ceramic pellets of 2-3 mm, which consist of a mixture of clay soil, rice brand and zero valent iron (ZVI) powder at a ratio of 80:20:40, respectively, and de-ionized water. The iron mixed ceramic pellets effectively adsorbed arsenic at neutral pH.

1.2.2 Application of ZVI for arsenic removal and inactivation of microorganisms

Various studies have proposed ZVI as an effective adsorbent for arsenic. One of the most promising available HWTS for the removal of arsenic is the SONO filter developed by Hussam & Munir (2007), shown in Figure 1-2.

The active material for arsenic adsorption in this filter is Composite Iron Matrix (CIM), which is inexpensive and locally available ZVI. The SONO filters consist of tow buckets: the upper one is filled with coarse sand and a layer of CIM (cast iron) and the lower one is filled with a layer of coarse sand, a layer of fine sand and wood charcoal. This filter is very well capable to remove arsenic to meet the WHO standards for a long period of time.

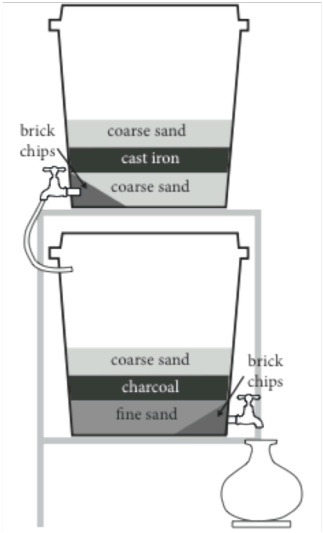

Figure 1–2| Schematic illustration of the SONO filter (Van Halem, 2011[3])

Especially ZVI nanoparticles (nZVI) are well able to remove arsenic because of their much smaller size and hence greater surface area compared to micro particles. Several studies have proven that arsenic can adsorb strongly and rapidly onto the corrosion products of nZVI (Kanel et al., 2005; Kanel et al., 2006; Mosaferi et al., 2014; Alfred & Ramos, 2011).

Furthermore, a study by Kim et al., (2011) showed that nZVI exhibits virucidal and bactericidal properties. They showed that both the metal ions released from the particles and the direct interaction of the nanoparticles and MS2 contribute to the toxicity of the nanoparticles against viruses.

1.3 Problem description

It can be concluded that although CPFs are used worldwide and are recommended by the WHO, they do not consistently provide safe water that complies with the guidelines set by the WHO. The main limitations are the poor virus removal capacities and the incapability of removing arsenic. Since the user often does not know which contaminants the raw water contains a multi-functional HWTS, capable of removing turbidity, bacteria, viruses as well as arsenic, is desired. At present such a low cost multifunctional CPF has not yet been developed. Therefore the problem description of this thesis is:

The performance of current available CPFs is not sufficiently effective to consistently meet the guidelines set by the WHO on water quality, particularly with respect to arsenic and viruses removal.

1.4 Objective

From the literature review, it followed that the current available CPFs have several limitations; but the review of previous research also showed opportunities to potentially improve the CPFs. It was found that ZVI particles, especially at nanoscale, are excellent arsenic adsorbents. Besides, nZVI also has possible capabilities for virus inactivation. With the problem description and the opportunities that resulted from previous research, the following overall objective is established:

Provide reliable experimental data to investigate whether it is feasible to extend the capabilities of the CPF with arsenic removal properties and enhanced virus inactivation by the incorporation of nZVI before firing.

From the overall objective the following sub-objectives were formulated:

I. Study the arsenic adsorption capacities of CPFs with nZVI fired-in.
II. Determine the microbiological inactivation efficiency by CPFs with nZVI.
III. Evaluate the leaching of the incorporated nZVI.
IV. Provide knowledge on the effect of incorporating nZVI into the CPFs before firing.

1.5 Research approach

In this study Ceramic Disk Filters (CDFs) were manufactured with nZVI incorporated before the firing process. To investigate whether it is possible to improve the current available CPFs, several requirements were formulated for the CDFs. With these CDFs several batch experiments and filter experiments were conducted to test the following requirements:

I. Arsenic must be removed to below the provisional WHO guideline of 10 µg/L[3].
II. A LRV of 2 or greater should be reached for bacteria[4].
III. A LRV of 3 or greater should be reached for viruses[4].
IV. The amount of leached metals must not exceed the WHO guidelines. For silver the maximum concentration is 0.1 mg/L. The WHO does not recommend a health-based guideline value for iron in drinking water.
V. CDFs should have a flow rate of 0.08-0.24 L/h, which corresponds to 1-3 L/h for a full-size CPF[5]. CPFs must be sustainable and have a long life span of at least 1 year.

1.6 Outline report

In order to understand the content of this thesis theoretical background information is provided in Chapter 2. Subsequently, the materials and methods used for the different experiments conducted in this study are discussed in in Chapter 3. The experiments are subdivided in batch experiments, filter experiments and experiments to determine the characteristics of the CDFs. Chapter 4 discusses the results of the following techniques to characterise the CDFs; X-ray Diffraction (XRD) results, ^{57}Fe Mössbauer spectra, optical microscopy images, Scanning Electron Microscope – Energy Dispersive X-ray spectroscopy (SEM-EDX) images, flow rates and the results of a conservative tracer test. The results of the batch experiments with ground CDFs are presented in Chapter 5. First the experimental data of the batch experiments with MS2 bacteriophages are evaluated and thereafter the results of the arsenic adsorption kinetics experiments. Chapter 6 deals with the obtained measurements in the filter experiments of *E. coli* and MS2 bacteriophages removal. In addition, the breakthrough of arsenic of particular CDFs is analysed. At last, in Chapter 7 the conclusions of this study are drawn and recommendations for future research are provided.

[3] In this study an influent concentration of 200 µg/L is used (see Chapter 3 Materials and methods), but actual source water might contain much higher arsenic concentrations.

[4] These requirements are based on the guidelines set by the WHO for a 'protective' HWTS (WHO, 2011a).

[5] The translation of the flow rate of a CDF to a CPF is discussed in Chapter 4.

2 Theoretical background

To get a better understanding of the content of this thesis, relevant theoretical background information is provided in this chapter. The first section elaborates on ZVI particles. In the second section the mechanisms of arsenic removal by ZVI and clay minerals are explained. Thereafter, insight is given on the inactivation of bacteria by means nZVI and silver nanoparticles (nAg). Subsequently, virus adsorption and virus inactivation by nZVI and nAg are discussed. The last section of this chapter deals with the processes that take place during the firing of CPFs.

2.1 ZVI particles

ZVI particles have a core-shell structure consisting of a metallic core enclosed by a thin layer of iron oxyhydroxides (Figure 2-1 a). This shell presumably develops directly after production as a result of passivation of the reactive ZVI core (Ramos et al., 2009).

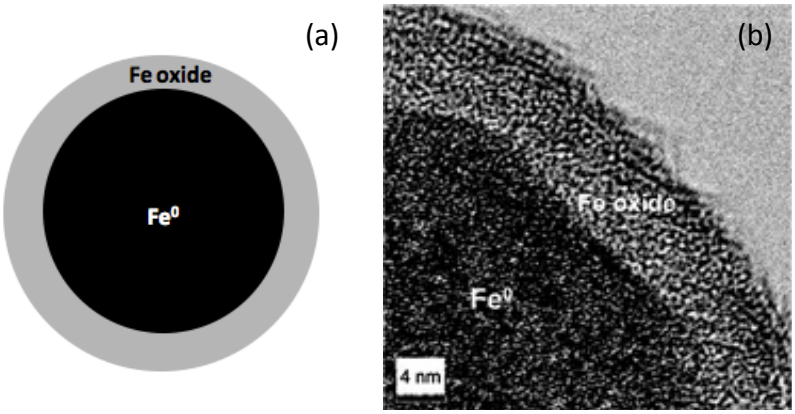

Figure 2–1|(a) Schematic picture of the core-shell structure of a ZVI particle. (b) High resolution transmission electron microscopy micrograph of a nZVI particle (Ramos et al., 2009).

In an aqueous environment first the ZVI surface oxidizes to Fe(II) (Kim et al., 2011):

$$Fe^{0}_{(s)} + O_2 + 2H^{+} \rightarrow 2Fe(II) + H_2O_2 \quad (2.1)$$

$$Fe^{0}_{(s)} + H_2O_2 + 2H^{+} \rightarrow Fe(II) + 2H_2O \quad (2.2)$$

Fe(II) reacts further to yield Fe(III). This involves the production of reactive oxygen species (ROS): hydrogen peroxides (H_2O_2), superoxide-radicals ($\bullet O_2^-$) and hydroxyl radicals ($\bullet HO$). Also Fe(IV) is formed due to these reactions (Kim et al., 2011):

$$Fe(II) + H_2O_2 \rightarrow Fe(III) + \bullet HO + OH^- \quad (2.3)$$
$$Fe(II) + O_2 \rightarrow Fe(III) + \bullet O_2^- \quad (2.4)$$
$$Fe(II) + \bullet O_2^- + 2H^+ \rightarrow Fe(III) + H_2O_2 \quad (2.5)$$
$$Fe(II) + H_2O_2 \rightarrow Fe(IV) + H_2O \quad (2.6)$$

Subsequently, an oxyhydroxides layer is formed by the following reactions (Li et al., 2006):

$$Fe(III) + 3OH^- \rightarrow Fe(OH)_3 \quad (2.7)$$
$$Fe(III) + 2H_2O \rightarrow FeOOH + 3H^+ \quad (2.8)$$
$$Fe(OH)_3 + 3H^+ \rightarrow FeOOH + H_2O \quad (2.9)$$

Transmission electron microscopy imaging indicated that the core has a crystalline structure (Nurmi et al., 2005). In the outer-layer no periodic lattice fringes were observed, which implies that it is an amorphous material (Figure 2-1 b) (Ramos et al., 2009). This amorphous character makes it difficult to determine the exact composition of the oxide layer. In addition, the type of synthesis of the ZVI particles and the particle's environment might also have an influence on the speciation of the oxide layer (Li et al., 2006).

2.2 Arsenic removal mechanisms

The main mechanism to remove arsenic by a CPF with ZVI incorporated is adsorption. There are two types of forces that play a role in the adsorption of arsenic: (i) the relatively weak Van der Waals forces, which are a result of physical attraction and (ii) the Coulomb forces, which are a result of electrostatic attraction. The charge of both the adsorbent and the adsorbate can thus play an important role in the adsorption process. Therefore, first more insight is given on the charge of a mineral surface. Subsequently, the chemistry of arsenic is explained and thereafter the removal processes of arsenic by CPFs with ZVI incorporated are discussed.

2.2.1 Charge of a mineral surface

The net total charge of a mineral surface consists of different components, as described by equation 2.10 (Essington, 2004).

$$\sigma_p = \sigma_0 + \sigma_H + \sigma_{is} + \sigma_{os} \quad (2.10)$$

where σ_0 is the permanent structural charge, σ_H the proton charge, σ_{is} inner-sphere complex charge and σ_{os} the outer-sphere complex charge. The permanent structural charge of clay depends on the combination of broken bonds, charge deficiencies and cations substitution in the lattice. The proton charge is a variable pH-depending charge, which occurs due to the adsorption of H^+ and OH^- ions. This takes place in the s-plane of the mineral surface (see Figure 2-2). The permanent structural charge and charge due protons form together the intrinsic charge of a mineral surface.

The inner-sphere complex charge and the outer-sphere complex charge result from the formation of inner-sphere surface complexes in the is-plane and outer-sphere surface complexes in the os-plane, respectively. These types of complexes will be discussed in more detail later on.

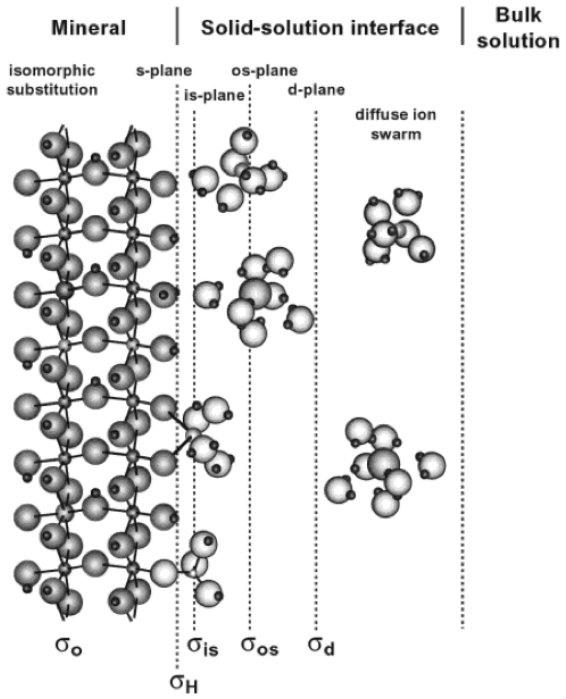

Figure 2–2| Illustration of the different adsorption planes with the associated charge components (Essington, 2004).

The solid-solution interface is considered to have an electric double layer structure. The inner layer, or Stern layer, consists of the surface charge σ_p and the outer layer is the diffuse layer, or Gouy layer, which balances the charge of the surface with freely mobile counter ions (see Figure 2-3). The total net surface charge of σ_p is thus counter balanced by the charge of the diffuse layer σ_d: $\sigma_p + \sigma_d = 0$.

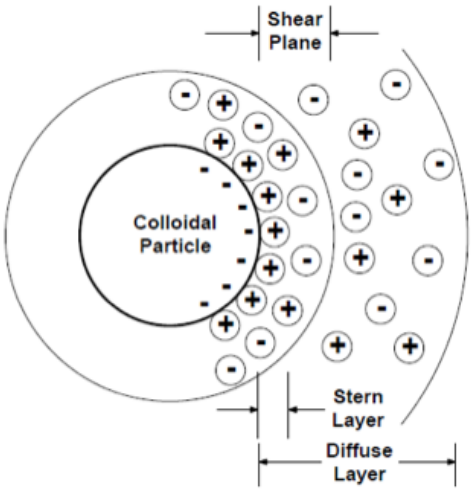

Figure 2–3| Schematic illustration of the diffuse layer around a colloidal particle.

The surface charge of a mineral can be determined with its point of zero charge (pH_{pzc}). The pH_{PZC} is defined as the pH value at which the net total charge of a mineral surface σ_p is zero. When the pH is lower than the pH_{PZC} the surface is positively charged and when the pH is higher than the pH_{PZC} the surface is negatively charged.

Kanel et al. (2005) reported a pH_{PZC} for untreated nZVI of 7.8. Under the experimental pH conditions of this study (pH around neutral[6]) the nZVI is thus slightly positively charged. The clay that is used in this study for manufacturing of CDFs consists of several minerals: quarz, albite, kaolinite and montmorillonite[7]. In Table 2-1 pH_{PZC} values for the diffferent clay minerals obtained from literature are reported. All the clay minerals have low pH_{PZC} values and are hence strongly negatively charged. However, it should be kept in mind that not only the pH has an effect on the charge of a mineral surface, the charge might also change because interactions with other compounds at the mineral surface. The surface of clay minerals can become positively charged due to edge defects, as for example an exposed broken Al-OH at which protonation takes place (Lin & Puls, 2000).

Table 2-1| pH_{PZC} values for different clay minerals reported in literature.

	pH_{PZC}	Reference
Quartz	2.8	Churchill et al. (2004)
Albite	2.6	Churchill et al. (2004)
Kaolinite	3.5 -3.6	Scroth et al. (1997)
Montmorillonite	3.4	Ijagbemi et al. (2009)

2.2.2 Arsenic chemistry

Arsenic is a metalloid, which can occur in the oxidation states +5, +3, 0 and -3. In natural waters it is generally present in the trivalent (arsenite, As(III)) or pentavalent (arsenate, As(V)) state. In an oxidative environment As(V) prevails, whereas As(III) is dominant under reducing conditions.

The speciation of arsenic depends mainly on the redox potential (Eh) and the pH (see Figure 2-4). Under reducing conditions uncharged As(III) species ($H_3AsO_3^0$) predominates at a pH below 9.2. In an oxidative environment, As(V) is prevalent in the form of $H_2AsO_4^-$ in the pH range of 2-6.9, whilst between pH 6.9-11 it is prevalent in the form of $HAsO_4^{2-}$ (Smedley & Kinniburgh, 2002).

Although As(III) is unstable under oxidizing conditions, the reaction from As(III) to As(V) by dissolved oxygen is kinetically slow, so that both arsenic species can be present in oxidizing conditions (Kim & Nriagu, 2000).

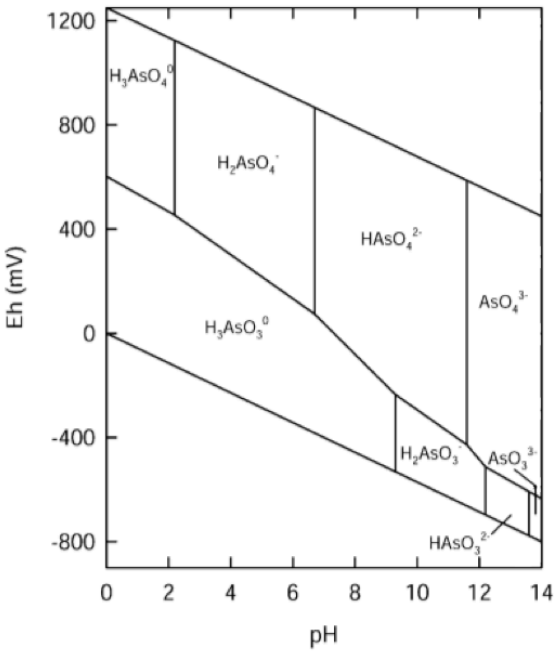

Figure 2-4| Eh-pH diagram for aqueous arsenic species in the system As-O_2-H_2O at 25°C and 1 bar total pressure ((Smedley & Kinniburgh, 2002)

[6] The experimental conditions will be discussed in Chapter 3 Materials and methods.

[7] The different clay minerals of which the clay of the CDFs consists were identified by means of XRD-analysis. The results of this XRD-analysis are discussed in Chapter 4 CDF characterisation.

2.2.3 Arsenic adsorption

The following three steps can be distinguished in the adsorption process of arsenic; (i) migration of arsenic species towards the adsorbent surface, (ii) dissociation/deprotonation process and (iii) formation of surface complexes (Zhu et al., 2009).

Migration of arsenic species

As(III) prevails as uncharged species under the experimental conditions (pH 7) in this study. Therefore, only intrinsic chemical attraction determines the adsorption of As(III). As(V) is mainly present as anions, while ZVI is slightly positively charged in this study's experiments, which means that electrostatic attraction might influence the migration of As(III) species. The clay however, is under the experimental pH conditions of this study negatively charged. This negative charge can cause repulsion of $HAsO_4^{2-}$ and $H_2AsO_4^-$ species.

Deprotonation process and formation of surface complexes

Arsenic is adsorbed onto mineral surfaces by a ligand-exchange reaction with surface hydroxyl groups. Arsenic undergoes a deprotonation process and subsequently forms a surface complex with the oxyhydroxides layer of ZVI or with the clay. Due to the corrosion of ZVI, new adsorption sites are formed. The adsorption of anionic As(V) species ($H_2AsO_4^-$ and $HAsO_4^{2-}$) onto ZVI can occur through reactions 2.11 and 2.12. Uncharged As(III) species (H_3AsO_3) are adsorbed onto ZVI as described by reaction 2.13 (Dixit & Hering, 2003).

$$\equiv FeOH + H_2AsO_4^- \rightarrow \equiv FeHAsO_4^- + H_2O \quad (2.11)$$

$$\equiv FeOH + HasO_4^{2-} \rightarrow \equiv FeAsO_4^{2-} + H_2O \quad (2.12)$$

$$\equiv FeOH + H_3AsO_3 \rightarrow \equiv FeH_2AsO_3 + H_2O \quad (2.13)$$

There are two types of surface complexes that can be formed: inner-sphere surface complexes and outer-sphere surface complexes. Inner-sphere complexes are 'specific' adsorption complexes, which are formed due to a chemical reaction (ligand-exchange) between the surface plane and the ion or molecule. These complexes can be monodentate or bidentate, which determines how many positions of adsorbates are involved in the surface complex. A bidentate bond is much tighter than a monodentate binding (see Figure 2-5). Outer-sphere complexes result from the electrostatic attraction between the surface and the ion. In the case of outer-sphere surface complexes the adsorption is 'non-specific'.

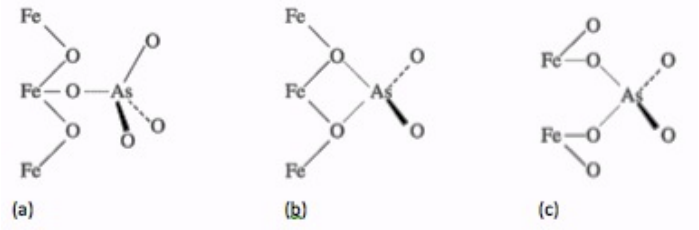

Figure 2–5| Schematic representation of a (a) monodentate mononuclear, (b) bidentate mononuclear and (c) bidentate binuclear bindings (Eick et al., 1999).

Since, arsenic is adsorbed onto mineral surfaces by ligand-exchange reactions, inner-sphere surface complexes are formed. This was confirmed by several studies that reported that As(III) and As(V) form inner-sphere adsorption complexes with ZVI or ZVI corrosion products with a bidentate configuration (Manning et al., 2002; Sherman & Randall, 2003; Farrell et al. , 2001). Furthermore,

Mohapatra et al. (2007) suggested the binding between As(V) and the clay minerals, kaolinite and montmorillonite, is also inner-sphere.

2.2.4 Other arsenic removal processes

Next to the adsorption of arsenic several other processes occur in the removal of arsenic by ZVI: oxidation of arsenic, reduction of arsenic and precipitation of arsenic. These processes are shown in Figure 2-6 and are further discussed below.

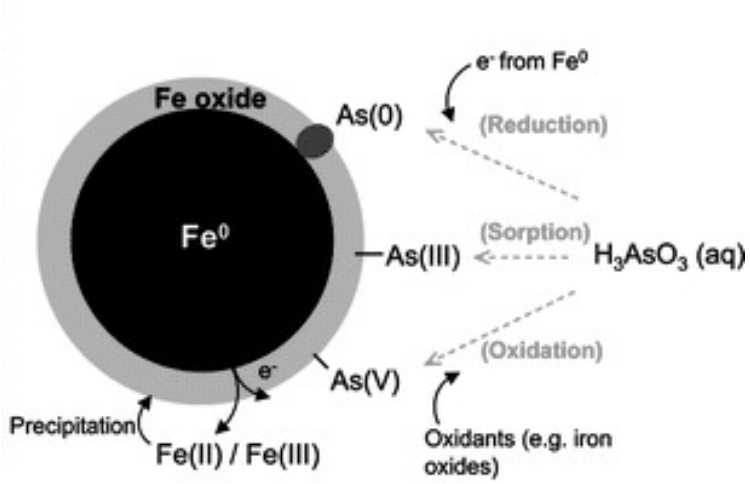

Figure 2–6| Schematic picture of the core-shell structure of ZVI together with the As(III) removal processes by ZVI (Ramos et al., 2009).

Oxidation of arsenic

As described before Fe(IV) species and •OH are formed during the oxidation of ZVI. The Fe(IV) species and •OH radicals are able to oxidize As(III) to As(IV), as described in the reactions 2.14 and 2.15.

$$As(III) + Fe(IV) \rightarrow As(IV) + Fe(III) \quad (2.14)$$

$$As(III) + {\bullet}OH \rightarrow As\ (IV) \quad (2.15)$$

Thereafter, As(IV) reacts further to As(V) in a corrosion process:

$$As(IV) + O_2 \rightarrow As(V) + {\bullet}O_2^- \quad (2.16)$$

Reduction of arsenic

According to Ramos et al. (2009) reduction of arsenic takes place simultaneously to the oxidation of arsenic. They observed As(0) species when ZVI had reacted with an As(III) or As(V) solution to which the ZVI was added. This indicated the reduction of As(III) to As(0) and the reduction of As(V) to As(III) and eventually to As(0). It is hypothesized that arsenic reduction occurs due to mass and charge transfer through the strains and defects of the thin oxide film to the metallic core of ZVI, which is able to reduce the arsenic. It must be noted that oxidation and adsorption of As(III) happens faster than As(0) accumulation (Ramos et al., 2009).

Arsenic precipitation

Next to arsenic adsorption onto ZVI surfaces arsenic can also be removed via precipitation. Both Fe(II) and Fe(III) precipitate with As(III) and As(V) (Ramos et al., 2009).

2.3 Bacteria removal and inactivation

According to Van Halem et al. (2007) mechanisms, such as diffusion, sedimentation and adsorption, play an important role in the removal of bacteria by CPFs. Van Halem et al. (2007) concluded that mechanical screening could not be main mechanisms since Van Halem measured an effective pore size for CPFs 40 µm, which is larger than the typical size of bacteria (0.5-5 µm). Furthermore, metals that are applied on CPFs can inactivate bacteria. Below the inactivation of bacteria by nAg and nZVI is discussed.

The inactivation of bacteria by nAg is thought to consist of the flowing three processes: (i) cell membrane damage upon contact with the nAg (ii) penetration of released silver ions into the cells and (iii) formation of ROS causing further damage (Zhang et al. 2012). Inactivation by nZVI occurs probably due to similar mechanisms.

Membrane damage

Damage of cell walls of *E. coli* by nAg was also reported by Feng et al. (2000) and Sondi & Salopek-Sondi (2004). In the latter study, results show the formation of "pits" in the cell membrane of the *E. coli* bacteria. In addition, Tolaymat et al. (2010) stated that nAg could adhere onto the cell membrane surface, which might have an adverse affect on the respiration of aerobe organisms. Furthermore, the damage of the cell might also cause problems with the permeability (Morones et al., 2005).
Similarly, serious damage to cell membrane integrity due to nZVI was observed by Kim et al. (2010) and by Lee et al. (2008).

Influx metal ions into cell

Further damage by access of released metal ions into the cells, following the damage of the cell, was reported by different studies. Feng et al. (2000) found that silver ions released from nAg were sorbed into the cell membranes of *E. coli* and *Staphylococcus aureus*. They suggested that due to the silver ions DNA molecules are not able to replicate anymore and that proteins are inactivated. But, not only the ions are able to penetrate into the bacteria, the nAg itself are also able to get inside bacteria, where they can cause further damage (Morones et al., 2005).

Reactive oxygen species

Park et al. (2009) reported that ROS, mainly $\bullet O_2^-$ radicals, were generated inside the bacteria cell by nAg. ROS can cause permanent damage of cellular components and inhibition of the respiration chain, which can lead to more ROS production.
Lee et al. (2008) reported that ROS produced by nZVI might play a role in inactivation of bacteria. Also, Kim et al., (2010) concluded that the produced oxidants ·OH and Fe(IV) reduced the respiratory activity. However, it must be noted that the latter two studies found a larger *E. coli* inactivation efficiency of nZVI under deaerated condition than under aerated conditions. This indicates that *E. coli* is not primarily inactivated by the oxidative stress of ROS. Hence, direct physical and chemical interactions between nZVI and *E. coli* must play a major role in bacteria inactivation by nZVI.

It must be noted that the degree of inactivation may vary per type of bacteria. Barzan et al. (2014) for instance observed that the Gram-negative bacteria *Erwinia amylovora* and *Xanthomonas oryzae* have less resistance towards nZVI than the Gram-positive bacteria *Bacillus cereus* and *Streptomyces*

spp. This is presumably because the cell walls of Gram-negative bacteria have a thin peptidoglycan layer.

2.4 Virus adsorption and inactivation

Viruses are much smaller than the effective pore size of CPFs, mostly in the range of 20 – 300 nm. Hence, viruses cannot be removed by mechanical screening. Virus reduction by CPFs occurs due to adsorption and inactivation by applied metals. Below first the adsorption of viruses is discussed and thereafter the inactivation of viruses by nAg and nZVI.

2.4.1 Virus adsorption

Also for the removal of viruses the adsorption mechanisms plays a large role. A virus is composed of nucleic acid, either DNA or RNA, which is enclosed by a protein shell, the capsid. Some viruses have also an envelope of lipids, which surrounds the capsid. Amino acids are incorporated in the capsid. Protons can be released or attach onto these amino, sulfhydryl and carboxyl groups, which results in an electrical charge. The charge of a virus thus depends on the pH. Each virus has a specific isoelectric point (IEP), which can also be defined as the pH value at which the net electric charge is zero.

In this study MS2 bacteriophages are used as indicator organisms for viruses[8]. The IEP for MS2 bacteriophages is 3.9 (Gerba, 1984). This means that the MS2 bacteriophages are negatively charged for the pH values used in this study (pH 7.2[7]).

The primarily mechanisms for adsorption of viruses are double-layer interactions and van der Waals forces (Gerba, 1984). Under the experimental conditions of this study the negatively charged MS2 bacteriophages might be weakly attracted towards the slightly positively charged surface of nZVI (see previous section about the pH_{PZC} of nZVI). On the contrary, clay minerals are negatively charged, resulting in repulsion of the virus. When the attractive van der Waals forces become greater than the double layer repulsion forces the virus can be adsorbed by the clay mineral.

Furthermore, hydrophobic interactions also play a role in the adsorption of viruses (Chattopadhyay & Puls, 1999). This is the case for viruses that have an envelope of lipids. Viruses that do not have an lipid envelope, such as coliphages and enteroviruses, are more hydrophilic (Gerba, 1984). MS2 bacteriophages, also called MS2 coliphages, do not have a lipid envelope and therefore hydrophobic interactions will probably not occur.

2.4.2 Virus inactivation by nAg and nZVI

There is much less known about inactivation of viruses by metals compared to inactivation of bacteria. Below several possible mechanisms by nAg and nZVI are briefly discussed.

Inactivation by nAg

Viruses are far less sensitive to nAg compared to bacteria. This was shown by You et al. (2011) by comparing the inactivation due to nAg of *E. coli* and MS2 bacteriophages.

Elechiguerra et al. (2005) found that the size of nAg determines whether they can directly interact with HIV-1 viral particles. The nAg was probably attracted to gp120 glycoprotein knobs sites of the

[8] The experimental procedures and conditions will be discussed in Chapter 3 Materials and methods.

HIV-1 virus particles, which are responsible for attachment of the host-cell. Hence, this interaction caused that HIV-1 viral particles were not able to enter their host cells. It is thought that this direct interaction plays a major role in the inactivation of viruses by metal nanoparticles.
A similar inactivation mechanism of Respiratory Syncytial Virus (RSV) by poly(N-vinyl-2-pyrrolidone) coated nAg was hypothesized by Sun et al. (2008). The nAg probably interacted with G proteins on RSV, which has the same function of gp120 glycoprotein knobs, and hence attachment to the host-cell was not possible.

A study by Lu et al. (2008) investigated the antiviral effects of nAg against Hepatitis B Virus (HBV). It was found that the HBV RNA could be constrained by nAg. TEM images showed that nAg were able to directly interact with HBV double-stranded DNA, probably because they are in the same size range.
Furthermore, silver ions, which are released from the metallic surface, can also interact with viral DNA and proteins, leading to inactivation of viruses (You et al., 2011).

Inactivation by ZVI nanoparticles
Ryan et al. (2002) examined the inactivation of PRD1 and MS2 bacteriophages by iron-oxide coated sand. According to them viruses are attracted to ferric oxyhydroxides by electrostatic forces and are subsequently inactivated at the surface. The surface inactivation might be mainly due to interaction with the protein capsids, leading to virus break down (Ryan et al., 2002).
Several findings of Kim et al. (2011) also suggested that MS2 phages interacted directly with nZVI, which resulted in inactivation.

Furthermore, Kim et al. (2011) reported that the released Fe(II) contributed significantly to the virucidal activity of nZVI. Also to Sagripanti et al. (1993) reported that ferric ions can inactivate the bacteriophages ϕX174, T7 and ϕ6, the Junin virus and the herpes simplex virus.

Moreover, Kim et al. (2011) observed that more MS2 bacteriophages are inactivated by nZVI and Fe(II) under air-saturated conditions than under deaerated conditions. This suggests that the MS2 is damaged by formed ROS.
As discussed earlier, Kim et al. (2010) and Lee et al. (2008) found lower bactericidal effects of nZVI against *E. coli* under air saturation compared to deaerated conditions. This implies that bacteria and viruses have different inactivation mechanisms.

2.5 Processes that take place during firing of CPFs

As previously discussed, a CPF is made by firing a mixture of clay, water and burnout material. The firing process ensures that the clay mixture becomes a strong ceramic filter. During the firing process a number of chemical and physical transformations take place: (i) evaporation of physical water, (ii) oxidation, (iii) dehydroxylation/decomposition, (iv) modification of quartz and (v) vitrification (Bickley Remmey Jr., 1994).

Firstly, the drying process is completed: when the temperature in the kiln is around 100-200°C, the physical water evaporates. Secondly, during the oxidation phase the organic matter, such as sawdust, burns out at a temperature of 300-400°C. The combustion of sawdust creates a porous ceramic material. Furthermore, the carbon of the organics oxidizes to carbon dioxide at this temperature. All

the carbon should be oxidized and volatilized out of the ceramic disks to avoid black coring[9]; this requires a slow firing rate. Thirdly, dehydroxylation of clay minerals takes place between 480 -700°C. In this process materials are decomposed and the "chemical bound water" is driven off.
Furthermore, quartz is modified: below 573°C silica is present as alpha quartz or low quartz and between 573°C and 867°C as beta quartz or high quartz. When the ceramic material is not cooled down gradually, the beta quartz will change suddenly back to alpha quartz, which can potentially cause cracks to form. The last process during firing is vitrification. During the vitrification process, which occurs for most clays around 800°C, the clay particles bind further together (see Figure 2-7). Due to this contraction of the clay, the ceramic material becomes strong. Since vitrification causes shrinkage and reduces the porosity, it is important that the CPF is not fire at a too high temperature. But at the same time the required strength of the ceramic material must be met.

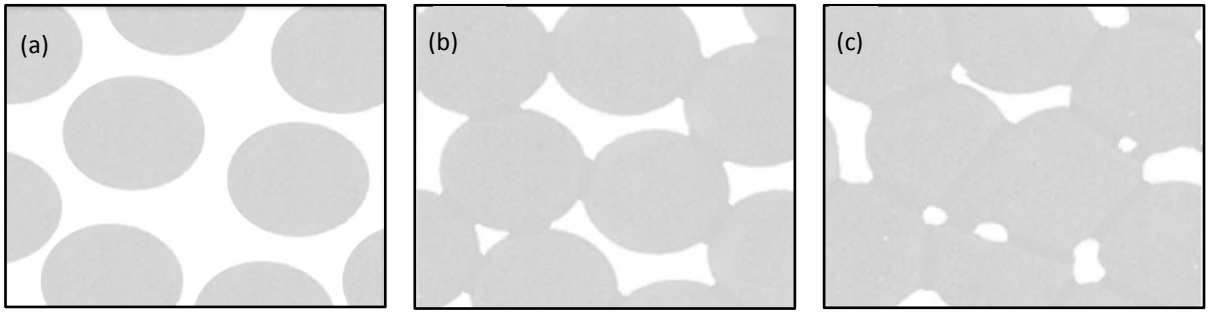

Figure 2–7|The development of the ceramic structure during vitrification: (a) loose clay particles, (b) initial stage of vitrification and (c) intermediate stage of vitrification.

[9] Black coring was observed in the first fired batch of ceramic disks. Therefore the firing process was adapted to the process as described in paragraph 1.6.

3 Materials and methods

In this chapter the materials and methods of the different experiments performed in this study are outlined. Firstly, a description is given of the used chemicals and test waters. Secondly, the manufacturing process of the CDFs is presented. Thereafter, an overview is given of the experiments that were conducted to characterise the CDFs, which include: XRD-analysis, ^{57}Fe Mössbauer Spectroscopy, optical microscopy, SEM and SEM-EDX analysis, flow rate experiment and conservative tracer experiment. The experimental procedures of the batch experiments with MS2 bacteriophages and arsenic are elaborated in the following section. Subsequently, the experimental set-up of the filter experiment is presented together with the experimental procedures to determine the removal of *E.coli* and MS2 bacteriophages and the breakthrough of arsenic by CDFs. The analysis techniques for the different types of samples are described in the last section of this chapter.

3.1 Chemicals and test waters

3.1.1 Metals

The nZVI aqueous dispersion (NanoFer 25), which consists of 30% nZVI and 70% water, was purchased from NanoIron S.R.O. (Rajhrad, Czech Republic). The average particle size of the nZVI is smaller than 50 nm. The CIM was obtained from a SONO filter, made in Bangladesh. The CIM was made from local available iron turnings, handled in a proprietary process with food-grade acids to boost the formation of hydrous ferric oxide. The CIM particles were grinded with a mortar and a pestle and sieved through a 40-mesh sieve, which corresponds to a particles size of 420 µm. The nAg solution that was used was supplied by Ames Goldsmith Cooperation (New York, United States) and has an average size of 30nm.

3.1.2 Test water microbes

A phosphate buffered saline (PBS) solution was added to de-ionized water to create a 1:10 PBS solution. This PBS solution is a standard solution that is commonly used in microbiological test in the United States. A PBS solution is made from demineralized water with sodium chloride (8 g/L), sodium phosphate (1.42 g/L), potassium chloride (0.2 g/L) and potassium phosphate (0.24 g/L). The desired pH of 7.2 was reached by adding hydrochloric acid to the solution. Subsequently test microbes were added and the mixture was stirred to homogenize it.

In this study the non-pathogenic test bacteria *E. coli* WR1 was chosen as an indicator organism for pathogenic bacteria. *E. coli* is a Gram-negative bacterium with the shape of a rod. It has a diameter of around 0.5 µm and a length of 1.0-3.0 µm. This bacteria strain is often used in Dutch laboratories for modelling bacteria in drinking water since it has similar characteristics as the pathogenic bacteria *Campylobacter, Shigella, Salmonella, Vibrio cholera* and pathogenic *E. coli.*
For the modelling of viruses, MS2 bacteriophages were chosen. Bacteriophage MS2 is a non-pathogenic RNA virus with a size of 23-25 nm. It is often used as surrogate for pathogenic viruses as entero viruses, polioviruses, hepatitis A viruses and noro viruses, which are viruses that can be present in drinking water sources. Furthermore, this type of bacteriophage is easy to produce and to enumerate.

3.1.3 Test water arsenic

An As(III) stock solution (5 mg/L) was prepared freshly every measuring day by mixing sodium arsenite ($NaAsO_2$) with degassed ultrapure water. 1 mL nitric acid was added to the solution, to prevent oxidation from As(III) into As(V). Sodium arsenate ($Na_2HAsO_4 \cdot 7H_2O$) was dissolved in ultrapure water to make an As(V) stock solution. The solution was conserved in a dark place at room temperature.
The arsenic solutions for the experiments were made by diluting the arsenic stock solutions with synthetic water. The synthetic water was prepared fresh for each experiment by adding 1 mM sodium chloride and 4 mM sodium bicarbonate to demineralized water. This bicarbonate concentration was based on a small data collection of measuring points in Nicaragua where corresponding arsenic concentration were measured (see Appendix I). The initial pH of the synthetic water was adjusted to 7 by adding hydrogen chloride or sodium hydroxide. All chemicals were reagent grade obtained from Sigma Aldrich.

3.2 CDF synthesis

3.2.1 Metal content CDFs

In this study ceramic filters in the form of a disk were manufactured. Different amounts of metals were added to the clay mixture before the firing process. Figure 3-2 gives an overview of the different CDF that were manufactured, together with the type of experiments that were conducted. Since there is not much known about arsenic removal by ceramics amended with ZVI, two different types of ZVI were used: low-cost CIM micro-particles and nZVI. Furthermore, CDFs with nAg were manufactured, because most currently produced CPFs have a silver application. In this way the bacteria and virus removal capacities of the CDFs containing nZVI could be compared to the currently produced CPFs with nAg. In addition, CDFs with a combination of nAg and nZVI were produced to see whether those two metals together have an additive effect on bacteria and virus removal. Lastly, blank CDFs were produced as control filters.

Table 3-1| Overview of the different CDFs that were manufactured and their metal composition as a percentage of the dry clay weight.

Type of CDF:	Metal composition CDF:	Test for the removal of:
CIM	5 % CIM	Arsenic
nZVI	5 % nZVI	Arsenic
	0.5 % nZVI	Microbes
	0.05% nZVI	Microbes
nZVI + nAg	0.5% nZVI + 0.05 % nAg	Microbes
nAg	0.05 % nAg	Microbes
Blanks	-	Arsenic and microbes

The metal content of the CDFs was based on the initial results of an unpublished study of Friedman (2015), in which the effectiveness of bacteria and virus inactivation by CDFs[10] with nAg and copper micro-particles (Cu) was examined. Friedman (2015) found that the optimal nAg and Cu content was 0.05% or 0.5%, based on the dry clay weight. This was not only based on the best microbial inactivation capacity, the influence on the filtration rate[11] and the costs of the metals were also taken into account. Since the silver concentration of CPFs is commonly around 0.05%, this silver concentration was also chosen for this study. Because there is less know on the inactivation of microbes by nZVI, both CDFs with 0.05% nZVI and 0.5% nZVI were made.

For effective arsenic adsorption even higher ZVI concentrations are needed. With the use of the arsenic adsorption capacity of nZVI reported by Kanel et al. (2005) it was calculated that around 25 g of nZVI was needed per CDF. This calculation can be found in Appendix I. The amount of 25 g nZVI corresponds to an iron content of around 7.5% (dry clay weight is 333g). An iron content of 5% was hence a logical choice regarding the other metal concentrations of 0.05% and 0.5%.

3.2.2 Metal application technique

Most currently produced CPF are impregnated with nAg or a silver salt, such as $AgNO_3^-$. However, Ren & Smith (2013) found that significantly less silver was released from ceramic filters where nAg was incorporated in the clay mixture before firing compared to filters where nAg was applied after firing by means of painting of dipping. Hence, according to Ren & Smith applying nAg with the fire-in method would improve the performance of CPF in terms of the retention of Ag. Therefore also in this study the metals were incorporated in the clay mixture before firing.

[10] In the study by Friedman the same type of CDFs as in this study were used.

[11] Friedman (2015) noticed that the copper micro-particles caused a decrease in porosity and therefore a decrease in flow rate.

3.2.3 Manufacturing process at FilterPure (Dominican Republic)

The CDFs were manufactured at a local factory of the non-profit organisation FilterPure in the Dominican Republic. In Figure 3-1 a diagram of the manufacturing process of CDFs is presented. In Appendix I pictures can be found of the manufacturing process.

The CDFs were made in batches of 5 CDFs. Each CDFs was made of a mixture of 333 g clay soil, 67 g sawdust and 110 g demineralized water. The soil sample and the sawdust were dried and passed through a 35-mesh sieve prior to use. The particular metal was suspended in the demineralized water together with some of the clay - in order to get a well-suspended metal solution - and mechanically mixed for 10 minutes. The dry mixture of the rest of the clay soil and sawdust was mixed for 5 minutes with a mechanical mixer. Subsequently, the metal solution was added to the dry clay mixture and homogenously mixed for 20 minutes. Afterwards, the mixture was mixed for 5 minutes by hand and moulded into balls of around 510 g. The clay was placed in a mould and pressed into disks with a diameter of 13 cm and a thickness of 1.9 cm by means of a press under 2200 psi. This thickness is around the same thickness of CPFs of FilterPure. The simple geometric shape of a disk instead of a pot-shaped filter was chosen for the ease of manufacturing and testing.

The disks were dried for 2-3 days and fired in a kiln. In 3 hours the temperature of the kiln gradually increased to a peak temperature of 860°C, which means a ramp rate of 2.4°C/min. The dwell time was 40 minutes at peak temperature. After that the disks were allowed to cool overnight.

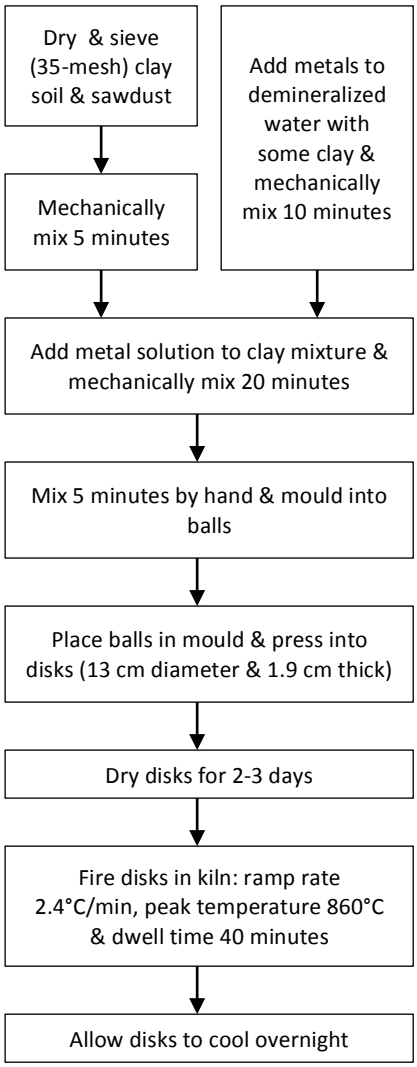

Figure 3–1| Process diagram for the manufacturing of CDFs.

3.3 CDF characterization

3.3.1 XRD analysis

XRD analysis was performed with powdered material of the CDFs containing 0.05% nZVI, 5% nZVI and 5% CIM to identify the phases of the CDF material. In order to provide knowledge on chemical changes that take place due to firing, both samples of fired CDFs and unfired CDFs were analysed. XRD is a technique for structural characterisation of crystalline materials. The method uses an incident beam of monochromatic X-rays, which diffract from the sample. By comparing the measured intensities and incident angles of these scattered X-ray beams to reference values compounds can be identified. A detailed description of the XRD technique can be found in Appendix I.

The Department of Material Science and Engineering of the Delft University of Technology conducted the analysis with a BrukerD8 Advance diffractometer with Bragg-Brentano geometry and Lynxeye

position sensitive detector. The used instrument generates copper radiation with K_α energy. The measurements were performed with a coupled θ-2θ scan over a range of 10° to 110°, with a size step of 0.034° 2θ and a counting time of 0.5 s per step. The CDF samples were analysed in duplicates.

3.3.2 Mössbauer spectroscopy

Powdered samples of a fired blank CDF, an unfired CDF containing 5% nZVI and a fired CDF containing 5% nZVI were analysed with ^{57}Fe Mössbauer spectroscopy to determine the different iron phases. This technique, based on the "Mössbauer effect", makes use of the emission and absorption of gamma rays by the nucleus ^{57}Fe. With a Mössbauer spectrometer the small changes in energy, caused by hyperfine interactions between a nucleus and its environment, are measured. There are three most important hyperfine interactions, which can be used to identify a compound,: an "isomer shift", which is induced by electron density differences, "quadrupole splitting", which occurs due to a charge asymmetry at the iron atoms, and "hyperfine magnetic splitting", which originates from the presence of a magnetic field.

The Reactor Institute Delft collected transmission ^{57}Fe Mössbauer absorption spectra at 300 K with a conventional constant-acceleration spectrometer using a ^{57}Co(Rh) source. The Mosswin 4.0 program was used to fit the Mössbauer spectra.

3.3.3 Material analysis microscopy

The material of the manufactured CDFs was analysed by means of a Keyence VHX digital microscope. To gain insight on the effect of incorporating ZVI in the clay mixture before firing, the visible differences between unfired and fired CDFs were investigated and the dissimilarities between CDFs with ZVI and without were studied. The CDF material was inspected as a powder. The CDFs were pulverized to a powder by means of a mortar and a pestle.

3.3.4 SEM and SEM-EDX

The CDF material was studied in more detail with SEM and SEM – EDX. With SEM images are obtained from signals that are produced by a focused electron beam. In addition, with SEM – EDX an element analysis of the sample can be conducted. The electron beam interacts with the sample resulting in the emission of X-rays. With the different emitted X-rays elements can be identified since each element has a particular atomic structure.

The SEM-EDX analyses were performed with a JEOL JSM-7500 device. Small pieces, in the order of several centimeters, were broken off from the CDFs for analysis. The samples were coated with thin layer of gold beforehand, to make the samples conductive. This was done with a gold sputter device Balzers Union SCD040.

3.3.5 Flow rates of CDFs

The flow rates of the CDFs were determined at the 3rd, 9th and 15th measuring day of the filter experiment. For these flow rate measurements the experimental set-up of the filter experiment was used, as presented in Figure 3-2. One hour after the water columns were filled with 5 L of test water, the produced amount of water captured in the receptacles was weighted.

3.3.6 Conservative tracer transport through CDFs

The water flow through the CDFs was characterized by means of conservative tracer tests with sodium chloride (NaCl). Also for this experiment the experimental set-up of the filter experiment was

used (see Figure 3-2). The CDFs were flushed beforehand with a demineralized water solution containing 0.05 g/L NaCl: the conductivity baseline solution. When a stable concentration was reached the water columns were emptied and subsequently filled with 5 L demineralized water containing 0.5 g/L NaCl, which corresponds to a conductivity of approximately 1050 µS/cm. Effluent samples were frequently collected and the conductivity was measured with a WTW pH Electrode SenTix 41-3 device. When a stable conductivity was reached, the water columns were emptied and refilled with the baseline solution. Again samples were taken until a stable baseline value was observed.

3.4 Batch experiments

3.4.1 Material preparation

The CDFs were finely ground with a mortar and a pestle. The ceramic material of the non-fired CDFs was sieved through a 40-mesh sieve to remove the sawdust from the clay material.

3.4.2 Batch experiment MS2 bacteriophages adsorption and inactivation

The objective of this experiment was not only to test the degree of MS2 removal by the manufactured CDFs, but also to make a distinction between the viruses that are only adsorbed and viruses that are actually inactivated. Therefore, first the adsorption of MS2 by the different ceramic media was tested. Secondly, it was examined how much MS2 could be recovered from the surface of the media and if those viruses were still infectious. The experiments were performed in duplicates. In addition, the amount of metals that leached of the ceramic material was measured.

Adsorption MS2- bacteriophages

In this experiment 2 mL polypropylene tubes were filled with 1 mL of test water containing $10^5 – 10^8$ PFU/mL of MS2-bacteriophages. To this solution 0.25 g crushed ceramic material was added. The ground ceramic material was for this experiment sieved to obtain a particle range of 75-250 µm. The tubes were horizontally shaken for 30 minutes on a shaker plate at 150 rpm. These 30 minutes of contact time approximately correspond to the residence time of water in CPFs. Afterwards, the tubes were centrifuged for 10 minutes at 8000 g. The supernatant was assayed for MS2-bacteriophages[12].

Recovery of MS2- bacteriophages

After centrifugation a ceramic pellet remained. This pellet was resuspended in a 1 mL eluant solution in order to recover the adsorbed viruses. This eluant is a solution of distilled water with 3% beef extract by weight, 2 M $NaNO_3$ and a pH of 9.5. The tubes were again shaken on the shaker plate for 1 h and subsequently centrifuged for 10 minutes at 8000 g. After that, the supernatant was removed again for MS2 assay. This recovery experiment was repeated with a similar beef extract eluant but with a pH of 5.5 instead of 9.5[11].

3.4.3 Batch experiment arsenic adsorption

To examine the adsorption of arsenic by CDFs batch experiments were performed with crushed CDFs. Also the arsenic removal capacities of solely nZVI dispersion and CIM particles, which are the metals that were added to the ceramic disks, were investigated.

[12] The conditions of this experiment were adopted from a study by Brown & Sobsey (2009) in which the removal of viruses by ceramic media amended with metal oxide was tested.

The arsenic adsorption kinetics was investigated in 250 mL closed bottles containing 250 mL arsenic solution with an initial concentration of 200 µg/L. To this solution ground ceramic material, nZVI aqueous dispersion or CIM powder was added. The bottles were continuously stirred at 150 rpm in a closed incubator and were hence kept in a relatively dark surrounding[13]. The temperature in the incubator ranged between 28°C and 29°C[14].

A 10 mL sample was taken with a syringe after 0 – 1440 min of contact time. Due to the frequently opening of the bottles it was assumed that the experiments were conducted under aerobic conditions. The samples were filtered through a 0.45 µm membrane filter (Whatman). Since it was impossible to filter the samples from experiments with unfired CDF material immediately through a 0.45 µm membrane filter, they were first vacuum filtered through a 4-12 µm cellulose filter paper (Whatman).

Each experiment was run in duplicate. The temperature and the pH were monitored at the beginning of the experiment, after 1.5 h, after 6 h and at the end of the experiment. This was done with a WTW pH Electrode SenTix 41-3 device.

3.5 Filter experiments

3.5.1 Experimental set-up

The experimental set-up of this study is shown in Figure 3-2. The set-up consisted of 10 PVC pipes of 1 m length and a diameter of 125 mm with a pipe connector attached to each pipe. The PVC pipes and pipe connector functioned together as the water column. Before use, the CDFs were fired for 3 h at 200°C for disinfection. Furthermore, a thin layer of epoxy harder was applied on the edges of the CDFs to ensure that all the produced water passed the whole CDF thickness. The ceramic disks were then placed at the bottom of the pipe connector with a rubber O-ring. The CDFs were secured with a bead of silicone around the edge where the CDF met the inside of the CDF holder. The water columns were covered with aluminium foil to prevent contamination. A funnel was connected to the pipefittings, e.g. CDF holders, so that to the water could flow into the collection receptacles.

[13] It is tried to mimic the conditions of the CPF in practice as much as possible. Therefore it was chosen to have a place the bottles in a dark surrounding.

[14] These relatively high temperatures were due to the warm summer months when the experiments were performed.

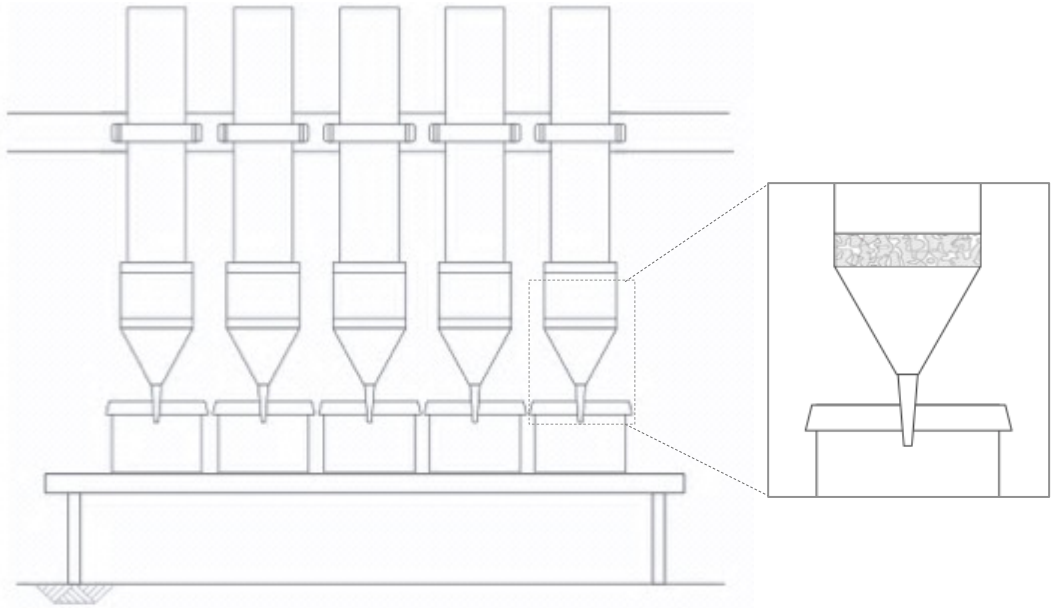

Figure 3–2| Schematic drawing of a part of the experimental set-up of the filter experiment.

3.5.2 Experimental procedure *E. coli* and MS2 bacteriophages experiment

In a 16-day loading experiment the removal of both *E. coli* and MS2 bacteriophages by the different CDFs was quantified. Next to the *E. coli* and MS2 bacteriophages reduction that was monitored during this experiment, the leached metals concentration was measured.

Experimental set-up preparation

Before the experiments were started, the collection receptacles were first rinsed with a chlorine bleach dilution, then rinsed with de-ionized water and dipped into a solution of sodium thiosulfate (100 mg/L). After that they were rinsed again with de-ionized water.

Experimental procedure filter experiment

Before the actual experiment was started, 5 L of test water without microbes was dispensed into each CDF, to flush and wet the CDFs. Thereafter, every day 5 L of prepared test water, spiked with 10^5 – 10^8 PFU/mL of MS2-bacteriophages and around 10^8 CFU/mL of *E. coli,* was poured into the CDFs.

Each measuring day (day 1,2,3,4,9 and 16) two samples of 5 mL were taken of each CDF: the first sample after approximately one hour of initial filtration[15] directly from the CDF and the second sample from the receptacle at the start of the next day. It was ensured that the time between the direct sample and the overnight samples was 16-18 h. The samples were collected into a 15 mL centrifuge tube with 500 µL of ethylenediamine-tetraacetic acid (EDTA) and 250 µL of silver quencher, in order to stop the reactions between the metals and microbes. The samples were immediately vortexed and refrigerated. In addition, at the start of the next day, a 10 mL sample was collected from the receptacle to analyse the amount of leached metals. Furthermore, the pH was of the monitored at the start of the next day. This was done with a WTW pH Electrode SenTix 41-3 device. This experiment was performed in duplicate.

[15] This 1 h of filtration before sampling was to ensure that all the water from the last filter run was flushed out of the filter.

3.5.3 Experimental procedure arsenic breakthrough experiment

The breakthrough of arsenic was investigated for two different configurations: (i) for a blank CDF and a CDF with 5% nZVI and (ii) for a CDF in combination with a layer of CIM. The latter configuration is discussed in more detail below.

The water columns were filled with 5 L of arsenic test water containing 200 µg/L As(III). At regular time intervals, a 10 mL sample was collected directly from the CDF and analysed for total arsenic concentration. This was repeated until a total breakthrough was observed.

CDF combined with layer of CIM

The arsenic breakthrough of CDFs with 5% CIM was not investigated in this study. Instead, the arsenic-breakthrough experiment was repeated with on top of the ceramic disk a layer of CIM, as shown in Figure 3-3. This was done as a preliminary study, since it might be a good option to combine the CPF with pre-treatment of CIM for enhanced removal of arsenic. The CIM layer had a thickness of 1.5 cm, which was based on the maximum amount of available material. The CIM grain size was in the range of the grain size used in the SONO filter: 0.05 – 6 mm (Hussam, 2008).

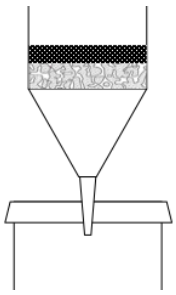

Figure 3–3| Schematic illustration of a CDF combined with a layer of CIM.

With the results of this experiment a comparison can be made between the performance of a CDF with and without a layer of CIM. Due to time limits it was not possible to determine the arsenic breakthrough of this combination filter.

Oxidation of arsenic by CDF

To investigate whether the As(III) was oxidized to As(V) by the blank CDF and the CDF with 5% nZVI, some samples were passed through a 10 mL syringe filled with an Amberlite®IRA-400 chloride resin (Sigma Aldrich). Since the chloride exchanges with the charged As(V) species in the sample, only the As(III) species will come out of the syringe. In this way, it is possible to differentiate between the concentration of As(III) and As(V) in a sample. In Figure 3-4 a schematic drawing is shown of the syringe filled with a chloride resin together with an indication of the different arsenic species.

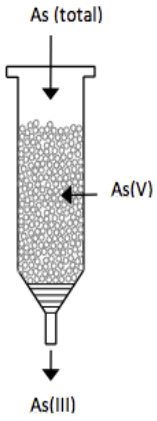

Figure 3–4| Illustration of a syringe filled with the resin, together with the As species.

3.6 Analyses

3.6.1 *E. coli* and MS2 bacteriophages

The *E. coli* was analysed using a standard spread plate method. Serial dilutions were prepared, and the appropriate dilutions were enumerated on lauryl sulphate agar. After incubation overnight, the number of Colony Forming Units (CFU) was recorded and converted to CFU/mL.

MS2-bacteriophages were assayed according to NEN-EN-ISO 10705-1 protocol using tryptic yeast glucose agar. Again, serial dilutions were made and only the relevant ones were analysed. After overnight incubation, the number of Plaque Forming Units (PFUs) was recorded and converted to PFUs/mL. All samples were analysed in duplicate.

3.6.2 Arsenic & metals

The total arsenic concentrations and the concentration of metals that leached out of the CDF material were quantified by means of Inductively Coupled Plasma Mass Spectrometry performed by the Waterlaboratory HWL (Haarlem, the Netherlands). This was done according to the NEN-EN-ISO 17294-2 method.

4 CDFs characterisation

In this chapter the results of the experiments to characterise the CDFs are presented and reflected. In the first four sections the results of the following material characterisation techniques are outlined respectively: XRD, ^{57}Fe Mössbauer spectroscopy, optical microscopy and SEM-EDX. With these techniques insight was gained on the effect of firing ZVI into ceramic material. Thereafter, the measured flow rates of the CDFs are discussed and translated to flow rates of CPFs. Penultimately, the results of the conservative tracer test, performed to study the hydraulic properties of the CDFs, are evaluated. Lastly, the conclusions with regard to the CDFs characterisation are summarised.

4.1 XRD analysis

In Table 4-1 the identified minerals, besides quartz and ordered albite, which are the major phases in all samples, are listed per type of CDF. In Appendix II one the measured XRD patterns is shown.

Table 4-1|The minerals per type of CDF that were identified by means of XRD, besides quartz and ordered albite, which are present in each sample.

		Kaolinite -1A	Montmorillonite -22A	Nontronite heated	Iron oxide hydroxide	Hematite	Iron (ZVI)
Unfired	0.05% nZVI	x	x				
		x	x				
	5% nZVI*		x			x	x
			x			x	x
	5% CIM	x	x				
		x	x				
Fired	Blank*					x	
						x	
	0.05% nZVI						
	5% nZVI	x		x	x		
		x			x		
	5% CIM				x		
					x		

* These CDFs were measured separately from the rest with a longer measuring time - a counting time of 20 seconds per step, instead of 0.5 seconds per step - in order to have a better chance of detecting the iron.

4.1.1 Identification of clay minerals

In all samples the major phase is quartz SiO_2. Quartz is a tectosilicate, or "framework silicate", and is one of the most common minerals in the Earth's crust. It has a crystal structure of interconnected silicon-oxygen tetrahedra SiO_4 (see Figure 4-1 a). Each silicon atom is linked to four oxygen atoms at the corners of the tetrahedron and each oxygen atom is shared by two SiO_4 tetrahedra. This results in an overall chemical formula of SiO_2, referred to as silica.

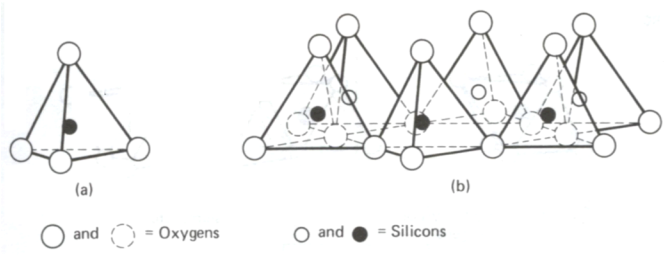

Figure 4–1|(a) Silicon tetrahedron. (b) Silicon tetrahedral sheet (Weaver & Pollard, 1973).

The other compound, which is present in all the samples, is ordered albite $NaAlSi_3O_8$, a sodium aluminosilicate. Albite belongs to the feldspar family of the tectosilicates. The framework consists of tetrahedral coordinated silicon and aluminium elements (see Figure 4-1 b) with sodium ions located in the void spaces of the structure. The distribution of the aluminum and silicon elements is ordered, which corresponds to the structural modification at low-temperature.

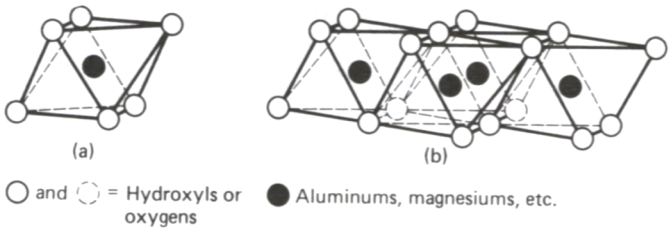

Figure 4–2|(a) Aluminium octahedron. (b) Octahedral sheet (Weaver & Pollard, 1973).

Kaolinite $Al_2Si_2O_5(OH)_4$ is a 1:1 phyllosilicate, also called a sheet silicate. It is composed of alternating silicon tetrahedral layers (Figure 4-1 b) and octahedral layers of alumina (Figure 4-2 b). The interlayer bonding is by van der Waals forces and hydrogen bonding. The structure of kaolinite is shown in Figure 4-3.

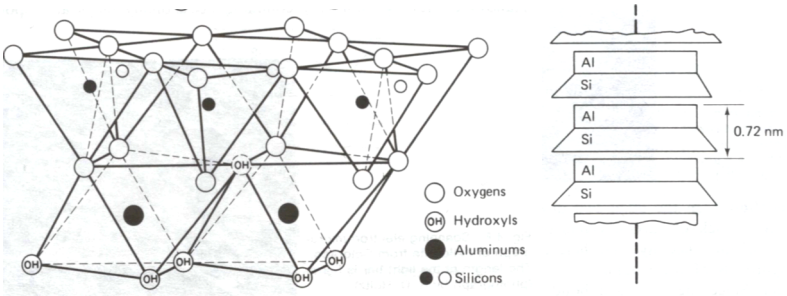

Figure 4–3|Structure of kaolinite (Weaver & Pollard, 1973).

Montmorillonite $Na_{0.3}(Al,Mg)_2Si_4O_{10}(OH)_2 \cdot 8H_2O$ is a 2:1 phyllosilicate, which is build-up of two tetrahedral sheets with an octahedral sheet in between (see Figure 4-4). In the octahedral layer magnesium replaces every sixth aluminum atom. The layers are attached through van der Waals

forces and sodium ions, which make up the charge balance between the sheets creating adsorption complexes for H_2O molecules. The amount and position of the water molecules differ per structure.

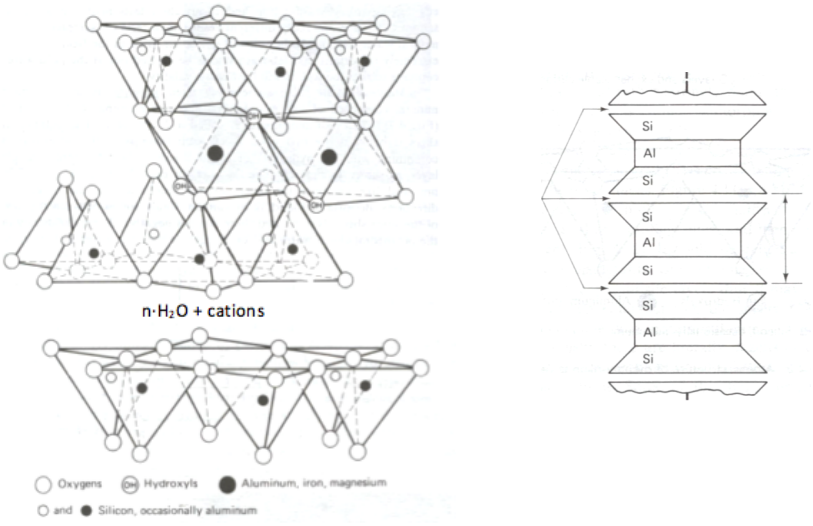

Figure 4–4|Structure of montmorillonite (Weaver & Pollard, 1973).

Nontronite $(Na,Ca)_{0.3}Fe_2(Si,Al)_4O_{10}(OH)_2{\cdot}xH_2O$ is an iron rich clay mineral, that usually consisting of more than 30% of Fe_2O_3. It is 2:1 layered silicate mineral composed of mainly silicon tetrahedral sheets and iron octahedral sheets. Cations balance the charge deficiencies of the layers.

4.1.2 Transformations clay compounds due to firing

In Chapter 2 the processes that take place during the firing of ceramics are outlined. During the dehydroxylation process, decomposition of the clay material takes place.

It can be seen in Table 4-1 that the unfired samples all contain montmorillonite-22A, while this clay compound is not detected in any of the fired samples. This implies that a phase change took place from a crystalline structure to an amorphous structure, because a diffractometer is only capable of detecting crystalline materials. This is in line with the findings of Temuujin et al. (2000), who reported that the crystalline structure of the montmorillonite clay destructs at 800°C and changes into an amorphous structure.

Furthermore, according to Murad & Wagner (1998) kaolinite decomposes into metakaolinite by the following reaction when the firing temperature approaches 500°C:

$$Al_4Si_4O_{10}(OH)_8 \rightarrow Al_4Si_4O_{14} + 4H_2O \qquad (4.1)$$

This conversion goes together with geometric transformation, resulting in an amorphous structure (Fernandez et al., 2011). The above suggests that kaolinite would not be present in fired samples. This is the case for the samples of CDFs containing 0.05% nZVI and 5% CIM, but not for the samples of CDFs with 5% nZVI. It is unclear what the reason for this is.

4.1.3 Transformation iron compounds due to firing

Firstly, it can be seen in Table 4-1 that no iron phases were detected in all the samples with 0.05% nZVI. This is because the minimum detection limit of a diffractometer is higher than 0.05%. The clay minerals probably caused a lot of disturbances, making the iron phases undetectable.

Secondly, iron (ZVI) was detected in the unfired sample containing 5% nZVI, while in the fired samples only iron oxide hydroxides were found. This implies that during the firing process ZVI was oxidized, which is indeed an expected process. Shafiquzzaman et al. (2011) also reported that the firing process of their manufactured iron mixed ceramic pellets[16], which consisted of 24 h drying at 105°C and subsequently 1.5 h firing at 600°C, caused that the added ZVI was oxidized: into hematite. The reason that no ZVI was found in the unfired samples with CIM is probably because the measuring time of the diffractometer was too short. Initially also no ZVI was found in the samples of the unfired CDF with 5% nZVI. But these samples were analyzed again with a longer measuring cycle. This was not done for the samples containing CIM.

Another notable result is that hematite and goethite were detected in the unfired sample with 5% ZVI. This suggests that part of the ZVI is already oxidized before firing. This oxidation before firing was indeed noticed during the manufacturing of the CDFs. The oxidation caused the clay to heat up and to dehydrate. However, hematite was also identified in the blank fired samples. So it might be that the detected hematite in the unfired sample with 5% nZVI was already present in the clay.

4.2 ^{57}Fe Mössbauer spectroscopy

With ^{57}Fe Mössbauer spectroscopy the incorporation of nZVI in the clay mixture before firing was further studied. The obtained ^{57}Fe Mössbauer spectra of the samples from an unfired CDF with 5% nZVI, a fired CDF with 5% nZVI and a fired blank CDF are depicted in Figure 4-5.

The black line in Figure 4-5 reflects the measured spectra. Two types of Mössbauer signals are visible: doublet signals, displayed in red, and sextuplet signals, displayed in blue. All Mössbauer subspectra have an isomer shift (IS), which determines the oxidation state of the iron, and a line width (Γ), which results from the uncertainty in the energy of the states involved in the transition. Doublets signals occur when a charge asymmetry is present at the Fe atoms and hence quadrupole splitting (QS) is measured. When also a magnetic field is present a hyperfine field is measured and a sextet pattern is observed.

[16] See paragraph 1.2 Previous research.

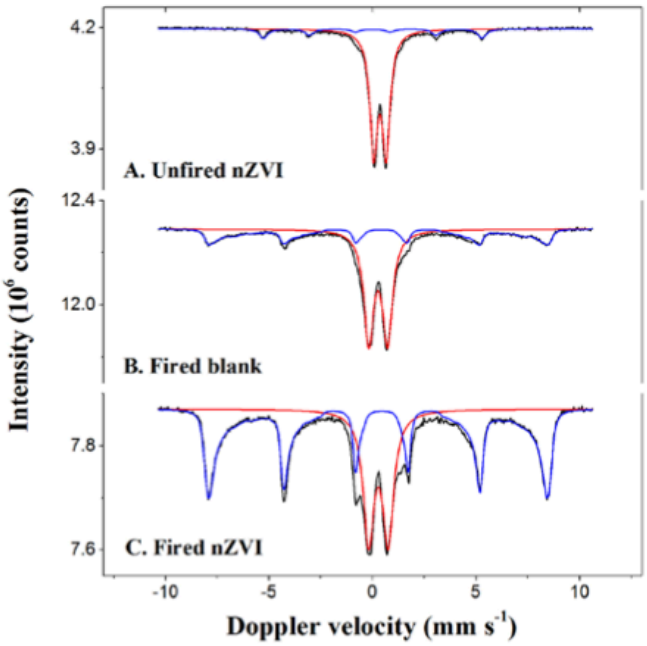

Figure 4–5| Mössbauer spectra obtained at 300 K for the samples from an unfired CDF with 5% nZVI, a fired CDF with 5% nZVi and a fired blank CDF.

In Table 4-2 the fitted parameters of the Mössbauer spectra are presented. Also the identified phases and their spectral contributions in percentages are shown.

Table 4-2| The Mössbauer fitted parameters of the samples from an unfired CDF with 5% nZVI, a fired CDF with 5% nZVi and a fired blank CDF. Experimental uncertainties: Isomer shift: I.S. ± 0.01 mm·s^{-1}; Quadrupole splitting: Q.S. ± 0.01 mm·s^{-1}; Line width: Γ ± 0.01 mm·s^{-1}; Hyperfine field: ± 0.1 T; Spectral contribution: ± 3%. [a] Mean hyperfine field.

CDF	IS [mm·s^{-1}]	QS [mm·s^{-1}]	Hyperfine field [T]	Γ [mm·s^{-1}]	Phase	Spectral contribution [%]
Unfired 5% nZVI	0.37	0.61	-	0.45	Fe^{3+}	85
	0.02	-	32.8	0.50	Fe^{0}	15
Fired blank	0.28	0.91	-	0.57	Fe^{3+}	64
	0.36	-0.15	45.2[a]	0.29	Fe^{3+} (α-Fe_2O_3)	36
Fired 5% nZVI	0.29	0.95	-	0.63	Fe^{3+}	39
	0.36	-0.19	47.2[a]	0.28	Fe^{3+} (α-Fe_2O_3)	61

The doublet signals are unambiguously assigned to Fe^{3+}, representing a superparamagnetic signal. A superparamagnetic signal occurs when structures that usually have a magnetic field become really small (below approximately 10-13 nm). This results in spins that are fluctuating very fast and because of this singlet or doublet signals are observed instead of sextuplet signals. The superparamagnetic Fe^{3+} signal is most likely hematite α-Fe_2O_3.

The unfired sample with 5% nZVI is the only sample that contains ZVI (Fe^0): about 15%. Metallic iron, i.e. ZVI, has a cubic symmetric structure and hence no QS was observed. It is interesting to see that even though this CDF was not fired, only a part of the initially added nZVI was still present as nZVI. The rest was probably oxidized to hematite. This is in accordance with the results of the XRD analysis. It must be kept in mind that a part of the hematite detected in the unfired CDF in not a corrosion product of the added nZVI but was already present in the clay.

The fired blank CDF appeared to contain hematite. This is in accordance with the XRD results and again proves that there was also iron present in the clay. A mean hyperfine field was measured for this sample because of this distribution in particle size.

In the fired CDF with 5% nZVI only hematite was found. With the XRD-analysis the identified compound was oxide hydroxide. Although the identified compounds differ, these results prove that all the added iron is oxidized during firing.
Additionally, the fitted Mössbauer parameters indicated that the hematite is sintered. This is an important discovery, because this could have influence on the distribution of the iron in the CDF and it might decrease the total available surface area of the iron.

4.3 Material analysis microscopy

The powdered samples were analysed with the Keyence VHX digital microscope, and several images were made. To gain insight on the effect of firing iron into the CDFs, both samples of blank CDFs and samples of CDFs containing iron were studied. In addition, both samples of unfired and fired CDFs were investigated. A selection of the images is shown below in Figure 4-6.

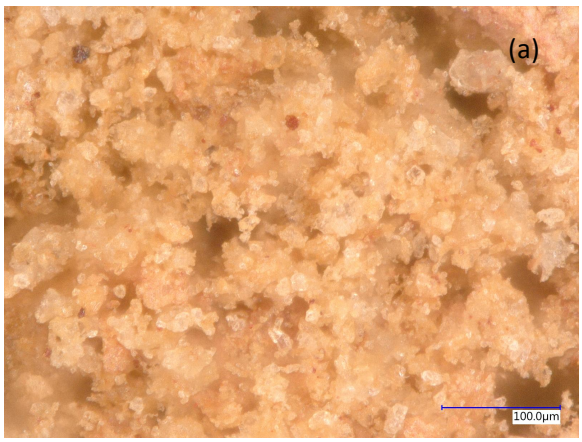

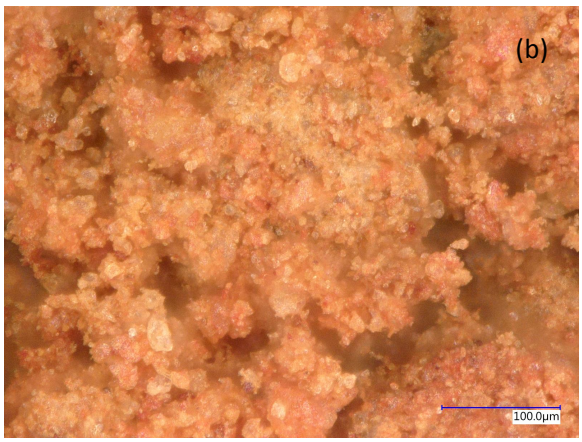

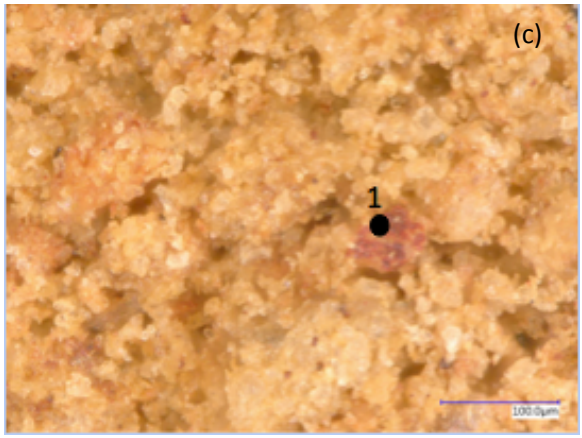

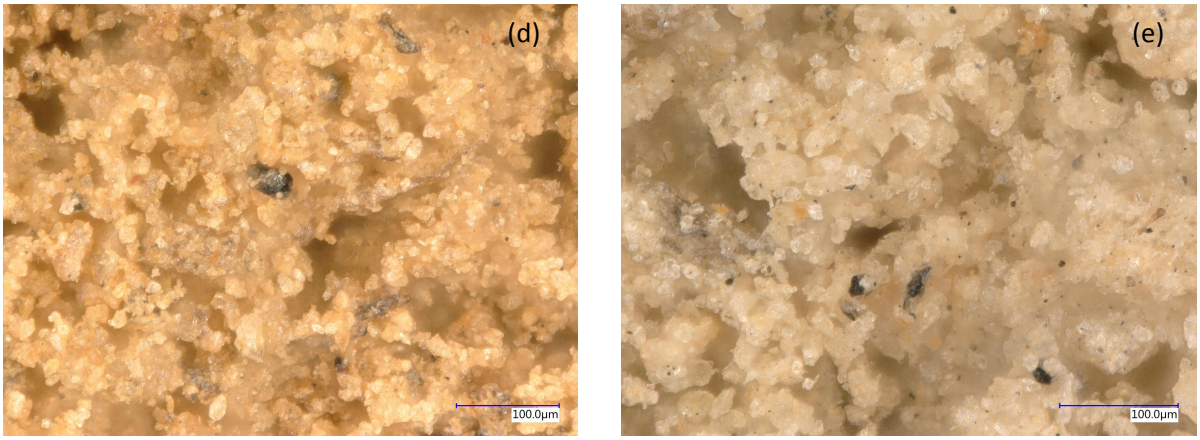

Figure 4–6|Microscope images of powdered samples of (a) fired blank CDF (b) fired CDF containing 5% nZVI, (c) fired CDF containing 5% CIM, (d) unfired CDF containing 5% nZVI and (e) unfired CDF containing 5% CIM.

There is a clear difference in colour between the analysed samples. All fired samples are redder in colour than the unfired samples. The firing process probably causes this colour change. A similar colour transformation due to firing was observed by, among others, Murad & Wagner (1998) and Ngun et al. (2012).
The fired sample containing 5% nZVI has clearly a redder hue than the unfired sample containing 5% nZVI. This might be due to the corroded nZVI that is mixed through the clay. The samples of blank fired CDFs are also orange-red in colour, but to a much less extent than the sample containing nZVI. This might suggest that the same corrosion process took place, since iron is also present in the clay, as confirmed by the XRD-results and ^{57}Fe Mössbauer spectroscopy results.
On the images of the fired samples with 5% CIM, concentrated red dots are visible, indicated with number 1. This might be a corroded CIM particle.

4.4 SEM an SEM-EDX

Since the microscopy results were not conclusive about the effect of incorporating ZVI particles in the clay mixture before firing, further research was done with SEM and SEM – EDX.
SEM was used to attempt to locate the added nZVI particles in CDFs containing 5% nZVI to provide knowledge on the iron particles itself and its surrounding area. Unfortunately, the nZVI particles appeared to be too small to distinguish them from the iron that is present in the clay. The disturbances in the clay make this analysis technique thus not suitable to gain further insight on the effect of incorporation nZVI in the clay mixture before firing.

For the fired CDF with 5% CIM, it was possible to detect a CIM particle. In Figure 4-7 (b) there is a clear accumulation of iron elements visible, which is likely assigned to a CIM particle. The rest of the visible iron elements are thus present in the clay it self. Figure 4-7 (c) shows that there was also oxygen present at the location of the CIM, suggesting that the CIM was oxidized, which is in line with the XRD-results.
The CIM particle found with SEM-EDX is of the same order of magnitude as the red “spot” observed with the Keyence VHX digital microscope (see Figure 4-6). It is thus likely that the observed red “spot” is indeed a corroded CIM particle.

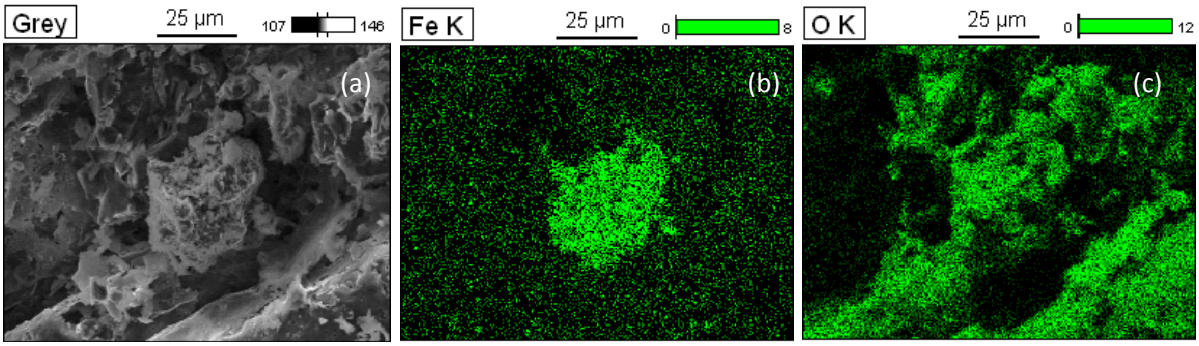

Figure 4–7| (a) SEM image of the sample from a fired CDF with 5% CIM and the corresponding distributions of (b) iron and (c) oxygen, determined with SEM-EDX.

Although it was not possible to locate nZVI particles, it was possible to evaluate the distribution of the iron in the clay with SEM-EDX. The following samples were analysed with SEM-EDX: a fired blank CDF, a unfired CDF with 0.05% nZVI, a fired and unfired CDF containing 5% nZVI and a fired and unfired CDF with 5% CIM. For all the samples an element analyses was performed at 1000x magnification. The weight percentages of iron were obtained from this elemental analysis and presented in Table 4-3. Besides iron and oxide, all the samples contained silicon, carbon, aluminium and potassium. The elements sodium, magnesium, calcium and titanium were detected in some of the samples at lower concentrations.

Table 4-3| Iron percentages per CDF, obtained from the SEM-EDX elemental analyses, performed with SEM-EDX at 1000x magnification.

CDF	Percentage Fe
Fired blank	4.47 %
Unfired 0.05% nZVI	4.04 %
Fired 5% nZVI*	10.6 % ; 18.6 %
Unfired 5% nZVI	6.11 %
Fired 5% CIM*	5.18 % ; 15.42 %
Unfired 5% CIM	1.62 %

* For these CDFs two element analyses were performed instead of one.

The 4.47% iron in the blank CDF indicates that the clay itself contained a significant amount of iron. If the iron in the clay were evenly distributed, it would be expected that each sample contained at least 4.47% iron, which is not the case. Nevertheless, the iron looks evenly distributed as can be seen in Figure 4-8, which shows an SEM image of the sample and an SEM-EDX image that shows where the iron elements are located.

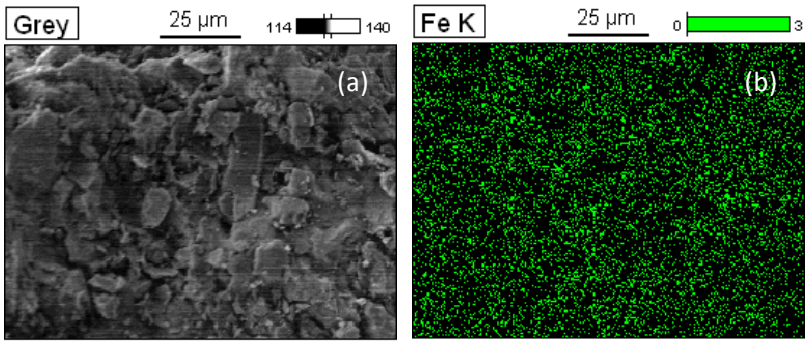

Figure 4–8| (a) SEM image of the sample from a blank CDF and (b) the corresponding distribution of iron determined with SEM-EDX.

With a first measurement of the fired CDF with 5% nZVI, an iron content of 10.6% was found. Compared with the 4.47% iron in the blank CDF this would indeed correspond to an addition of approximately 5% nZVI. This indicates that the iron was evenly spread over the CDF. The SEM images of the sample and the SEM-EDX image of the accompanying locations of the iron elements are shown in Figure 4-9 (a) and (b). The iron element image of the fired CDF with 5% nZVI looks similar to the fired blank CDF, the iron distribution is only clearly denser compared to the blank CDF.
A second measurement resulted in 18.6 % iron for the fired CDF with 5% nZVI, which invalidates that the iron was totally homogenously distributed over the whole CDF. Yet, there is no extreme agglomeration visible in the SEM-EDX images of this CDF (see Figure 4-9 (c) and (d)). Therefore, it can be carefully concluded that the nZVI is well spread in the ceramic material. Although, actually more replicate measurements should have been done to give a more reliable conclusion about this.

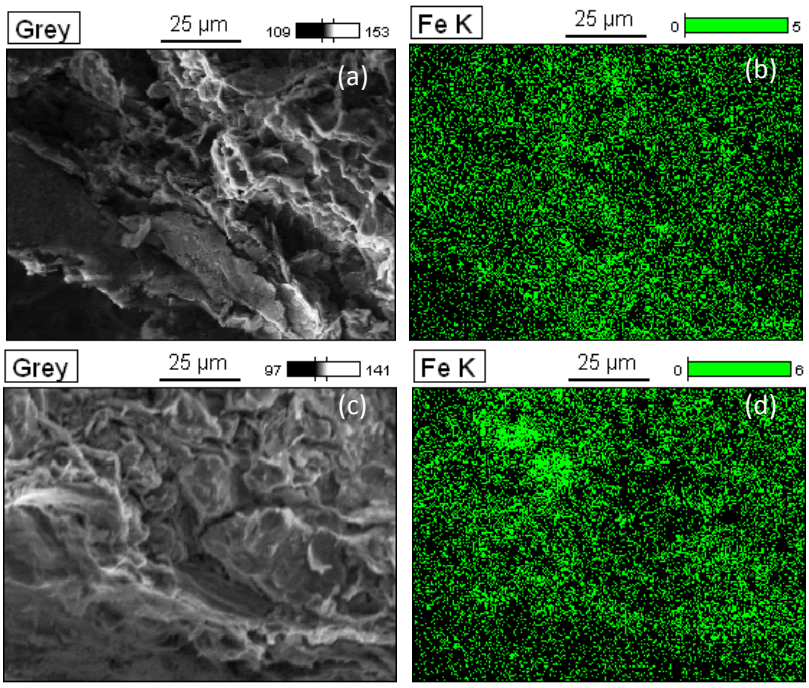

Figure 4–9| In figure (a) and (c) SEM images of the sample from a fired CDF with 5% nZVI are shown (measurement one and two, respectively) and in figure (b) and (d) the corresponding distributions of iron, determined with SEM-EDX, are depicted.

Since CIM particles have a much larger size than the nZVI particles, the total iron content in the CDFs with 5% CIM is less well distributed over the CDFs compared to nZVI. This agglomeration of iron is clearly visible in Figure 4-7 (b).

There were no clear differences found between the distribution of the iron in the fired CDFs and the unfired CDFs. In Appendix II the SEM and SEM-EDX images of the samples of the unfired CDFs are presented. The iron looks evenly spread. The iron content of the unfired CDFs is for all measurements lower than the fired CDFs. This might be coincidence, since only one measurement was done. Or, it might be that there has been some slight agglomeration of iron due to firing and that SEM-EDX images were made at the locations with these slight iron agglomerations. According to the ^{57}Fe Mössbauer spectra the firing process results indeed in the presence of a sintered form of nZVI in the fired CDF with 5% nZVI.

4.5 Flow rates of CDFs

The measured flow rates of the CDFs in the first hour after filling the water columns with 5 L of test water are presented in Figure 4-10. The CDF containing 5% nZVI was not included in the three-week filter experiment, in which the removal of *E. coli* and MS2 was studied, and therefore the flow rates of this CDF were only measured two times: after approximately 10 and 40 L of test water had run through. This roughly corresponds to the week 1 and week 2 measurements of the three-week filter experiment, since at the 3rd (week 1), 9th (week 2) and 15th (week 3) measuring day the water columns were filled in total with 15L, 45L and 75L respectively.

It should be kept in mind that this measured flow rate values were the maximum flow rates of the CDFs, since the water level gets lower with time. The lowering water level directly affects the flow rate of the CDFs.

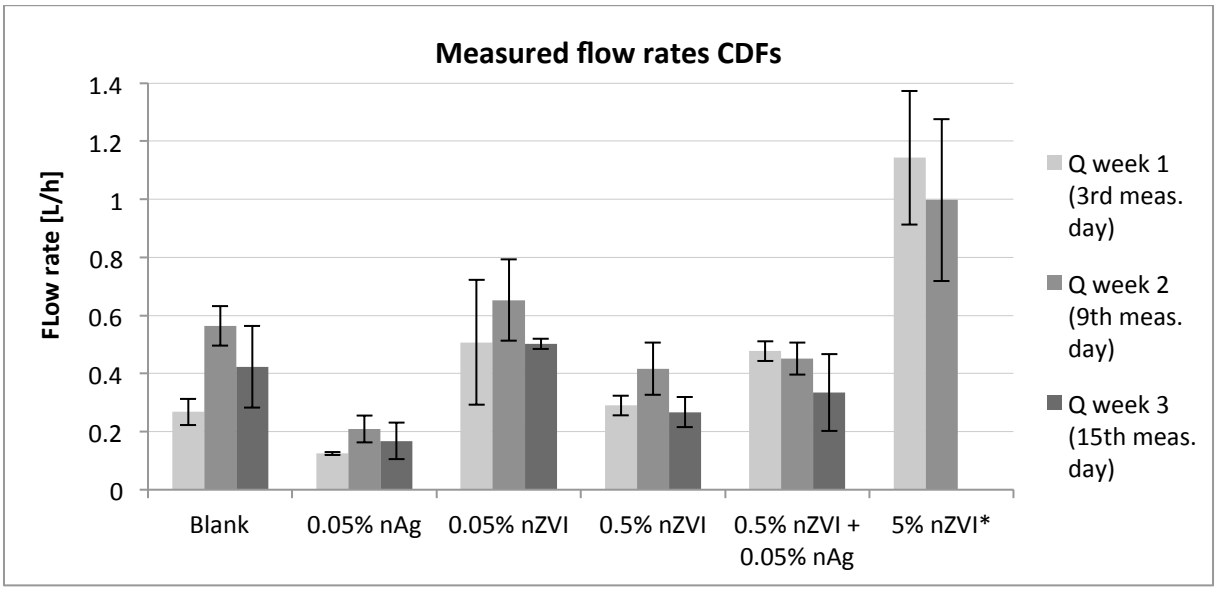

Figure 4–10| Measured flow rates of the CDFs of the first hour after filling the water columns with 5L test water.

It can be seen in Figure 4-10 that for all CDFs, except for the CDF with 0.5% nZVI + 0.05% nAg and the CDF with 5% nZVI, the flow rate increased in the second week and decreased again in the third week. The increase of flow rate in the first week was probably because the pores first had to fill up before they were all connected and the water could easily flow through. Although the test water did not contain any turbidity, it seems that the CDFs got slightly clogged in the third week, since all CDFs have a lower flow rate compared to the second week. This clogging is presumably due to some particulate matter that was still present in the CDFs, such as some sawdust or other impurities.

Initial results of an unpublished study by Friedman (2015) indicated that the addition of metals could cause a decrease in flow rate. The results of this study do not confirm this. The flow rates of the CDF with 5% nZVI even suggest the opposite: the addition of nZVI increased the flow rate considerably. This might be due to successive expansion and shrinking of the nZVI during the firing process. The increase in flow rate is in line with findings of another study: the addition of laterite, which is a soil type with a high iron oxide content, caused a increase in flow rate of CPFs (The Ceramics Manufacturing Group, 2011)

Next to the addition of metals there are several other factors that could have affected the flow rate and can be different per CDF: the amount of burn-out material, the grain size of the burn-out material, inhomogeneity of the clay, heating temperature, heating ramp rate and the duration of heating (Reed, 1995).

Translation of the flow rates of a CDF to the flow rates of a CPF

As stated in Chapter 1, a CPF should be able to produce 1-3 L/h in order to be a sustainable HHWT technique. A flow rate of 1-3 L/h is the optimum value both to ensure a long enough contact time between the raw water and the filter and to ensure sufficient drinking water production for a family.

To test whether the requirement of a flow rate of 1-3 L/h for a CPF is met, the flow rates of the disks were translated to flow rates of a CPF with the shape of a truncate cone[17]. Van Halem (2006) presented a model for the total flow rate through a CPF with the shape of a truncate cone based on Darcy's law (equation 4.2 and 4.3).

$$Q_{Darcy} = \frac{KAh}{t} \tag{4.2}$$

$$Q_{Filter} = \frac{K}{t_f} 2\pi \left(\frac{r_1 - r_2}{6L} h_w^3 + \frac{1}{2} r_2 h_w^2 \right) + \frac{K}{t_b} \pi r_2^2 h_w \tag{4.3}$$

Q	filter discharge [m^3/s]
K	hydraulic conductivity [m/s]
L	height of the filter from r_1 to r_2 [m]
r_1	radius at the top of the filter [m]
r_2	radius at the bottom of the filter [m]
h_w	water level in the filter [m]
t_f	thickness of the filter wall [m]
t_b	thickness of the bottom of the filter [m]

With the measured flow rates of the CDFs the hydraulic conductivity K was calculated using Darcy's law. The dimensions of a CPF were obtained from the study by Van Halem (2006), which are presented in Appendix II. The average flow rates for a CPF translated from the different CDFs are shown in Figure 4-11 for a water level of 18 cm. The water level of 18 cm was assumed to be an average water head for the first hour of use. Hence, for some filters an underestimation is made and for some an overestimation. Especially, the filter with 5% nZVI would have in reality a lower flow rate since the head will drop much faster compared to the other filters.

The calculations showed that the flow rate of 1-3 L/h for a full-size CPF corresponds to a flow rate of 0.08-0.24 L/h for a CDF.

[17] The bottom of CPFs made by the non-profit organisation FilterPure, which is the organisation where the CDFs were manufactured, is bowl-shaped. In this study a CPF with a truncated cone shape is assumed.

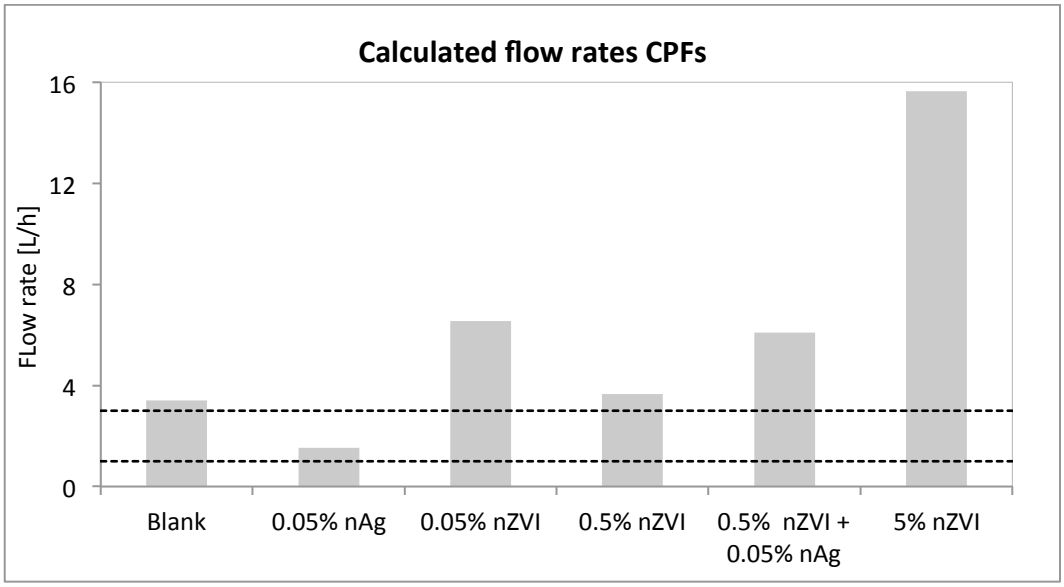

Figure 4–11 | Calculated flow rates of a CPF, which are translated from the measured flow rates of the CDFs tested in this study with a water level at half the height of the CPF. The flow rates are both averaged for difference between the duplicate disks and for the differences in time. The lower and upper dotted line indicates the minimum and maximum desired flow rate for a CPF, respectively.

Figure 4-11 shows that the translated flow rates of almost all CDFs produced in this study were outside the range of the desired flow rate of 1-3 L/h for a CPF, except the CDF with 0.05% nAg. The CDF with 5% nZVI had such a high flow rate that the contact time is really low, which will likely result in less removal of contaminants.

4.6 Conservative tracer transport through CDFs

The water flow through the CDFs was characterized by means of conservative tracer tests with NaCl. The flow through the CDFs can be described with the following advection- dispersion equation:

$$\frac{\partial c}{\partial t} = D_L \frac{\partial^2 c}{\partial x^2} - v \frac{\partial c}{\partial x} \qquad (4.4)$$

where c is the NaCl concentration, t is the time, D_L is the hydrodynamic dispersion coefficient, x is the distance and v is the advection coefficient. At the beginning of the tracer experiment the effluent NaCl concentration is equal to the baseline concentration of 0.05 g/L. The actual tracer solution has a concentration C_0 of 0.5 g/L NaCl and the time the tracer was added is t_0. After the stable effluent concentration was reached the columns were emptied and filled again with demineralized water with the baseline concentration (0.05 g/L NaCl). This gives the following initial- and boundary conditions.

$$c\,(x,0) = c_{baseline} \quad \text{for } x > 0 \qquad (4.5)$$

$$c\,(0,t) = c_0 \quad \text{for } 0 < t < t_0 \qquad (4.6)$$

$$c\,(0,t) = c_{baseline} \quad \text{for } t > t_0 \qquad (4.7)$$

Bringham (1974) showed that although the advection-dispersion equation has substantial different solutions for different initial- and boundary condtions, the calculated results are almost similar. Therefore, the following simplified solution is used (Fetter, 1999):

$$c = \frac{c_0}{2} \cdot erfc\left(\frac{L - v_x t}{2\sqrt{D_L t}}\right) \quad (4.8)$$

where *erfc* is a complementary error function [-], *L* is the flow distance (thickness of the CDF) [cm] and v_x is average linear velocity [cm/min]. This equation can be expressed as (Bringham, 1974):

$$\frac{c}{c_0} = 0.5 \cdot erfc\left(\frac{1 - U}{2\sqrt{\frac{UD_L}{v_x L}}}\right) \quad (4.9)$$

in which *U* is the total effluent pore volume, which can be calculated by dividing the discharge by one pore volume. The average linear velocity v_x was determined with the following formulas:

$$v_x = \frac{v}{n_e} \quad (4.10)$$

$$n_e = \frac{v * T_{res}}{L} \quad (4.11)$$

where *v* is the average flow rate during the experiment [cm/min], n_e is the porosity [-] and T_{res} is the average residence time. The average residence time is defined as the time from the start of tracer test till the point in time where 50% of the breakthrough took place. This is when the increase in conductivity is the largest.

The measured relative concentration C/C_0 was plotted versus the effluent pore volumes *U* and with the Matlab a best fit of the model was sought to determine the dispersion coefficient D_L. In Appendix II the breakthrough graphs of the tracers experiments are presented. In Table 4-4 the obtained residence time, linear velocity, porosity and dispersion coefficient are depicted. It must be kept in mind that only a singular tracer test was conducted per type of CDF, which makes it difficult to draw reliable conclusions.

Table 4-4| The CDF characterization parameters: linear velocity, porosity and dispersion coefficient per CDF, which were determine by means of tracer breakthrough experiment.

CDF type	Average residence time T_{res} [min]	Linear velocity v_x [cm/min]	Porosity n_e [-]	Dispersion coefficient D_L [cm^2/min]
Blank	21	0.090	0.62	0.006
0.05% nAg	37	0.051	0.54	0.006
0.05% nZVI	19	0.098	0.50	0.017
0.5% nZVI	26	0.073	0.53	0.006
0.5% nZVI + 0.05% nAg	24	0.079	0.50	0.014
5% nZVI	12	0.152	0.54	0.030

There is quite some variation in the average residence time of the CDFs. The CDF containing 0.05% nAg had an average residence time of 37 minutes, while for the CDF with 5% nZVI this was only 12 minutes. This means that in the CDF with 0.05% nAg there was a longer contact time between the

raw water and the CDF material compared to the other CDFs. Hence, removal mechanisms as adsorption, inactivation and sedimentation have more time to take place.

The porosity values for each type of CDF are similar, although the blank CDF had a slightly higher porosity. A reason for this might be that the addition of metals causes a decrease in porosity. Yet, there is no consistency in the relation between the porosity and the amount of metals added.
The found values for the porosity in this study were quite high compared to the values of ceramic disks manufactured by other researchers. Oyanedel-Craver & Smith (2008) found for instance porosities between 37-42%. But, they used flour as a combustible material and moreover the percentage of flour was only 10% on weight basis, while in this study 16.75% sawdust on weight basis was used. Also based on the initial results of Friedman (2015) slightly lower porosities were expected. Hence, it might be that the model used for the tracer test slightly overestimates the porosities.

The hydrodynamic dispersion coefficient consists of a mechanical dispersion term and a molecular diffusion term, as expressed with the following equation:

$$D_L = \propto_L v_x + D^* \qquad (4.12)$$

in which α_L is the longitudinal dispersion coefficient [cm] and D^* is the molecular diffusion coefficient [cm^2/min]. Molecular diffusion is caused by the concentration gradient. Mechanical dispersion is the mixing of water due to differences in velocities in the pores and due to the different flow paths water particles travel because of the tortuosity of the ceramic filters. The tortuosity of ceramic filters play an important role in the removal of contaminants, since a high tortuosity makes removal processes as sedimentation and adsorption more likely to happen (van Halem et al., 2007).
The blank CDF, the CDF with 0.05% nAg and the CDF with 0.5% have the lowest dispersion coefficient. The CDF containing 5% nZVI has the highest linear velocity and dispersion coefficient, which illustrates that in this CDF the tracer spread most rapidly. If in indeed a slight overestimation of the porosities was made with the used model and in reality the porosities values would be slightly lower, this would result in higher values for the dispersion coefficient.

4.7 Conclusions CDF characterisation

The material of fired and unfired CDFs was analysed by means of XRD. In all samples a quartz peak and an ordered-albite peak were detected. The other predominant clay minerals were kaolinite and montmorillonite. It is thought, based on the XRD results, that kaolinite and montorilonite turn into amorphous material during the firing process.

Only in the samples of the unfired CDFs with 5% nZVI, iron (ZVI) was actual identified by XRD and ^{57}Fe Mössbauer spectroscopy. According to the XRD-results and the ^{57}Fe Mössbauer spectroscopy all the nZVI that was added to the clay mixture was during firing oxidized to iron oxide hydroxides and a sintered form of hematite, respectively. The sintering of nZVI particles could have an effect on the distribution of iron over the CDF and on the total available surface area of the iron. Also in the unfired CDFs part of the added nZVI was corroded into hematite, as shown by the XRD-results and the ^{57}Fe Mössbauer spectroscopy

Although it was not possible with SEM-EDX to locate the added nZVI particles in the samples due to the background noise of the clay, the SEM-EDX results did provide some insight on the iron distribution. In all samples of the CDFs with nZVI no clear agglomeration of iron elements was visible on SEM-EDX images. Therefore, it can carefully be concluded that the nZVI is relatively homogenously spread. Furthermore, the SEM-EDX results showed that the clay itself contains quite a large amount of iron (4.47%).

CPFs should produce 1-3 L/h to ensure both a long enough contact time between the raw water and the filter and sufficient drinking water for a family. If a whole CPF would be manufactured from the same material as a CDF and the water head would be 18 cm, all the CPFs have higher flow rates than the requirement (3.4 – 15.6 L/h), except for the filter with 0.05% nAg (1.5 L/h).
The flow-rate measurements suggest that the addition of nZVI particles leads to a considerable increase of flow rate, probably as a result of successive expansion and shrinking of the nZVI during the firing process. Contrary to the expectations, this implies that higher iron concentrations are possible by adapting the 'recipe' of the ceramic filter. It was concluded that there are several other factors that can have effect on the flow rate: amount and size of the burnout material, inhomogeneity of the clay, and the firing process. These factors can slightly differ per batch of manufactured CDFs and even per CDF in case the clay mixture was not homogenously mixed.

A conservative tracer-test with NaCl was performed to characterize the water flow through the CDFs. As expected from the flow rate measurements, the average residence times of the CDFs vary noticeably: the CDF with 0.05% nAg and the CDF with 5% nZVI having the longest (37 minutes) and shortest (12 minutes) residence times, respectively. The CDFs have a similar porosity, although the porosity of the blank CDF is slightly higher. The water dispersed most rapidly in the CDF containing 5% nZVI, since this CDF type has the highest linear velocity and dispersion coefficient.

5 Batch experiments

After the characterization of the CDFs, batch experiments were conducted with ground CDFs and MS2 bacteriophages to get more insight on the virus adsorption and inactivation by the material of different CDFs. The results of these experiments are evaluated in the first section of this chapter. Subsequently, the results of the arsenic adsorption kinetics experiments are discussed. These experiments were conducted to make predictions about whether the contact between the contaminated water and the adsorbent would be long and effective enough for sufficient arsenic adsorption. This section deals successively with the arsenic removal by solely ZVI, the arsenic removal by fired CDFs with ZVI incorporated and the arsenic removal by unfired CDFs with ZVI incorporated.

5.1 MS2 bacteriophage batch experiments

The LRV is commonly used to evaluate the removal performance of water treatment systems. LRVs were calculated as a function of the initial concentration of infectious MS2 bacteriophages in the test water before contact with the ceramic material (pre-contact) and the concentration of unadsorbed infectious MS2 bacteriophages in the supernatant water after 30 minutes of contact time with the ceramic material and 10 minutes of centrifugation (post-contact), as shown in equation 5.1 The concentrations of MS2 bacteriophages were calculated as an average of the countable plate counts (those between 1 – 360) of PFUs of the duplicate samples. In case several dilutions were analysed, the weighted average concentration of these dilutions was calculated.

$$LRV_{adsorption} = \frac{\log_{10}(pre - contact)}{\log_{10}(post - contact\ )} \tag{5.1}$$

The MS2 bacteriophages were recovered by means of a beef extract eluant. This was done to make a distinction between the viruses that were only adsorbed onto the ceramic material and the viruses that were actually inactivated. The MS2 recovery was calculated as a LRV and as a percentage with equation 5.2 and equation 5.3, respectively. The concentrations of the total amount of MS2-phages that were recovered after the first and second re-suspension are referred to as “post-elution”.

$$LRV_{recovered} = \frac{\log_{10}(pre - contact)}{\log_{10}(post - contact \ + \ post - elution \ )} \quad (5.2)$$

$$Per\ cent\ recovery = \frac{[post - elution]}{[pre - contact] - [post - contact]} * 100\% \quad (5.3)$$

Furthermore, a LRV was computed for the eventual irreversible adsorption of MS2 bacteriophages. The irreversible adsorption is defined as the initial adsorption of MS2 phages minus the MS2 phages that were recovered by the first and second elution.

The calculated values per type of CDF material are presented in Table 5-1. All types of CDFs have a lower $LRV_{irreversible}$ than 3.
The 30 minutes of contact time of this experiment is approximately equal to the residence time of raw water in currently produced CPFs. Although the results of this batch experiment cannot directly be translated to the effectiveness of an actual CDF, the results give a first indication that the requirement for virus removal of the WHO to be a protective HWTS (LRV ≥ 3) can probably not be met.

Table 5-1| Overview of the calculated LRVs for the initial adsorption of MS2 bacteriophages by the ceramic material, the LRVs and percentages for the recovered phages during the first and second elution and the LRVs for the eventual irreversible adsorption of MS2 bacteriophages.

CDF type			**Adsorption**		**1st elution (pH 9.5) MS2 recovery**		**2nd elution (pH 5.5) MS2 recovery**		**Irreversible adsorption**	
		n*	Mean LRV	Std. Dev.	Mean LRV	%	Mean LRV	%	Mean LRV	Std. Dev.
Unfired	0.05% nAg	2	-0.05	0.01	0.04	-99.5	0.01	-12.8	-0.10	0.01
	5% nZVI	2	2.58	0.10	2.40	65.9	0.08	12.6	0.11	0.02
Fired	Blank	2	0.89	0.08	0.01	0.4	0.01	0.2	0.87	0.07
	0.05% nAg	2	0.92	0.11	0.01	0.3	0.00	0.1	0.91	0.10
	0.5% nZVI	2	0.46	0.03	0.04	4.6	0.01	1.0	0.42	0.03
	5% nZVI	2	0.95	0.04	0.02	0.5	0.01	0.3	0.92	0.04
	0.5% nZVI + 0.05% nAg	4	1.62	0.17	0.08	0.6	0.02	0.2	1.52	0.18

* Number of experiments.

5.1.1 MS2 bacteriophage sorption and inactivation by ground CDFs

First of all, some conclusions can be drawn with regard to the procedure of this batch experiment. The mean $LRV_{adsorption}$ of the unfired material containing 0.05% nAg shows that all initially added MS2 bacteriophages could be found back in the supernatant. This means that no viruses disappeared during the different actions of the experimental procedure. Hence, this CDF material functioned (unintentionally) as a control filter.
Furthermore, the mean $LRV_{recovered}$ for the first elution of the unfired CDF with 5% nZVI indicates that the chosen eluant (pH 9.5) functions well, because the majority of the phages were recovered.

Adsorption and inactivation by the unfired CDF material with 5% nZVI

At first sight the unfired material with 5% nZVI is well capable MS2 bacteriophages ($LRV_{adsorption}$ 2.58). Nevertheless, the low eventual $LRV_{irreversible}$ of 0.11 for this CDF material shows that a large part of the MS2 phages is not removed or inactivated by the media, but only temporarily sorbed to the surface.
First it was thought that the clay perhaps absorbed the test water containing MS2 phages, since clays can easily swell and take up water. However, if absorption by clay was indeed the reason for the sorption of MS2 phages it would be expected that the unfired material with 0.05% nAg also has a high $LRV_{adsorption}$, which is not the case. This indicates that the nZVI in the unfired material played an important role in adsorption of MS2 phages.

As explained in Chapter 2, under the pH conditions of the adsorption experiment (pH=7.2) nZVI is slightly positively charged and MS2 bacteriophages are negatively charged. Theoretically nZVI would thus attract phages during the adsorption experiment, as shown in Figure 5-1 (a). This is in accordance with the results of the unfired material with 5%: the unfired material with 5% nZVI has namely a high $LRV_{adsorption}$ of 2.58.
The pH of the first elution was 9.5. This means that theoretically the charge of the nZVI would have changed to a negative value during the first recovery experiment, leading to the repulsion of viruses, as shown in Figure 5-1 (b). This is also in line with the measurements: a large amount of viruses were recovered from the unfired material with 5% nZVI during the first recovery experiment ($LRV_{recovery}$ 2.40).
However, it must be kept in mind that this theory is based on several assumptions. Firstly, the pH_{PZC} of the material, which determines the charge of the material, is based on literature, the actual pH_{PZC} is not known. Secondly, the pH of the test water might have changed during the experiment[18], which also has an influence on the charge of the material.

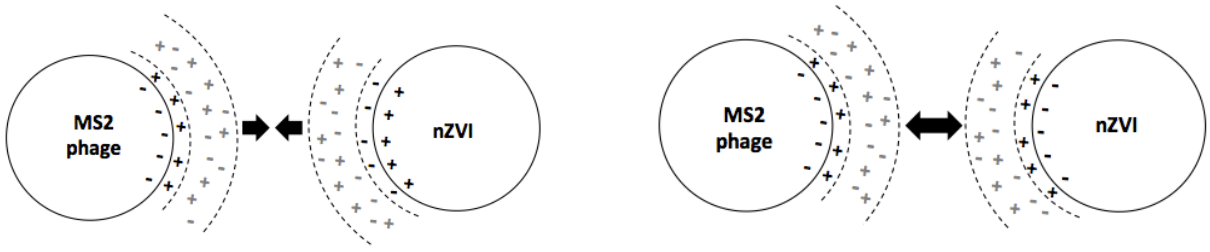

(a) Adsorption experiment: pH 7.2 (b) First elution: pH 9.5

Figure 5–1| Schematic illustration of (a) the potential attraction in the adsorption experiment with pH7.2 between the negatively charged MS2 bacteriophages and positively charged nZVI particles and of (b) the potential repulsion during the first elution with pH 9.5 between the negatively charge MS2 bacteriophages and the negatively charged nZVI.

In Table 5-1 it can be seen that a lot of infectious MS2 bacteriophages were recovered from the unfired material with 5% nZVI. It was expected that following the sorption of the MS2 phages by the unfired material with 5% nZVI, inactivation would take place. Kim et al. (2011) demonstrated namely a high LRV of 5 after 30 minutes of contact time with approximately 0.05 g/L nZVI, under aerated conditions. The nZVI content of 5% of the crushed CDF material in this study corresponds to a much higher concentration of 12.5 g/L nZVI. Besides, the high $LRV_{adsorption}$ for this CDF material suggests that direct interaction between the nZVI and MS2 phages could take place. It is therefore unclear why the adsorption of phages was not followed by inactivation.

[18] The pH was not measured during this experiment.

As explained in Chapter 2, released Fe(II) play a considerable role in the inactivation of MS2 bacteriophages. As can be seen in Table 5-2, a lot of iron leached of from the unfired clay material with 5% nZVI, so this can not be the reason why the phages were not inactivated. As indicated with ^{57}Mössbauer spectra, large part of the nZVI in the unfired CDFs is present as hematite. It might be that nZVI is better capable of inactivating viruses than hematite. Furthermore, might be that a higher oxygen concentration in the study of Kim et al. (2011) - they used open containers, while in this study closed tubes were used - played a role. Under deaerated conditions Kim et al. (2011) observed a LRV of 2.6 instead of 5. As discussed in Chapter 2, under aerated conditions ROS are namely formed, which contribute considerably to the virus inactivation by nZVI.

Table 5-2| Amount of metals that leached of from the ceramic material in the batch experiment with MS2 bacteriophages.

CDF		Ag (µg/L)	Fe (µg/L)
Unfired	0.05% nAg	107.2	
	5% nZVI		559
Fired	Blank*		149.2
	0.05% nAg	62	
	0.5% nZVI		132
	5% nZVI		213
	0.5% nZVI + 0.05% nAg	53.3	267.6

* The blank CDF was only tested for leached iron and not for silver.

In addition, inactivation of viruses by the unfired CDF with 5% nZVI was expected because Brown & Sobsey (2009) found high irreversible MS2 adsorption values by fired ceramic media amended with hematite ($LRV_{irreversible}$ 3.5). According to the ^{57}Fe Mössbauer spectra 85% of the iron in the unfired CDF with 5% nZVI is present as hematite and hence inactivation would be expected. However, Brown & Sobsey (2009) used fired ceramic material while in this case unfired material was used. As will be discussed later on, it was found that the fact whether the clay is fired or not has an influence on the adsorption and inactivation of MS2 bacteriophages.
In conclusion, it remains unclear why the unfired CDF with 5% nZVI is not able to inactivate the MS2 bacteriophages.

Adsorption and inactivation by the unfired CDF material with 0.05% nAg

The unfired CDF material with 0.05% nAg was not able to adsorb or inactivate the MS2 phages. nAg have typically a negative charge, which in theory would lead to repulsion of the negatively charged MS2 bacteriophages (El Badawy et al., 2010). This is in agreement with the results of this study: the mean $LRV_{adsorption}$ is -0.05.
The effect of nAg on virus inactivation is not yet clearly understood. Some studies report enhanced virus removal with the application of silver on CPFs while others reported a decrease in viral activity with silver amendment. It is however generally acknowledged that viruses are far less sensitive to nAg compared to bacteria. You et al. (2011) observed no MS2 bacteriophage inactivation after 1 h exposure to 5 mg/L nAg. This is in line with the results of this study. No MS2 bacteriophage inactivation was found for the unfired CDF with 0.05% nAg, which corresponds to 125 mg/L nAg.

Adsorption and inactivation by fired CDF material

In contrast to the unfired CDFs, the fired CDFs all had a $LRV_{irreversible}$ close to the $LRV_{adsorption}$. This indicates that almost all the MS2 bacteriophages were no longer infectious after sorption to these types of media. It is unlikely that the eluant was not able to recover the phages, as discussed previously.

The fired material with 5% nZVI, the fired material with 0.05% nAg and the fired blank material all had about the same performance: they all had a $LRV_{irreversible}$ of around 0.9. The fact the fired CDFs with 5% nZVI, 0.05% nAg and the blank CDFs had similar $LRV_{irreversible}$ suggests that not the added metals were responsible for the inactivation of the viruses but the ceramic material it self. It seems that after firing, the ceramic material becomes more effective against MS2 bacteriophages.

As mentioned earlier, Brown & Sobsey (2009) found increased sorption and inactivation of MS2 phages by fired ceramic media amended with iron oxide hydroxide and hematite, compared to unmodified material. Iron oxide hydroxides and hematite were also the main corrosion products of nZVI in the fired CDFs of this study, according to the XRD-analysis and ^{57}Fe Mössbauer spectroscopy results. The media of this study is thus similar to the media of Brown & Sobsey (2009): both media were fired and the iron phases were the same. Hence, it was expected that also in this study the fired CDF containing 5% nZVI would have higher MS2 adsorption and inactivation capacities compared to a fired blank CDF. However, Brown & Sobsey (2009) tested ceramic material with 16.7% iron oxides, while in this study only 5% nZVI was added to the clay. Furthermore, it must be noted that the media with magnetite Fe_3O_4 - another possible corrosion product of nZVI, which may develop from hematite that oxidizes further in water - did not show improved adsorbed sorption and inactivation in the study of Brown & Sobsey (2009).

The reason that the added metals in the fired ceramic material had no effect on MS2 bacteriophages might be that the metals were enclosed by the ceramic structure and were therefore not able to interact with the viruses. As discussed in Chapter 2, several reactions take place during the firing of ceramics. During firing the clay decomposes and binds together as described by the following equation (Breuer, 2012):

$$[clay]–OH + HO–[clay] \rightarrow [clay]–O–[clay] + H2O_{(g)} \quad (5.4)$$

Although, there is limited literature available on the reaction between clay and metals during firing, one could image that a linkage between the clay and iron oxides is also possible. This reaction between silica and ferrous forms was also reported by Stolboushkin et al. (2013), who studied the ceramic matrix composite produced from iron-ore. During the clay decomposition process and the vitrification process the metal particles probably become enclosed in the ceramic structure, which is illustrated in Figure 5-2. This results in less available surfaces sites for adsorption and inactivation, also when the material is crushed up.

The considerable lower $LRV_{adsorption}$ of the fired material with 5% nZVI compared to the unfired material with 5% nZVI confirms this theory. Also the difference between leached amount of iron between the fired and unfired CDF supports this theory. The leached amount of iron of the fired CDF is considerably lower than of the unfired CDF with 5% nZVI, which suggests that part of the iron in the fired CDF is somehow connected to the ceramic structure (see Table 5-2). However, other factors might also contribute to the difference is phage sorption between the unfired and fired material with

5% nZVI. It might namely be that the electrostatic attraction of unfired nZVI is stronger than of fired nZVI, resulting a higher $LRV_{adsorption}$. In the fired CDF all the iron is present as hematite, which has a lower pH_{PZC} of 7.5 than nZVI (pH_{PZ} 7.8), which results in less virus attraction (Plaza et al. 2002). However, the difference in pH_{PZC} is really small.

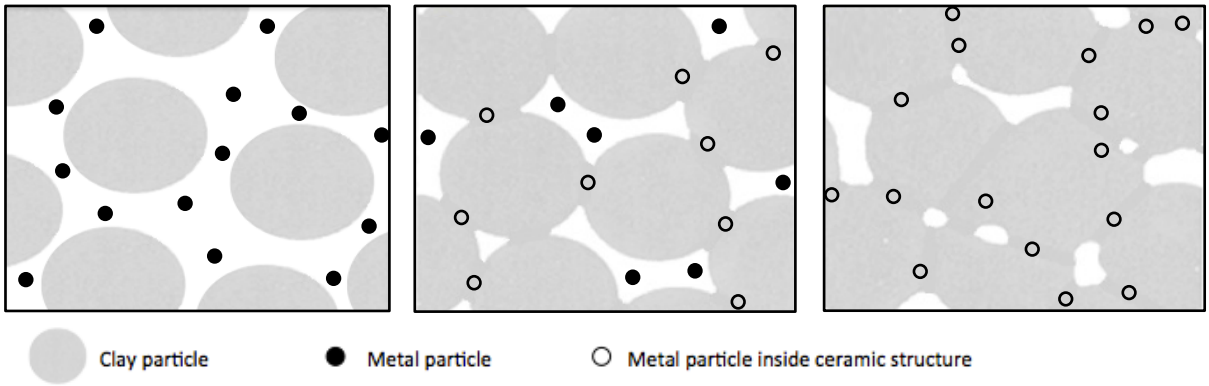

Figure 5–2| The development of the ceramic structure during vitrification: (a) loose clay particles and loose metal particles, (b) initial stage of vitrification and (c) intermediate stage of vitrification.

Adsorption and inactivation by the fired CDF material with 0.5% nZVI + 0.05% nAg

A last interesting result is that although the fired CDF containing 0.5% nZVI has a $LRV_{irreversible}$ of 0.42 and the fired CDF containing 0.05% nAg has a $LRV_{irreversible}$ of 0.91, the CDF with the combination of nZVI and nAg achieves a $LRV_{irreversible}$ of 1.52. The $LRV_{irreversible}$ 1.52 of the combination CDF is still low, but with different concentrations even higher LRVs might be possible.

Additive or even synergistic effects of metal combinations against microbes are reported before. For example, Lin et al. (1996) observed synergisms of copper and silver ions in the inactivation of the bacteria *Legionella pneumophila* at higher concentrations of copper and silver ions (0.04/0.04 mg/L) and a additive effect at lower concentrations (0.02/0.02 mg/L).

5.1.2 Conclusions on sorption and inactivation of MS2 bacteriophages

All types of CDFs have a lower $LRV_{irreversible}$ than 3 after 30 minutes of contact time, which corresponds to the average residence time of raw water in CPFs. Although the results of this batch experiment cannot directly be translated to the effectiveness of an actual CDF, the results give a first indication that the requirement for virus removal of the WHO to be a protective HWTS (LRV ≥ 3) can probably not be met.

The crushed unfired CDF with 5% nZVI showed a strong attraction of MS2 bacteriophages, but was not able to inactivate them. It might be that hematite, which is the main iron phase in the unfired CDFs with 5% nZVI, as indicated by the ^{57}Fe Mössbauer spectra, is able to adsorb viruses but is less able to inactivate viruses compared to nZVI.

It was expected that the fired CDF containing 5% nZVI would have higher MS2 adsorption and inactivation capacities compared to a fired blank CDF, since Brown & Sobsey (2009) found increased sorption and inactivation of MS2 phages by fired ceramic media amended with iron oxide hydroxide and hematite, which also the main corrosion products of nZVI in the fired CDFs of this study according to the XRD-analysis and ^{57}Fe Mössbauer spectroscopy.

The reason that the added metals in the fired ceramic material had no effect on MS2 bacteriophages might be that the metals were enclosed by the ceramic structure and were therefore not able to

interact with the viruses. This explains however not the differences in findings between this study and the study by Brown & Sobsey (2009).
Lastly, it was found that the combination of nZVI and nAg leads to enhanced virus removal compared to the CDFs with solely nAg or nZVI.

In order to better understand the adsorption of viruses onto different media and to give reliable explanations on it, it is advise for future research to determine the actual pH_{PZC} of the used media. In this study the explanations are only based or pH_{PZC} found in literature, while the exact values are not known. Furthermore, the pH of the test water should be measured during the experiment. The pH does not only influence the charge of the materials, it has also a direct effect on the viability of viruses. Moreover, it is remarked that every virus has its own IEP and therefore in future research other viruses than MS2 bacteriophages should also be studied.

5.2 Arsenic batch experiments

In this section the results of the arsenic sorption experiments are presented. The results are discussed by comparing the As(III) removal capacity of (i) solely nZVI particles versus solely CIM particles, (ii) blank fired CDFs versus fired CDFs containing nZVI or CIM and (iii) unfired CDFs versus unfired CDFs containing nZVI or CIM.

5.2.1 As(III) removal capacities of nZVI and CIM

First of all, the kinetics of the removal of As(III) by the two types of pure iron (nZVI and CIM) were investigated. The kinetic experiments with crushed ceramic material of the CDFs with 5% iron were performed at a concentration of 50 g/L. This iron content of 5% corresponds in the batch experiments to an iron concentration of 2.5 g/L. In order to compare the experiments with ceramic material and the experiments with solely iron, the experiments with solely iron were initially performed with 2.5 g/L iron.
The nZVI suspension consists of 20% nZVI and 80% water; therefore for the nZVI suspension a concentration of 12.5 g/L was used. With this concentration of nZVI all the arsenic of the initial 200 µg/L As(III) was removed within 5 minutes of contact time (see Figure 5-3).

Iron concentration

To obtain a clear kinetic arsenic adsorption curve an appropriate iron concentration was determined by means of initial As(III) adsorption experiments conducted with different amounts of nZVI. The results were analysed with anodic stripping voltammetry using the scTRACE Gold sensor (Metrohm, Switzerland). The detection limit of the instrument is 0.3 µm/L for As(III).
Satisfying results for As(III) removal were found at a concentration 0.3 g/L nZVI suspension, corresponding to 0.06 g/L nZVI. It was chosen to perform the CIM batch experiment with the same concentration as nZVI to be able to 'compare' the results. Hence, a concentration of 0.06 g/L CIM was used.

As(III) removal by solely nZVI and CIM

Figure 5-3 shows how much arsenic is removed with the addition of 2.5 g/L nZVI, 0.06 g/L nZVI and 0.06 g/L CIM.

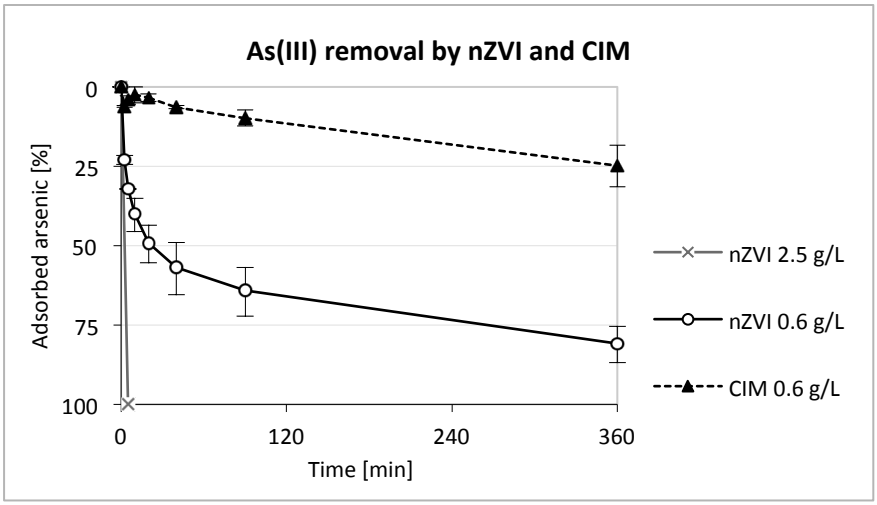

Figure 5–3| The adsorbed amount of arsenic in time with addition of 2.5 g/L nZVI, 0.06 g/L nZVI and 0.06 g/L CIM.

It must be noted that the comparisons that is made here is a comparison between two different iron products, nZVI suspension and CIM powder, and not between the iron contents of these products. CIM is not pure iron; it consists for more than 88 wt.% of iron oxide phases according to XRD-results. The compounds that were found in the CIM are Magnetite (Fe_3O_4), Hematite (Fe_2O_3), Wustite (FeO), Lipscombite ($Fe_3(PO_4)_2(OH)_2$), Iron (Fe) and Iron Carbonate Hydroxide ($Fe_6(OH)_{12}(CO_3)$). In addition, Si and Al compounds were detected. Therefore the specific iron mass of CIM is lower than that of nZVI. Although, according to the supplier NanoIron S.R.O. (Rajhrad, Czech Republic) also the nZVI suspension might contain some Magnetite (2-6%) and Carbon (0-1%). To confirm this, XRD-analysis was performed with the nZVI suspension. It indeed appeared that the nZVI suspension consists of two components: Iron (Fe) and Magnetite (Fe_3O_4).

It is clear that the arsenic adsorption capacity of nZVI is faster compared to CIM, as expected. The nZVI ensured an arsenic adsorption of more than 80% in 6 h of contact time, while the CIM only adsorbed around 20% of the arsenic during the experiment. The reaction with 2.5 g/L nZVI shows that the WHO guideline for arsenic of 10 µg/L can easily be met in a short contact time with the use of enough nZVI.

Several studies have shown that nanoscale ZVI exhibits higher arsenic adsorption rates compared to micron scale ZVI. For example, Kanel et al., (2005) reported 1-3 orders of magnitude higher As(III) adsorption rates constants by nZVI, studied by them, than by ZVI micro particles, examined by Su & Puls, (2001a).
The faster As(III) removal of nZVI compared to CIM can first of all be explained by the smaller particle size of nZVI particles and thus the larger specific surface area providing more reaction sites. According to the producer NanoIron S.R.O. (Rajhrad, Czech Republic), the average particle size of the nZVI is smaller than 50 nm, and the specific surface is more than $25 m^2/g$. The CIM particles were passed through a 40-mesh sieve and are hence smaller than 425 µm.
Another explanation for the higher adsorption rates of nZVI than CIM is the higher reactivity of nano particles compared to micro particles. This higher reactivity might be because nanoparticles exhibit a higher inherent reactivity. Furthermore, nanoparticles might have a more dense surface of reactive surfaces sites (Nurmi et al., 2005).

In addition, the iron content of the products probably influences the arsenic adsorption capacity. Since nZVI consist of more ZVI than CIM, it therefore has a greater arsenic adsorption capacity than CIM.

Capacity of nZVI to remove As(III) and As(V)

The removal of arsenic by nZVI was further studied by performing kinetic batch experiments with both As(III) and As(V) as initial solution. Figure 5-4 shows how much arsenic is removed in time with the addition of 0.3 g/L nZVI aqueous dispersion, corresponding to 0.06 g/L nZVI, with As(III) as initial solution and As(V) as initial solution.

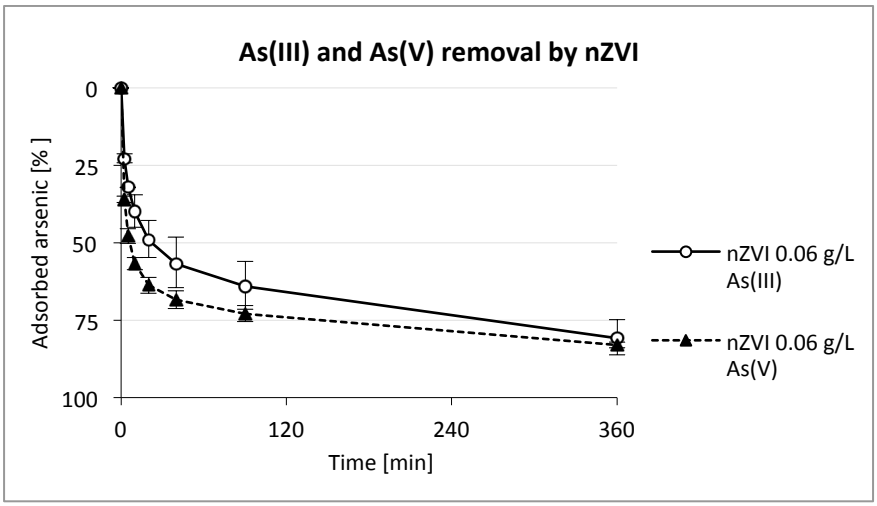

Figure 5–4|The adsorbed amount of arsenic in time by the addition of 0.06 g/L nZVI with As(III) as initial solution versus As(V) as initial solution.

The experimental data of the As(III) and As(V) adsorption by nZVI was evaluated using a pseudo-first-order kinetics model (equation 5.5) and a pseudo-second-order kinetics model (equation 5.6).

$$\frac{dq_t}{dt} = k_1(q_e - q_t) \tag{5.5}$$

$$\frac{dq_t}{dt} = k_2(q_e - q_t)^2 \tag{5.6}$$

where q_t (mg/g) and q_e (mg/g) are the amounts of arsenic adsorbed at contact time and at equilibrium time, respectively, and k_1 (1/min) and k_2 (g/(mg·min)) are the rate constants of the pseudo-first-order model and of the pseudo-second-order model, respectively. These equations can be linearized, which results in the following equations:

$$ln(q_e - q_t) = ln(q_e) - k_1 t \tag{5.7}$$

$$\frac{t}{q_t} = \frac{1}{k_2 q_e^2} + \frac{t}{q_e} \tag{5.8}$$

Since, the equilibrium concentrations were not measured in this study's experiments, they were estimated. This was done by extrapolation of the experimental data. To obtain the parameters of the pseudo-first-order and pseudo-second-order model, a linear regression analysis was performed by plotting $ln(q_e\text{-}q_t)$ and t/q_t, respectively, versus the time t. Linear regression was also used to

determine the best-fitted kinetic model. In Table 5-3, the kinetic parameters of the pseudo-first-order and the pseudo-second-order rate model for removal of As(III) and As(V) by nZVI are shown.

Table 5-3| Kinetic parameters of the pseudo-first-order and the pseudo-second-order rate model for adsorption of As(III) and As(V) on nZVI.

		Pseudo-first-order		Pseudo-second-order		
	Estimated q_e [mg/g]	k_1 [1/min]	R^2 [-]	k_2 [g/(mg·min)]	q_e [mg/g]	R^2 [-]
Removal of As(III)	2.78	0.0059	0.877	0.035	2.61	0.996
Removal of As(V)	2.83	0.0086	0.854	0.066	2.79	0.999

The estimated values of the equilibrium adsorption capacity are similar to the computed values. Both kinetic models were found to describe the obtained data adequately. The pseudo-second-order models have higher regression coefficient values compared to the pseudo-first-order models, which means that the pseudo-second-order model gives the best indication of the adsorption kinetics of both As(III) and As(V) on nZVI. This is in line with the findings of Mosaferi et al. (2014) who found that the adsorption of arsenic by nZVI stabilized with starch could best be described by the pseudo-second-order model. In addition, Shafiquzzam et al. (2013) also reported that arsenic adsorption by their manufactured iron mixed ceramic pellets best fitted the pseudo-second-order model.

The pseudo-second-order rate constants and Figure 5-4 illustrate that the adsorption rate of As(V) is greater than that of As(III). However, the difference in arsenic adsorption rate is small.
There are two major processes that take place by nZVI: oxidation of As(III) to As(V) and adsorption of As(III) and As(V). The experiments in this study are performed at around neutral pH and under relatively oxidising conditions. Hence, As(III) is present as $H_3AsO_3^0$ and As(V) mainly as $HAsO_4^{2-}$ and to a less extends as $H_2AsO_4^-$.
As explained in Chapter 2, under the experimental conditions of this study (pH around neutral) the nZVI is positively charged. Hence, the adsorption of the As(V) forms $H_2AsO_4^-$ or $HAsO_4^2$ onto ZVI particles might be enhanced by Coulombic attraction, while the adsorption of non-ionized As(III) happens only through a chemical reaction at neutral pH. This is a potential explanation for the higher adsorption rate of As(V).
Because of the better As(V) adsorption at around neutral pH conditions, As(III) is potentially first oxidized to As(V) before it is adsorbed. The small difference between the As adsorption rate with As(III) as initial solution and As(V) as initial solution indicates that the oxidation from As(III) to As(V) is effective and that the adsorption is the limiting factor.

5.2.2 As(III) removal capacities of fired CDF material

After the batch experiments with solely iron, batch experiments were conducted with crushed material of fired CDFs. For these experiments a concentration of 50 g/L was used, which was based on the maximum amount of available material. The arsenic removal percentages in time with addition of 50 g/L ground material of a blank CDF, a CDF with 5% nZVI and a CDF with 5% CIM are presented in Figure 5-5.

The manufactured CDFs have a contact time in the range of 12-37 minutes. In spite of the large quantity of material that was added to the test water (50 g/L), only a few per cent As(III) is removed by all three types of CDFs after this contact time. Although the results of this batch experiment cannot directly be translated to the effectiveness of an actual CDF, the results suggest that the guideline for arsenic of maximum 10 µg/L set by the WHO will probably not be reached.

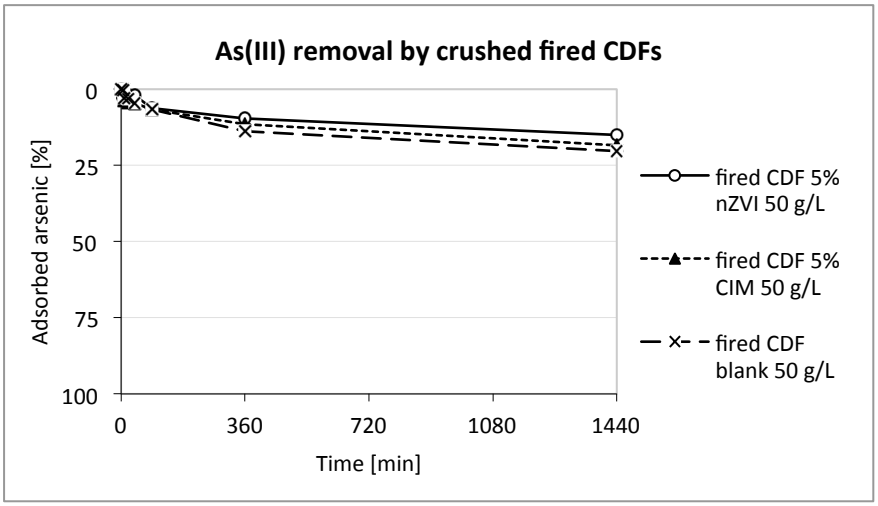

Figure 5–5| The adsorbed amount of arsenic in time with addition of 50 g/L ground material of a blank fired CDF, of a fired CDF containing 5% nZVI and of a fired CDF containing 5% CIM.

The results show that As(III) is also removed by crushed ceramic material without metals. This is as expected as mentioned in the Chapter 2.

There is no considerable difference between the sorption capacities of the ground material of the blank CDF and the CDFs with ZVI incorporated. This is noteworthy since the CDFs with nZVI contain 5% nZVI, which corresponds to a concentration of 2.5 g/L nZVI, and when solely 2.5 g/L nZVI was added to the As(III) solution no arsenic was measured after only 5 minutes of contact time (see Figure 5-3). This large difference in arsenic sorption by the same amount nZVI suggests that due to the incorporation into the clay before firing, the nZVI gets less effective against arsenic. This is studied more in detail in the next paragraph in which the As(III) removal by crushed material of unfired CDFs was tested.

5.2.3 As(III) removal capacities of unfired CDF material

Since the crushed material of fired CDFs with nZVI and with CIM showed slow arsenic removal rates, the effectiveness of unfired CDFs was also studied. In this way, insight was gained on the effect of the firing process. The results of the batch experiments with crushed material of a fired CDF versus an unfired CDF containing nZVI and CIM are depicted in Figure 5-6.

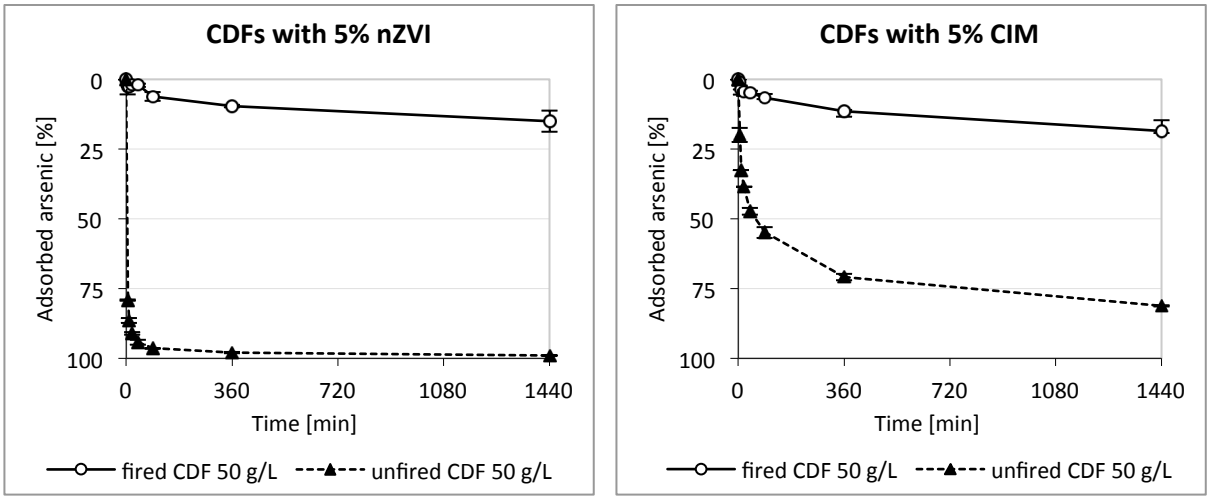

Figure 5–6| The adsorbed amount of arsenic in time with addition of 50 g/L ground material of (a) a fired CDF containing 5% nZVI versus an unfired CDF containing 5% nZVI and of (b) a fired CDF containing 5% CIM versus a unfired CDF containing 5% CIM.

It can be seen that the material of the unfired CDFs removes As(III) much faster than the material of the fired CDFs. The fired CDFs remove only a few per cent of As(III) in 12-37 minutes, which is the contact time of the manufactured CDFs, whereas the unfired CDFs remove approximately 90% of As(III) in the same contact time. This results in a final concentration arsenic concentration of approximately 20 µg/L, which is on the same order of magnitude as the WHO maximum of 10 µg/L. However, it must be kept in mind that these results cannot directly be translated to the performance of an actual CDF.

The large difference between As(III) removal by unfired and fired CDFs amended with ZVI implies that the firing process causes the ZVI to lose its arsenic adsorption capacities. There are several reactions that take place during firing that might influence the reactivity of the ZVI.
First of all, oxidation takes place, which was confirmed by the XRD and ^{57}Fe Mössbauer spectroscopy results, reported in Chapter 4. As explained before, arsenic is adsorbed onto the oxide(hydr)oxides, which are formed when the ZVI oxidizes. The firing process causes intensive oxidation, which might result in the formation of other corrosion products than when ZVI corrodes due to water (with oxygen). According to the ^{57}Fe Mössbauer spectroscopy results, all nZVI corroded into hematite, while in water, the main corrosion products of ZVI are oxyhydroxides. Moreover, the corrosion of ZVI in water leads to new-formed adsorption sites. When the ZVI is already totally oxidized during firing, it might be that this process not happens.
Different ZVI corrosion products have also a different ability to adsorb arsenic. Mamindy-Pajany et al. (2011) observed for example that ZVI exhibited the greatest adsorption of arsenic, secondly magnetite, then hematite and lastly goethite. Further, Manning et al. (2002) reported that goethite, lepidocrocite, and maghemite adsorbed As(III) within 24 h of contact time, while magnetite and hematite did not. Furthermore, Manning et al. (2002) found that As(III) was not oxidized to As(V) by goethite or lepidocrocite. The inability oxidizing As(III) to As(V) might also lead to slower arsenic removal, since As(V) is easier removed than As(III),as explained earlier.
Secondly, it might be possible that during the firing process a linkage between the ZVI and clay develops, as was explained in the previous section about the batch experiments with MS2 bacteriophages (see Figure 5-2). This can lead to less available surface sites for the adsorption of

arsenic. In addition, the ^{57}Fe Mössbauer spectra identified a sintered form of hematite. This could also result in less available adsorption sites for arsenic.

As explained above the difference in As(III) by the unfired and fired CDF material might be due to the differences in iron phases or because the differences in the iron-clay interactions, which leads to differences in available surface sites for adsorption. However, the clay/ceramic material it self is also different between the unfired and fired material. This might also be a reason for the differences in arsenic removal, especially because the sorbent:water ratio was high (50 g/L).
If the As(III) removal of the unfired material was only assigned to sorption by the clay, it would be expected that the kinetics curves of the unfired CDF with 5% nZVI and the unfired CDF with 5% CIM would be similar, which is not the case. The contribution of the unfired clay on the removal of As(III) was further investigated by performing an extra kinetic batch adsorption experiment with the material of an unfired CDF containing 0.05% nZVI, under identical experimental conditions as the other batch experiments. The CDF with 0.05% nZVI was chosen since there was no unfired blank CDF available for this control experiment.
The sorbed amount of arsenic in time by the unfired CDF with 0.05% nZVI is shown in Figure 5-7, together with the sorbed amount of arsenic by the unfired CDF with 5% nZVI. These results confirm that not only the clay is responsible for the As(III) removal, but also the nZVI that was incorporated in the clay mixture. Yet, the As(III) removal due to clay is significant. Since the nZVI content of unfired CDF with 0.05% nZVI is really low, it can be assumed that almost all the As(III) that is removed by the unfired CDF with 0.05% nZVI is due to the clay. Hence, the amount of arsenic that is adsorbed by the unfired CDF with 0.05% nZVI can be seen as the contribution of the clay, as indicated in Figure 5-7.

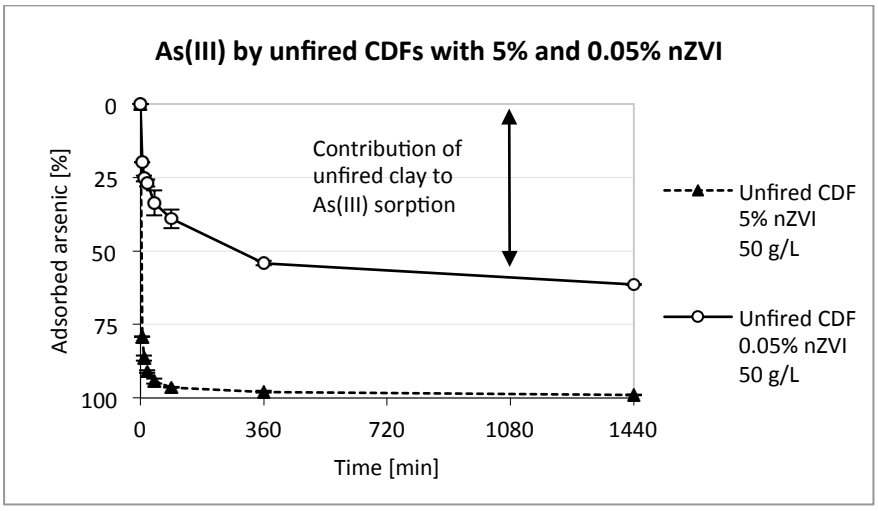

Figure 5–7| The adsorbed amount arsenic in time with addition of 50 g/L ground material of an unfired CDF containing 5% nZVI versus an unfired CDF containing 0.05% nZVI.

There is one other difference between the experiments with unfired and fired crushed CDFs that could have had an influence on the arsenic adsorption: the pH value. As can be seen in Figure 5-8 the fired ceramic material caused the pH to increase. With the unfired CDFs the pH did only increase slightly. As explained in Chapter 2, the pH has an influence on the surface charge of minerals and on which arsenic species are prevalent. The difference in pH between the experiments with unfired and fired CDFs is however small, so the effect on As(III) removal probably as well.

The increase in alkalinity due to a fired ceramic filter was also noticed by (Van Halem, 2006). Van Halem (2006) explained this increase of pH by means of a diffusion model for concrete materials. It is however unclear why no OH^- is released from unfired clay.

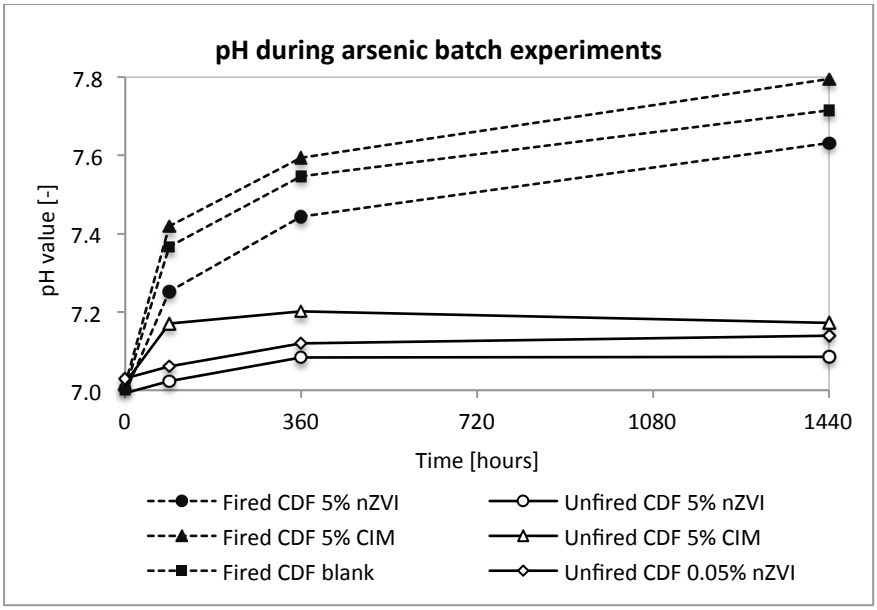

Figure 5–8| Average pH-values during the arsenic batch experiments with fired and unfired CDFs.

One last observation is that also when nZVI is incorporated in a CDF that is not fired, the ZVI becomes less effective against arsenic. The arsenic adsorption curves for the addition 0.06 g/L nZVI and 50 g/L clay containing 5% nZVI do not deviate a lot from each other. This while the amount of iron is around 40 times more for when 50 g/L of clay containing 5% nZVI (2.5 g/L nZVI) is added than when 0.06 g nZVI/L is added. Both curves are shown in Figure 5-9.

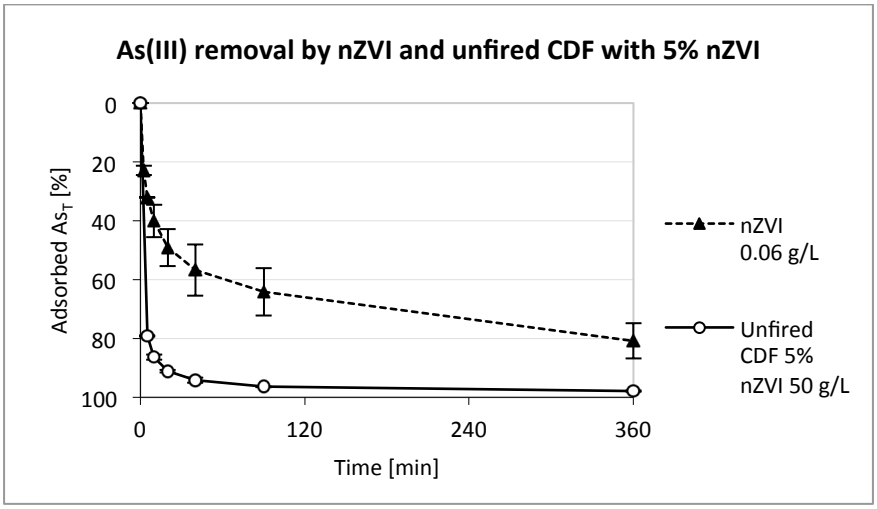

Figure 5–9| The adsorbed amount of total As in time with addition of 50 g/L ground material of an unfired CDF containing 5% nZVI versus 0.06 g/L of solely nZVI.

When the nZVI is added to the clay mixture and the clay mixture is pressed into a disk, the nZVI will probably stick to the clay. As a consequence of incorporating the nZVI in clay, there is thus probably less adsorption surface available for arsenic. Another, reason for this efficiency loss might be that part of the nZVI in the unfired CDF was oxidized. The results of the ^{57}Fe Mössbauer spectroscopy

analysis revealed that also in the unfired CDF a large part of the nZVI was oxidized to hematite. For the experiments with solely nZVI, the nZVI dispersion product was opened just before use to minimize the opportunity of oxidation. As discussed earlier, hematite adsorbs arsenic slower compared to nZVI.

5.2.4 Conclusions arsenic batch experiments

From the arsenic adsorption batch studies, it can first of all be concluded that ZVI is an effective arsenic adsorbent. This is in line with the current literature. Especially ZVI at nanoscale is able to rapidly adsorb arsenic, due to the small particle size and thus the larger specific surface area compared to CIM.

It was found however, that when ZVI is incorporated in clay and subsequently fired, the material becomes less effective. There was no considerable difference between the arsenic adsorption of ground material of a blank CDF and of a CDF with 5% ZVI incorporated. This while the nZVI content of 5% corresponds to a concentration of 2.5 g/L nZVI, and when solely 2.5 g/L nZVI was added to the As(III) solution no arsenic was measured after only 5 minutes of contact time.
Further research with unfired CDFs showed that unfired CDFs containing 5% nZVI or CIM remove As(III) much faster than fired CDFs: unfired material with 5% nZVI was able to remove approximately 90% of the initial 200 µg/L As(III) in 30 minutes of contact time, while fired material with 5% nZVI only removed a few per cent As(III). The results showed that both the clay of the unfired CDF material and the added nZVI contribute to the faster As(III) removal of the unfired material compared to the fired ceramic material.

There are several reactions that take place during firing that might influence the ability of ZVI to adsorb arsenic. First of all, oxidation takes place. According to the ^{57}Fe Mössbauer spectroscopy results, all nZVI corrodes into hematite, while in water the main corrosion products of ZVI are oxyhydroxides. Different ZVI corrosion products also have a different capacity to adsorb arsenic. Secondly, it is likely that during the firing process a link between the ZVI and clay develops, which leads to less available surface area for arsenic adsorption.

The results from these batch experiments suggest that it is not recommended to incorporate ZVI in the clay mixture before firing. The results do show that ZVI, especially at nanoscale, has potential for the removal of arsenic in HWTS – so incorporation in a different setting (e.g., unfired coating or amendment).

6 Filter experiments

After the batch experiments, several filter experiments were performed to test whether the in Chapter 1 established requirements for CPFs are potentially possible to fulfil. First, the removal and inactivation of bacteria and viruses by the CDFs was quantified. In section one of this chapter those results are presented. Subsequently, the amount of metals that leached out of the CDFs is discussed and thereafter the inactivation of *E.* coli and MS2 bacteriophages due to storage in the receptacle is elaborated. The final section deals with the results of arsenic breakthrough experiments. These experiments were performed to estimate the life span and thus the sustainability of the CDFs, in terms of arsenic removal.

6.1 Removal and inactivation of *E. coli* and MS2 bacteriophages with CDFs

6.1.1 LRVs of *E. coli* by CDFs

The *E. coli* removal by the CDFs was evaluated by means of LRVs. The LRVs were calculated with equation 6.1. For the concentration calculations of the samples, the average of the duplicate plate counts was used. In case several dilutions were analysed the weighted average concentration of these dilutions was calculated.

$$LRV = log_{10}(concentration\ influent) - log_{10}(concentration\ effluent) \quad (6.1)$$

The *E. coli* LRVs for the samples that were taken directly from the CDF are shown in Figure 6-1. In some of the *E. coli* analyses a detection limit was reached, which means that zero CFUs were detected. Therefor, for those cases it was not possible to report the actual LRV, but only the detection limit value by calculating the LRV with a plate count of one instead of zero. The cases, for which there was a detection limit for both duplicates, are indicated in the graph with larger than signs (>). In Appendix IV an overview can be found of all the LRVs, the detection limits are also indicated. Also the pH values, which were measured overnight from the receptacle, are presented in Appendix IV.

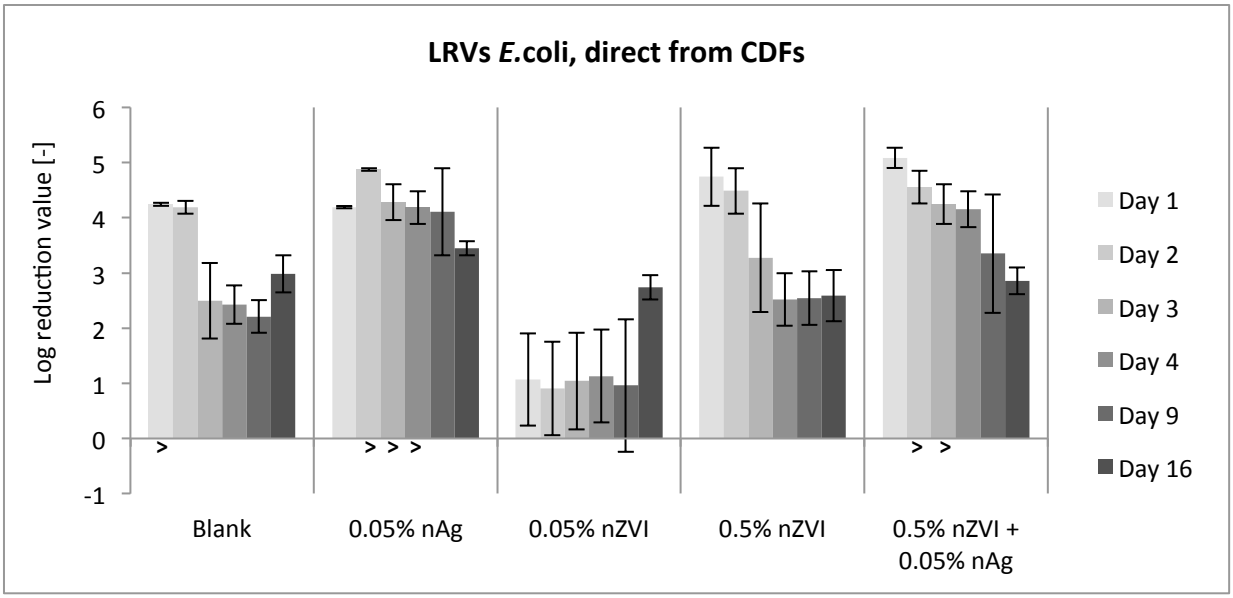

Figure 6–1| LRVs for *E. coli* of samples that were taken directly from the CDFs. The larger than signs (>) indicate the cases where there was a detection limit for both duplicates.

It can be seen from Figure 6-1 that the performance of the CDFs in most cases decreased over time. The reason for the higher LRVs on the first two test days, except for the CDF with 0.05% nZVI, is probably that not all pores were yet connected with each other, which resulted in removal of *E. coli*. This is also in accordance with the lower discharge of the CDFs in the first week.

To get an indication of the overall *E. coli* removal per CDF, total average LRVs were calculated by combining all the influent and all the effluent *E. coli* concentrations of the filter experiment. The calculated average LRVs are depicted in Table 6-1, together with the standard deviations σ.

Table 6-1| Average, minimum and maximum LRVs per CDF type, established by combining all the influent *E. coli* concentrations and all the effluent *E. coli* concentrations, together with the standard deviations.

CDF	LRV_{mean}	LRV_{min}	LRV_{max}	σ
Blank	2.61	1.81	4.30	0.91
0.05% nAg	4.28	3.31	4.90	0.56
0.05% nZVI	0.75	-0.24	2.96	1.07
0.5% nZVI	3.28	2.04	5.27	1.10
0.5% nZVI + 0.05% nAg	4.08	2.28	5.27	0.90

The required LRV for *E. coli* to be a protective HWTS is more than two, according to the WHO. As mentioned earlier, most currently produced CPFs reach this value. This is also the case for the CDFs manufactured in this study, except for the CDF with 0.05% nZVI.

For *E. coli* removal it appeared that a metal amendment is not necessary to obtain the required LRV of two. The high LRV for the blank CDF shows that bacteria were well removed by physical removal mechanisms. Although most pores are probably larger than *E. coli* (0.5 x 1.0-3.0 µm) - van Halem et al. (2007) measured an effective pore size of 40 µm for CPFs - *E. coli* could still be well removed by removal processes as diffusion, adsorption and sedimentation. Due to the high tortuosity of ceramic filters these removal processes can more easily take place (van Halem et al., 2007). In Figure 6-2 an illustration is given of ceramic material with a low and high tortuosity. In addition, with a high

tortuosity it is more likely that *E. coli* will encounter a smaller pore and hence is removed due to size exclusion.

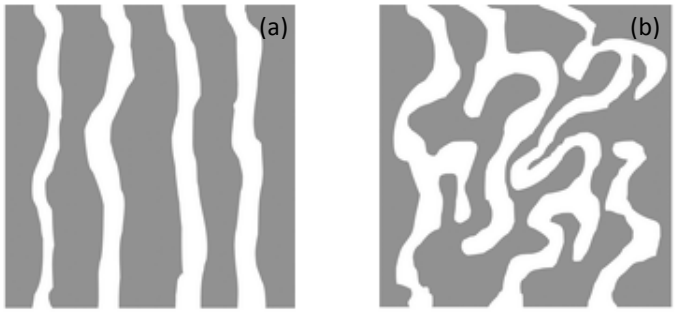

Figure 6–2| Illustration of the pores in ceramic filter material: (a) ceramic material with a low tortuosity and (b) ceramic material with a high tortuosity (adapted from: Peckham et al., 2007)

It is surprising that the LRV for the CDF with 0.05% nZVI is so much lower than the LRV of the blank CDF. The flow rate of the CDF with 0.05% nZVI is considerably higher than the flow rate of the blank CDF, which might indicate that the there were some larger pores or cracks present in the 0.05% nZVI CDF through which the *E. coli* could easily pass. It should be noted that there are a lot of factors that influence the characteristics of a CDF or CPF, and thus its ability to remove bacteria. As already mentioned before the characteristics of the clay, the characteristics of the burn-out material, the mixing procedure and the heating process can slightly vary per ceramic, resulting in different performances.

Furthermore, the CDF with 0.05% nAg performs considerably better than the blank CDF. This is in accordance with the findings of Oyanedel-Craver & Smith (2008), Bielefeldt et al. (2009) and Van Halem et al. (2007), who tested ceramic filters with colloidal silver application. On the contrary, Brown & Sobsey (2010) found no significant difference between CPFs with and without silver nitrate application (Brown & Sobsey, 2010).
In Chapter 2, the inactivation mechanisms of bacteria by nAg are explained. It is still an issue of debate whether the primarily killing mechanism of bacteria is the contact of bacteria with the metallic surface or the cell damaging via dissolved metal ions. Mathews et al. (2013) performed experiments with copper surfaces covered with contact arrays, made from inert polymer grids, to prevent direct bacterial-metal contact. No significant killing of *Enterococcus hirae* bacteria was observed, which implies that inactivation was restrained by the inability of bacteria to make contact with the copper surface. It was hypothesized by Mathews et al., (2013) that silver inactivates bacteria in the same way as copper. This could explain why Brown & Sobsey (2010) observed the same *E. coli* LRVs for filters with and without silver nitrate. Nevertheless, Van der Laan et al. (2014) found that with a longer storage time *E. coli* removal was enhanced by the silver ions applied on the filter. Hence, silver ions can also play a major role in bacteria inactivation.
Bielefeldt et al. (2009) reported that the removal efficiency of *E. coli* by CPFs impregnated with silver decreased in time. A limitation of this study is that only a short-term experiment was performed, hence is not known whether the efficiency of the CDFs will decrease more over time.

The results show that the CDFs containing nAg were better capable of removing *E. coli* compared to the CDFs with nZVI. CDFs with 0.05% nAg have a LRV of 4.28, while with a ten times higher iron

concentration the LRV is only 3.28. In addition, for the CDFs with nAg a detection limit often occurred, indicating potentially even better removal performances.
As mentioned above several studies have shown that silver has a positive effect on the inactivation of bacteria. Much less research has be done on inactivation of bacteria by ZVI. Lee et al. (2008) compared the bactericidal activity of nAg (15~20 nm) and nZVI (<100 nm) on *E. coli*. Under air saturated conditions nAg showed higher *E. coli* inactivation (0.41 log inactivation/(mg/(L·h))) than nZVI (0.029 log inactivation/(mg/(L·h))). Furthermore, the results of Lee et al. (2008) indicated that due to oxidative corrosion, nZVI becomes less effect against bacteria. Magnetite (9 mg/L) for instance did not significantly in activated *E. coli* after 1 h of contact time.

Lastly, it should be noted that, except for the CDF with 0.05% nZVI, even with flow rates much higher than the desired 1-3 L/h, sufficient LRVs for bacteria were obtained. This is in line with an unpublished study by Bloem (2008), which showed equal *E. coli* removal efficiencies for ceramic filters with an initial discharge of 2 L/h and an initial discharge of up to 6 L/h. This is an important finding since Van Halem et al. (2007) reported that the main deficiency of a CPF is the low filter discharge. Van Halem et al. found that the discharge decreases in time and scrubbing of the CPF cannot fully prevent the reduction in flow rate over time.

6.1.2 LRVs of MS2-bacteriophages by CDFs

In Figure 6-3 the LRVs for the removal of MS2 bacteriophages by the CDFs are shown. Also the average LRVs per CDF type were calculated, as shown in Table 6-2. In Appendix IV an overview can be found of all the LRVs.

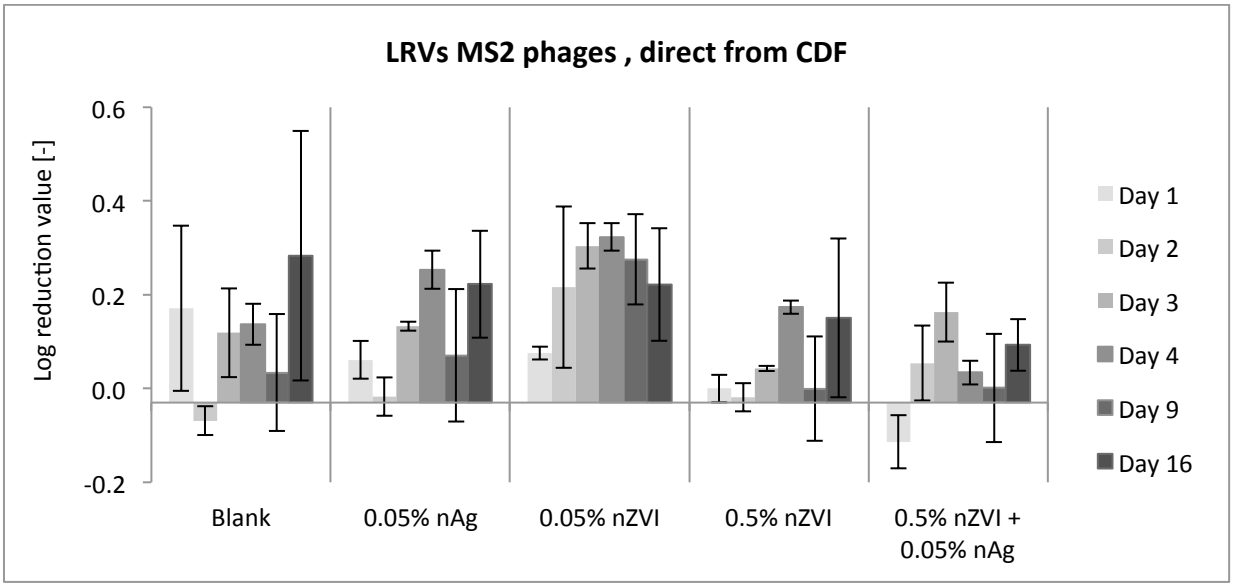

Figure 6–3| LRVs for MS2 bacteriophages of samples that were taken directly from the CDFs.

Table 6-2| Average, minimum and maximum LRVs per CDF type, established by combining all the influent MS2 concentrations and all the effluent MS2 concentrations, together with the standard deviations.

CDF	LRV_{mean}	LRV_{min}	LRV_{max}	σ
Blank	0.18	-0.07	0.58	0.18
0.05% nAg	0.20	-0.04	0.37	0.12
0.05% nZVI	0.24	0.07	0.42	0.13
0.5% nZVI	0.13	-0.08	0.35	0.11
0.5% nZVI + 0.05% nAg	0.11	-0.08	0.26	0.10

None of the manufactured CDFs reaches the WHO requirement of a LRV of 3 or greater for viruses. The LRVs are for all CDFs really low. There is no consistent trend visible for the dose-response relationship between nZVI concentration in the CDFs and performance of the CDFs.

The LRVs are considerably lower compared to LRVs reported in other studies. Tests with CPFs conducted by Brown & Sobsey (2010) resulted in mean LRV for MS2 bacteriophages of 4.1 within the first 100L throughput, which reduced to 1.2 on the long term. After 5 weeks of loading CPFs, Van Halem et al. (2007) obtained average LRVs between 0.6 and 1.2, while after 13 weeks the LRVs were between 1.1 and 2.1. An important difference between those experiments and the experiments in this study is the type of test water. In this study demineralized water is used, whereas Brown & Sobsey (2010) used rain water and surface water and Van Halem et al. (2007) utilized surface water. In contrast, Salsali et al. (2011) who also used demineralized water, evidenced similar LRVs for MS2 as this study: 0.21 – 0.45. It was hypothesized that viruses can more easily be removed in natural waters because they can attach to suspended solids and because the pores become clogged, so that they can be removed by filtration mechanisms such as straining, adsorption or sedimentation (Salsali et al., 2011). Furthermore, the build-up of a biofilm could probably also enhance the removal of viruses (Van Halem et al., 2007). However, Van der Laan et al. (2014) found an average LRV of 0.6 when utilizing surface water. Hence, they could not confirm this theory.

Looking at the results of the batch experiments with MS2 bacteriophages, higher LRVs were expected for MS2 phages in the filter experiment. The difference in LRVs is due to several differences in circumstances of the experiments. First of all, the contact between viruses and ceramic material was much more intensive in the batch experiment. In the batch experiment, the tubes with test water and ceramic material were shaken at 150 rpm. This enhances mechanisms such as diffusion and turbulence, which can lead to better adsorption and subsequent inactivation of viruses. Secondly, in the batch experiments crushed material of 75-250 µm was used, which probably resulted in larger surface area compared to the actual CDFs. Thirdly, the contact time was for most CDFs slightly longer in the batch experiment (30 min) than in the filter experiment (12-37), as can be seen in Table 4-4. Lastly, it might be that the added metals were not located at the surface of pores in the CDF but were hidden inside the ceramic material. In this way, it is not possible for a virus to be in contact with the metals, so that inactivation is inhibited. This is schematically illustrated in Figure 6-4.

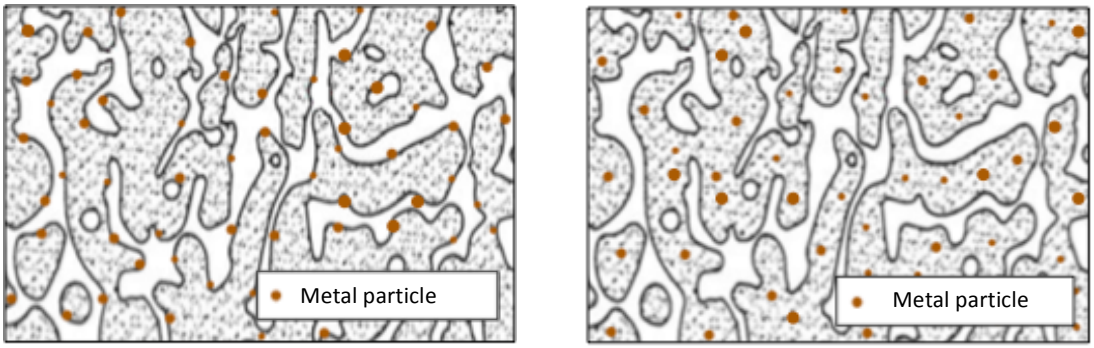

Figure 6–4| Schematic illustration of how the added metal particles might be located inside the CDFs. In the left figure an illustration is given of metal particles that are situated at the surface of the pores and in the right figure an illustration is given of metal particles that are hidden in the ceramic structure.

6.1.3 Metal leaching from CDFs

In Figure 6-5 the average iron and silver concentrations, which leached off from the different CDFs, are depicted. For the blank CDF it was chosen to analyse one CDF for iron and one for silver and copper, because the sample volume was too small to test all three in duplicates. The copper concentrations released from the blank CDF are shown in Appendix IV. It was found that the blank CDF also relased silver, but because the concentrations were so low this is not visible in Figure 6-5. Therefore, those are also shown in Appendix IV.

According to the guidelines from the WHO a maximum level of 0.1 mg/L of silver is allowed in drinking water (WHO, 2011b). This level is set to prevent arygria, a dermalogical disorder. Figure 6-5 shows that this level is not exceeded for any of the CDFs. The WHO does not recommend a health-based guideline value for iron in drinking water.

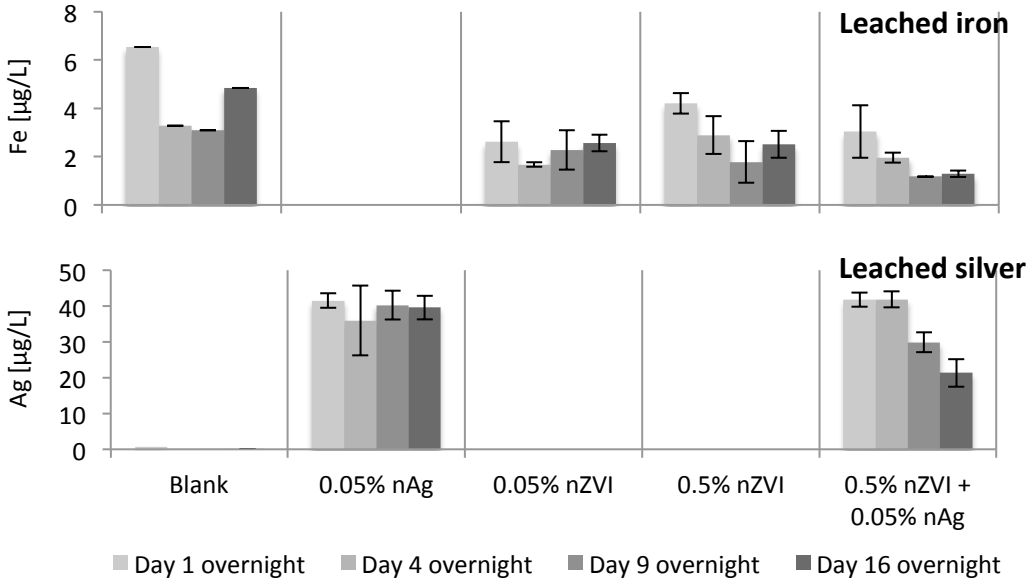

Figure 6–5| Average iron and silver concentrations, which leached off from the different CDFs.

The amount of silver leaching is relatively low and comparable to the amount of silver that leached of in the batch experiment with MS2 bacteriophages (see Chapter 5). This is as expected based on the conclusion of Ren & Smith (2013) that silver leaches off much less and more gradually when the nAg is apllied by means of a fire-in method instead of paining or impregnation. The incorporation of nAg in the clay mixture before mixing results in a better silver retention. This can be seen as an

improvement since other studies report silver concentrations that exceeded the WHO guideline in the first hour of use (Oyanedel-Craver & Smith, 2008; Kallman et al., 2011), although the silver leaching in those studies rapidly declined to below the maximum allowed value.
Mittelman et al. (2015) investigated the ratio of dissolved silver and nAg that leached of ceramic disks painted with nAg. They found that more than 90% of the released silver was in the ionic form.

Much less iron leached off from the CDFs compared to the amount of silver that leached off. It is interesting that the concentration of leached iron is considerably lower in the filter experiment than in the batch exerperiment with MS2 bacteriophages (see Chapter 5). Furthermore, the blank CDFs and the nZVI CDFs release similar amounts of iron, which indicates that the added nZVI does not leach off at all. These results imply that the nZVI particles are not located at the surface but are incorporated inside the clay structure, as illustrated in Figure 6-4.

6.1.4 Inactivation of *E. coli* and MS2 phages during storage in receptacle

In addition to the samples that were taken directly from the CDF, samples were taken 16-18 h later from the receptacle. In Figure 6-6 the average LRVs of the direct and overnight samples are shown per CDF for *E. coli*. An overall overview of the LRVs per day of both the direct and overnight samples can be found in Appendix IV.

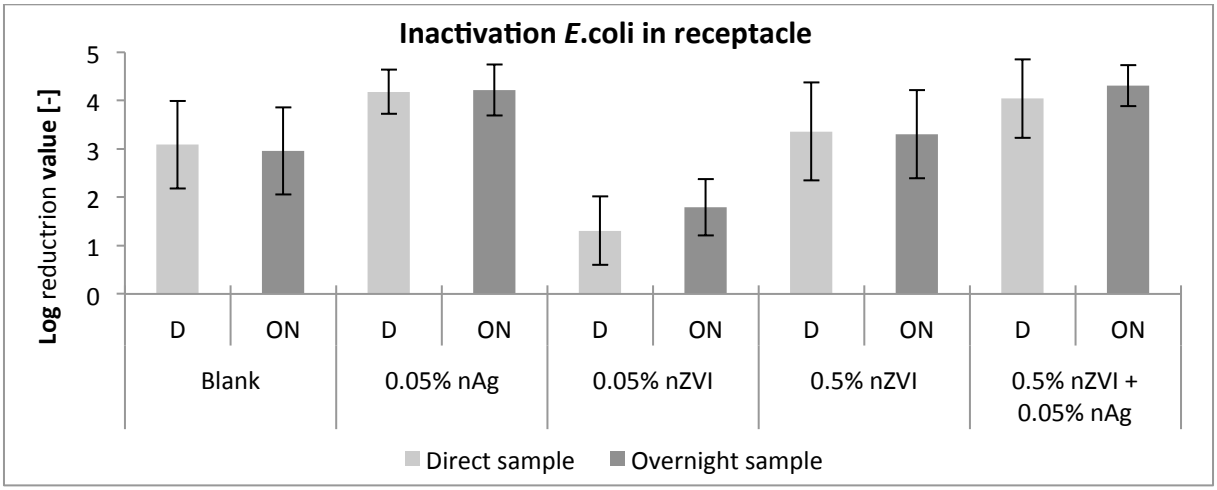

Figure 6–6| LRVs for *E. coli* of samples that were taken directly from the CDFs (D) and of samples that were taken 16-18 h later form the receptacle (ON).

The results of a study by Van der Laan et al. (2014) on the viral effectiveness of CPFs impregnated with an ionic silver solution ($AgNO_3$) implied that inactivation of *E. coli* by silver is predominantly dependent on the storage time in the receptacle and less on the contact time during filtration. In this study, no considerable effect of silver during storage on *E. coli* was observed. First it was thought that this was might be due to the difference in leached silver ions. Incorporating the nAg before firing decreases the amount of leaching compared to impregnating the filters with silver. In addition, this study used nAg while Van der Laan et al. (2014) impregnated their filters with silver nitrate. More ions leach off from a silver salt than from colloidal silver as observed by Mittelman et al. (2015). However, this was not the case, because Van der Laan et al. (2014) reported silver concentrations of 10-25 µg/L at the beginning of their experiments, while in this study, the values ranged between 26 and 46 µg/L (see Figure 6-5). It is therefore unclear why Van der Laan et al. (2014) found a significant inactivation of *E. coli* by storage in the receptacle.

Result of a study by Brown & Sobsey (2010) are in line with this study. They found approximately equal removal results for CPFs with and without silver even though the samples were collected after 5 h of storage time.
The results of this study support the hypothesis that the removal or inactivation of *E. coli* by metals happens mainly during the filtration phase and not during storage in the receptacle. This might be explained by how the inactivation mechanism of bacteria by metals works. As discussed earlier, according to Mathews et al., (2013) the primary mechanisms of contact killing is the direct contact between bacteria and the metallic surface. However, as explained previously, it is questioned whether the metals are located at the surface of the pores of the CDFs or are hidden in the clay structure, which would make direct contact impossible.

Also the leached iron ions do not seem to contribute to the inactivation of *E. coli*. The CDF with 0.05% nZVI does shows slightly higher LRVs for samples that were taken from the receptacle compared to samples that were taken directly from the CDF. However, this increase in *E. coli* removal due to storage in the receptacle is not visible for the CDF with 5% nZVI.
Chen et al. (2013) however, found that iron ions had strong inactivation effects on *E. coli* compared to nZVI. In this study, this was not clearly visible. This might be because the concentration of leached iron ions was quite low. Moreover, as previously discussed, it is thought that iron has less effect on bacterial inactivation than silver.

In Figure 6-7 the average LRVs of the direct and overnight samples are shown per CDF for MS2 bacteriophages. An overall overview of the LRVs per day of both the direct and overnight samples can be found in Appendix IV. As can be seen in Figure 6-7 the inactivation of MS2 is for every type of CDF slightly enhanced by storage in the receptacle. Although, the absolute increase in activation is really low. Statistical analysis should have been performed to give reliable conclusions on these results.

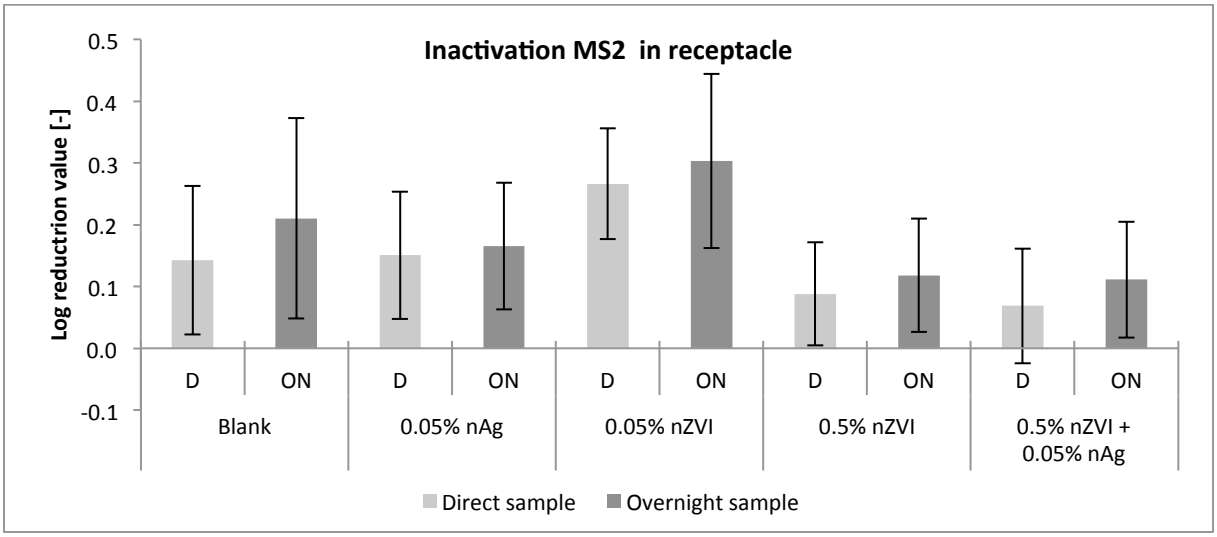

Figure 6–7| LRVs for MS2 bacteriophages of samples that were taken directly from the CDFs (D) and of samples that were taken 16-18 h later form the receptacle (ON).

6.1.5 Conclusions removal efficiency pathogenic microorganisms

In order to be a protective HWTS, the CDFs should have a LRV for *E. coli* of two or greater. This requirement is met for all the CDFs, except for the CDF with 0.05% nZVI. The low LRV for the CDF with 0.05% nZVI is probably due to presence of some larger pores or cracks. There are many variables in the manufacturing process that can cause this inconsistency in removal performance, such as the materials used, the mixing process en firing process.
The results of this study confirmed that nAg considerably enhances *E. coli* removal (LRV 4.28), while the increase in *E. coli* removal is less for nZVI (LRV 3.28). However, a metal amendment is not necessary to obtain sufficient bacteria removal: the blank CDF had a LRV of 2.61. Moreover, it was observed that even with flow rates much higher than the desired 1-3 L/h sufficient LRVs for bacteria were obtained.

The results of the filter experiment further showed that the virus removal remains a major concern of CPFs. Although in the batch experiment LRVs of 0.9-1.5 were found, in the filter experiment the LRVs were much lower: 0.11-0.24. This poor MS2 bacteriophage removal might be because the metal particles are not located at the surface of pores but are hidden in the clay. Furthermore, in this filter experiment, buffered demineralized water was used as test water. More natural challenged water will likely results in higher LRVs due to attachment to suspended solids. It is clear, that further investigation needs to be done to find solutions to improve the virus removal of CPFs.

In addition, it can be concluded that the concentration of leached metals stays far below the maximum guidelines set by the WHO. This confirms that incorporation of metals into the clay before firing results in low amounts of released metal ions, compared to applying metals by means of painting or impregnation.

In addition to samples that were taken directly from the CDFs overnight samples from the receptacle were collected in order to differentiate between the inactivation of *E. coli* and MS2 bacteriophages during the filtration phase and during storage in the receptacle. It was concluded that the removal or inactivation of *E. coli* happens mainly during the filtration phase and not during storage in the receptacle. For MS2 bacteriophages the LRVs were for both the direct and overnight samples really low.

6.2 Removal of arsenic by CDFs

6.2.1 Arsenic breakthrough of CDFs

With a blank CDF and two CDFs with 5% nZVI an arsenic breakthrough experiment was done. The measured total arsenic concentration in the effluent of these CDFs is displayed in Figure 6-8. Based on the results of the batch experiments it was calculated that arsenic breakthrough of the CDFs with 5% nZVI would occur after 1.3L of arsenic test water had gone through the CDF. This calculation is shown in Appendix IV. This theoretical breakthrough of arsenic is indicated in Figure 6-8 with the dotted black line.

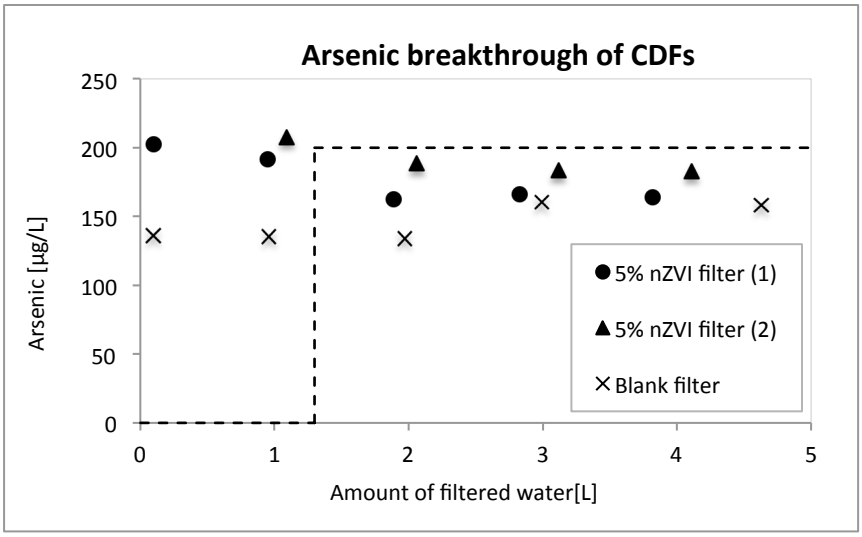

Figure 6–8| Removal of arsenic by a blank CDF and two CDFs containing 5% nZVI. The initial arsenic concentration was 200 µg/L As(III). The dotted black line indicates the theoretical breakthrough of arsenic, based on the results of the batch experiments.

For the CDFs containing 5% nZVI an immediate total breakthrough of arsenic was observed. Hence, the arsenic effluent requirement of maximal 10 µg/L is far from met. It is unclear why the arsenic concentration in the effluent of the CDFs with 5% nZVI slightly decreases.

Although a really quick breakthrough was indeed expected to happen, it is still noteworthy that an immediate total breakthrough took place. These results suggest there was insufficient contact between the iron (hydr)oxides. This insufficient contact can be because the iron (hydr)oxides were hidden in the clay structure and not located on the outside surface of pores of the CDFs, as illustrated in Figure 6-4 Another reason for the insufficient contact is that the contact time with the iron (hydr)oxides was too short.

In Table 6-3 the flow rates of the CDFs are depicted. As can be seen, the flow rates of the CDF with 5% nZVI are extremely high compared to the blank CDF, resulting in short contact times between the arsenic and iron (hydr)oxides.

Table 6-3| Measured flow rates of the CDFs of the first hour after filling the water columns with 5 L test water.

CDF	Flowrate [mL/h]
Blank	151
5% nZVI (1)	913
5% nZVI (2)	1374

The large difference in flow rates between the blank CDF and the CDF with 5% nZVI also explains why the blank CDF was slightly more capable to remove As(III) compared to the CDFs with 5% nZVI: the contact time was around 10 times longer. A long contact time between the raw water and the ceramic material makes adsorption of arsenic more likely to happen. As explained in Chapter 2 arsenic can be bind to the surface hydroxyl groups of clay minerals. Also from the batch experiment it appeared that the blank CDF was able to adsorb arsenic.

By means of an exchange resin insight was gained on the oxidation of As(III) by the CDFs. In Table 6-4 an overview is given of the measured total arsenic As_{Tot} concentration, the measured As(III) concentration and the calculated As(V) concentration, which is defined as the difference between the As_{total} concentration and the As(III). These samples were taken after approximately 4 L of throughput.

Table 6-4| Ratio of As(III) and As(V) concentration for the effluent samples of the blank CDF and the two CDFs with 5% nZVI after approximately 4 L of test water was passed through the CDFs. These values were determined by means of a chloride resin.

CDF	As_{Tot} [µg/L]	As(III) [µg/L]	As(V) [µg/L]
Blank	158	148	10
5% nZVI (1)	164	143	21
5% nZVI (2)	183	166	17

It can be seen in Table 6-4 that no considerable As(III) oxidation occurred. In addition, the small amount of As(III) that was oxidized might even took already place in the water column before it entered the CDFs. These results again imply that there was inadequate contact between the arsenic and the iron (hydr)oxides; either as a result of too high flow rates or of unreachable iron (hydr)oxides could, because they were enclosed by the ceramic structure.

6.2.2 Arsenic breakthrough of CDFs combined with CIM

To enhance arsenic removal it might be an effective option to combine a CPF with pre-treatment of CIM. Therefore, as a preliminary study, the arsenic-breakthrough experiment was repeated with on top of the CDFs with 5% nZVI a layer of CIM. In this experiment only one measurement was done per CDF. The results are shown in Figure 6-9.

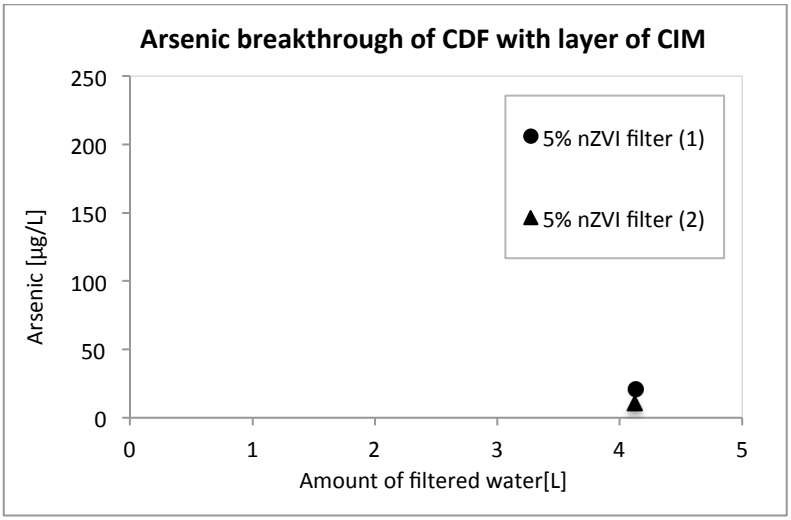

Figure 6–9| Removal of arsenic by CDFs containing 5% nZVI with a layer of 1.5 cm CIM on top of the CDFs. The initial arsenic concentration was 200 µg/L As(III).

It can be seen in Figure 6-9 that almost all the As(III) is removed by the CDFs with a layer of CIM. The arsenic is thus almost removed to below the provisional WHO guideline of 10 µg/L As.

The initial thickness of the CIM layer was 1.5 cm, which was based on the maximum amount of available material. A SONO filter contains between 5-10 kg CIM and has hence a much thicker layer of CIM compared to this study. SONO filters generally remove arsenic to below 10 µg/L and always to

below 50 µg/L for a period of up to 8 years (Neumann et al., 2013). Due to time limits it was not possible to determine the arsenic breakthrough of this combination filter. Nevertheless, the results show that this combination filter is much better capable of removing As(III) compared to the CDFs without a layer of CIM. The results of this study, together with the known arsenic removal capacities of a SONO filter (Neumann et al., 2013), indicate that a pre-treatment of CIM would be a potential alternative for the currently available CPFs.

7 Conclusions and recommendations

7.1 Conclusions

The primary goal of this study was to investigate whether it is feasible to extend the capabilities of CPFs with arsenic removal properties and enhanced virus inactivation by the incorporation of nZVI before firing. The specific objectives were (i) to study the arsenic adsorption capacities of CPFs with nZVI fired-in, (ii) determine the microbiological inactivation efficiency by CPFs with nZVI fired-in, (iii) evaluate the leaching of the incorporated nZVI and (iv) provide knowledge on the effect of incorporating nZVI into the CPFs before firing.

For this purpose, Ceramic Disk Filters (CDFs) were manufactured, according to the manufacturing protocol of the non-profit organisation FilterPure, in which metals were incorporated before firing. The manufactured CDFs were tested based on the following established requirements: (i) arsenic must be removed to below the provisional WHO guideline of 10 µg/L, (ii) for bacteria a LRV of 2 or greater is required, (iii) for viruses a LRV of 3 or greater is required, (iv) the leached amount of silver must not exceed the guideline of 0.1 mg/L set by the WHO and (v) CDFs should have a flow rate of 0.08-0.24 L/h, which corresponds to 1-3 L/h for a full-size CPF.

The following conclusions, with regard to the above-mentioned requirements were drawn:

i. Although this study showed that ZVI on itself is an effective arsenic adsorbent, especially at nanoscale, an immediate total breakthrough of approximately 200 µg/L As was observed the CDF containing 5% nZVI. Hence, it is concluded that the effluent requirement with regard to arsenic of maximal 10 µg/L was not met.

ii. All CDFs, except the CDF with 0.05% nZVI, were able to remove *E. coli* sufficiently to meet the requirements for bacteria removal. The results of this study showed that nAg significantly enhanced *E. coli* removal (LRV 4.28) compared to the blank CDF (LRV 2.61), while the increase in *E. coli* removal is much less for nZVI (LRV 3.28). However, the results also indicate that a metal amendment is not the crucial parameter to meet the WHO requirements for bacteria removal, but the production variables such as the mixing and firing process, are. Furthermore, it is concluded that removal and inactivation of *E. coli* happens mainly during the filtration phase and not during storage in the receptacle.

iii. The removal efficiency of the CDFs was with LRVs 0.11 and 0.24 for MS2 bacteriophages was below the required LRV of 3 or greater. Therefore it is concluded that the removal

effectiveness for viruses remains a major concern of CPFs. Moreover, there was no consistent trend visible for the dose-response relationship between the nZVI concentration of the CDFs and the performance of the CDFs with regard to MS2 bacteriophages removal.

iv. The amount of leached silver stayed below the maximum guideline of 0.1 mg/L set by the WHO (<50 µg/L). Also the Fe leaching was low (<7 µg/L). This confirms that incorporation of metals into the clay before firing results in low concentrations of released metal ions compared to applying metals by means of painting or impregnation.

v. The translated flow rates for CPFs were for all CDFs higher than the requirement of 1-3 L/h (3.4 – 15.6 L/h), except for the CDF with 0.05% nAg (1.5 L/h).

Overall, it can thus be concluded that it is not recommended to incorporate nZVI in CPFs before firing with the purpose to enhance the removal of arsenic and viruses.

ZVI on itself is well capable of removing arsenic, as confirmed by this study, particularly at nanoscale because of the small particles size and thus the large specific surface area. However, it appeared that when ZVI is incorporated into clay it looses effectiveness. In the batch experiments similar kinetics curves for the removal of As(III) were observed with 50 g/L unfired clay material containing 5% nZVI and with 0.06 g/L nZVI. When the clay with the nZVI incorporated is fired it looses even more effectiveness. In the batch experiments it was found that unfired CDF material containing 5% nZVI was able to remove approximately 90% of the initial 200 µg/L As(III) in 30 minutes of contact time, while fired material with 5% nZVI only removed a few per cent As(III). Although part of the faster As(III) removal of the unfired CDF was a result of sorption by the clay, the nZVI contributed considerably.

Although the LRVs for MS2 bacteriophages by fired CDF material were higher in the batch experiment (LRV 0.42-1.52) than in the filter experiment – probably due more intensive contact - there was also no enhanced MS2 bacteriophage reduction noticed for the fired CDFs with hematite or iron oxide hydroxides compared to the fired blank CDF. The unfired CDF with 5% nZVI, however, adsorbed the MS2 bacteriophages strongly compared to the fired CDF with 5% nZVI, but this did not result inactivation.

It is hypothesized that there are three main causes for this performance loss of ZVI, induced by the incorporation into ceramics before firing. The results of the filter experiments, with regard to arsenic and virus removal, indicated that there was insufficient surface contact with the nZVI particles; either due to too high flow rates or due to the unavailability of nZVI particles on the pore surface.

The flow rates measurements suggest that the addition of nZVI particles leads to a considerable increase of flow rate, probably as a result of successively expansion and shrinking of the nZVI during the firing process. Although sufficient LRVs for bacteria removal were obtained with flow rates higher than the desired 1-3 L/h, the high flow rates might have caused the low virus and arsenic removal in this study.

Furthermore, it is hypothesized that due to the vitrification process, in which the clay bonds together, the nZVI becomes enclosed in the clay structure. The corrosion products of the nZVI are hence not located at the surface of the pores, which inhibits the adsorption or inactivation of contaminants.

Lastly, the ^{57}Fe Mössbauer spectra evidenced that during firing all the added nZVI was oxidized into hematite, which probably affects the removal of arsenic. Different ZVI corrosion products have a

different ability to adsorb arsenic: ZVI exhibits the greatest As adsorption, secondly magnetite, then hematite and lastly goethite (Mamindy-Pajany et al. (2011)).

7.2 Recommendations

Overall, it can be concluded that it is not recommended to incorporate nZVI in CPFs before firing, to enhance the removal of arsenic and viruses. Since the CPF is one of the most socially accepted and effective HWTS in terms of bacteria removal, alternative solutions for enhanced arsenic and virus removal by CPFs need to be sought.

Concepts for potential alternative solutions of CPFs in combination with ZVI

This study confirmed that nZVI and CIM are effective arsenic adsorbents and have therefore potential for its applications in HWTS. The results of this study indicate that when designing a new type of CPF it is important to make sure that the iron (oxides) particles can be reached and that the flow rate is not too high so that the contact time with the iron (oxides) particles is long enough. The flow rate can be changed by adapting the "recipe" of a CPF: such as changing the amount and size of the burnout material, adding nZVI or changing firing process.

Several concepts for potential alternatives for CPFs in combination with ZVI are described below and illustrated in Figure 7-1.

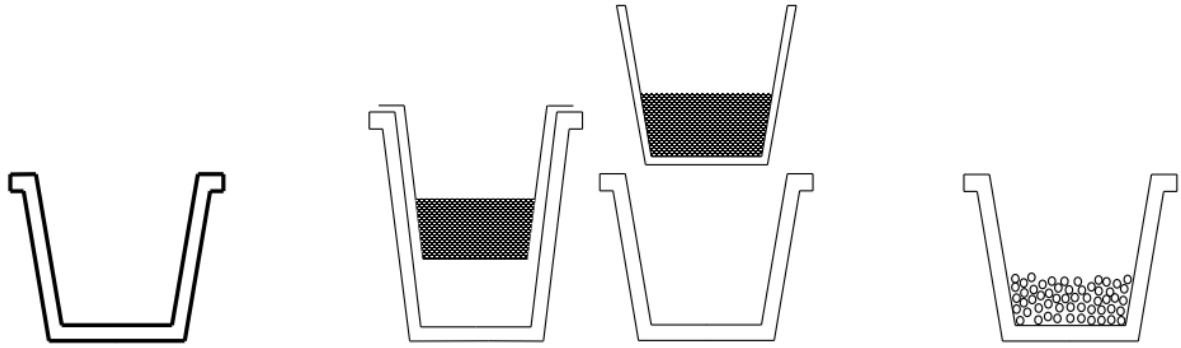

Figure 7–1| Schematic illustration of concepts of potential alternatives for CPFs in combination with ZVI. (a) Represents an CPF with an iron coating, (b) illustrates CPFs with pre-treatment of with ZVI and (c) shows a CPF in combination with iron mixed ceramic pellets.

i. **CPF with an iron coating** (Figure 7-1 a): An iron coating, applied after firing, can likely ensure that more iron is located on the surface and that the iron is hence better reachable. In an unpublished study Robbins (2011) performed experiments with ceramic micro-columns, which have the same thickness and properties as a CPF, coated with 0.510 M ferric-nitrate. Robbins observed an arsenic reduction from 250 µg/L to below 10 µg/L over 365 filter runs. This study thus shows the potential of an iron coating.

   There are several considerations that need to be taken into account when studying the possibilities of an iron coating. Firstly, a coating technique should be found that results in a high amount of iron, coated on the surfaces of the pores in the CPF. Secondly, it should be investigated what the best firing procedure would be. After applying an iron coating on the CPF, the CPF should be fired so that the coating will stick to the CPF. The temperature and the duration of firing might affect the types of iron corrosion products that are formed and the leaching of iron. Thirdly, it should be studied whether it is best to use a nZVI coating

solution or an iron salt coating solution. Lastly, it should be investigated whether an iron coating could have a positive effect on the inactivation of viruses.

ii. **CPF with a pre-treatment of ZVI** (Figure 7-1 b): The results of the arsenic breakthrough experiment with CDFs in combination with a layer of CIM, suggest that the combination of a CPF with pre-treatment of CIM could be a promising alternative. This might be for instance in the form of a separate element with CIM that can be hung in the CPF, or an extra bucket filled with CIM on top of the CPF. A main advantage of this option is that no firing is needed, resulting in large arsenic adsorption capabilities, as showed by the SONO filter (Neumann et al., 2013). However, there are many things that need to be taken into account when designing a new type of filter system: it should be socially accepted, cheap, easy to use etc.
It would be interesting to look at the use of nZVI instead of CIM, because nZVI has not only a higher surface area to adsorb arsenic it is also thought that nZVI could directly interact with viruses and inactivate them due to their small size (Kim et al., 2011). However, also the use of nanoparticles should be evaluated. Especially for local manufactures in developing countries it might be difficult to handle nanoparticles and it is more expensive than CIM.

iii. **CPF in combination with iron mixed ceramic pellets** (Figure 7-1 c): A study by Shafiquzzam et al. (2013) showed that porous ceramic pellets with ZVI incorporated before firing, have high arsenic removal capacities. The pellets consist of clay, rice-bran and ZVI with a ratio based on weight of 80:20:40, respectively. Since practical reasons will make it difficult to extremely increase the ZVI of CPFs - the CPFs will become too heavy, too brittle and more expensive – it might be an option to combine such ceramic pellets with a very high ZVI content with a CPF.
It is should be investigated whether the contact time with the ceramic pellets in the CPF is long enough for effective arsenic removal. Furthermore, it is important to consider whether the user is can easily and safely handle the (contaminated) ceramic pellets with ZVI.

The poor virus removal remains a major disadvantage of a CPF. For each of these concepts it is therefore recommended that more research is done on how virus removal and inactivation can be enhanced, since in this study no inactivation of MS2 bacteriophages by nZVI was observed. The results did show that unfired nZVI could effectively adsorb MS2 phages. Therefore, it is especially recommended to search additives that are able to inactivate viruses.
Furthermore, it was found in the batch experiments that the fired CDF material with a combination of nAg and nZVI showed an additive effect on MS2 phages inactivation compared to the CDFs with solely nAg or nZVI. Although, the LRVs for this combination CDF were still low it might have potential at higher concentrations. In addition, it is advised to look at other combination of metals, such as silver and copper, since synergism was reported for the inactivation of the bacteria *Legionella pneumophila* by copper and silver ions (Lin et al., 1996).

Additional recommendations for future research
In order to better understand the adsorption of viruses onto different media it is advised f perform zeta-potential measurements and to determine the actual pH_{PZC} of the used media. This is also of importance for the adsorption of arsenic.

Furthermore, it is recommended that in a later stage of future research also other viruses than MS2 bacteriophages are studied. Every virus has its own characteristics and hence its own IEP, which can result in the different removal efficiencies for different viruses. The same yields for bacteria.

Lastly, it is advised that in a later stage of future research experiments should be performed with more challenging water. There are a lot of parameters that can have an influence on both the removal of viruses and arsenic. These parameters included, among others:

- Turbidity: Turbidity can cause fouling and thus affects the discharge. It can also limit the available surface sites for arsenic adsorption. On the contrary, with a higher turbidity viruses can probably attach to suspended solids and subsequently be removed by filtration mechanisms such as straining, adsorption or sedimentation. Also the clogged pores and the formation of a biofilm could potentially enhance virus removal.
- pH: The pH plays an important role in the adsorption process; it influences the charge of adsorbents and adsorbates and hence the attraction or repulsion between those two. Furthermore, it determines which form of arsenic species prevails.
- Competing ions: Next to Natural Organic Matter, there are several ions, such as phosphate, and bicarbonate, that can cause inhibition of arsenic removal (Kanel et al., 2005). It might also affect the adsorption of viruses.
- Ionic strength: The ionic strength has a sizable influence on the balance between the double layer repulsive forces and the van der Waals attractive forces, since an increase of cations results in a reduction of the double layer thickness. Moreover, the amount of metal leaching is related to the ionic strength of a solution.
- Influent arsenic concentration: varying arsenic concentration should be studied.

Also mechanism as desorption of the arsenic should then be tested. Moreover, later on also long term studies are required.

Bibliography

Alfred, M., & Ramos, V. (2011). Sequestration of Arsenic by nanoscale Zero-Valent Iron (nZVI): Surface Reactions Characterized by High Resolution X-Ray Photoelectron Spectroscopy (HR-XPS).

Barzan, E., Mehrabian, S., & Irian, S. (2014). Antimicrobial and Genotoxicity Effects of Zero-valent Iron Nanoparticles. *Jundishapur Journal of Microbiology*, *7*(5), 1–5.

Bickley Remmey Jr., G. (1994). *Firing ceramics*. London: World Scientific.

Bielefeldt, A. R., Kowalski, K., Schilling, C., Schreier, S., Kohler, A., & Scott Summers, R. (2010). Removal of virus to protozoan sized particles in point-of-use ceramic water filters. *Water Research*, *44*(5), 1482–1488.

Bielefeldt, A. R., Kowalski, K., & Summers, R. S. (2009). Bacterial treatment effectiveness of point-of-use ceramic water filters. *Water Research*, *43*(14), 3559–3565.

Bloem, S. C. (2008). *Silver impregnated ceramic water filter*.

Breuer, S. (2012). The chemistry of pottery. *Education in chemistry*.

Bringham, W. E. (1974). Mixing Equations in Short Laboratory Cores. *Society of Petroleum Engineers Journal*, *14*(01), 91–99.

Brown, J., & Sobsey, M. D. (2009). Ceramic media amended with metal oxide for the capture of viruses in drinking water. *Environmental Technology*, *30*(4), 379–391.

Brown, J., & Sobsey, M. D. (2010). Microbiological effectiveness of locally produced ceramic filters for drinking water treatment in Cambodia. *Journal of Water and Health*, *8*, 1–10.

Chattopadhyay, S., & Puls, R. W. (1999). Adsorption of bacteriophages on clay minerals. *Environmental Science and Technology*, *33*(20), 3609–3614.

Chen, Q., Li, J., Wu, Y., Shen, F., & Yao, M. (2013). Biological responses of Gram-positive and Gram-negative bacteria to nZVI (Fe^{0}), Fe^{2+} and Fe^{3+}. *RSC Advances*, *3*(33), 13835.

Churchill, H., Teng, H., & Hazen, R. M. (2004). Correlation of pH-dependent surface interaction forces to amino acid adsorption: Implications for the origin of life, *89*, 1048–1055.

Cullity, B. D. (1956). *Elements of X-ray diffraction TT -*. *Addison-Wesley metallurgy series;* Reading, Mass. : Addison-Wesley Pub. Co.

Dixit, S., & Hering, J. G. (2003). Comparison of arsenic(V) and arsenic(III) sorption onto iron oxide minerals: Implications for arsenic mobility. *Environmental Science and Technology*, *37*(18), 4182–4189.

Eick, M. J., Peak, J. D., & Brady, W. D. (1999). The Effect of Oxyanions on the Oxalate-Promoted Dissolution of Goethite. *Soil Science Society of America Journal*, *63*(5), 1133.

El Badawy, A. M., Luxton, T. P., Silva, R. G., Scheckel, K. G., Suidan, M. T., & Tolaymat, T. M. (2010).

Impact of environmental conditions (pH, ionic strength, and electrolyte type) on the surface charge and aggregation of silver nanoparticles suspensions. *Environmental Science and Technology*, *44*(4), 1260–1266.

Elechiguerra, J. L., Burt, J. L., Morones, J. R., Camacho-Bragado, A., Gao, X., Lara, H. H., & Yacaman, M. J. (2005). Interaction of silver nanoparticles with HIV-1. *Journal of Nanobiotechnology*, *3*, 6.

Essington, M. E. (2004). *Soil and water chemistry : an integrative approach*. Boca Raton, CRC Press LLC, 322-330

Farrell, J., Wang, J., O'Day, P., & Conklin, M. (2001). Electrochemical and spectroscopic study of arsenate removal from water using zero-valent iron media. *Environmental Science & Technology*, *35*(10), 2026–2032.

Feng, Q. L., Wu, J., Chen, G. Q., Cui, F. Z., Kim, T. N., & Kim, J. O. (2000). A mechanistic study of the antibacterial effect of silver ions on Escherichia coli and Staphylococcus aureus.

Fernandez, R., Martirena, F., & Scrivener, K. L. (2011). The origin of the pozzolanic activity of calcined clay minerals: A comparison between kaolinite, illite and montmorillonite. *Cement and Concrete Research*, *41*(1), 113–122.

Flanagan, S. V, Johnston, R. B., & Zheng, Y. (2012). Arsenic in tube well water in Bangladesh: health and economic impacts and implications for arsenic mitigation. *Bulletin of the World Health Organization*, *90*, 839–46.

Friedman, K. C. (2015) Unblished results of prilimenary results of a study on ceramic filters amended with copper and silver for enhanced virus removal.

Gerba, C. P. (1984). Applied and theoretical aspects of virus adsorption to surfaces. *Advances in applied microbiology* (Vol. 30).

Hunter, P. R. (2009). Household water treatment in developing countries: Comparing different intervention types using meta-regression. *Environmental Science and Technology*, *43*(23), 8991–8997.

Hussam, A. (2008). An iron composition based water filtration system for the removal of chemical species containing arsenic and other metal cations and anions. Google Patents. Retrieved from http://www.google.com/patents/WO2008127757A2?cl=en

Hussam, A., & Munir, A. K. M. (2007). A simple and effective arsenic filter based on composite iron matrix: development and deployment studies for groundwater of Bangladesh. *Journal of Environmental Science and Health. Part A, Toxic/hazardous Substances & Environmental Engineering*, *42*, 1869–1878.

Ijagbemi, C. O., Baek, M.-H., & Kim, D.-S. (2009). Montmorillonite surface properties and sorption characteristics for heavy metal removal from aqueous solutions. *Journal of Hazardous Materials*, *166*(1), 538–546.

Kallman, E. N., Oyanedel-Craver, V. A., & Smith, J. A. (2011). Ceramic Filters Impregnated with Silver Nanoparticles for Point-of-Use Water Treatment in Rural Guatemala. *Journal of Environmental Engineering*, *137*(June), 407–415.

Kanel, S. R., Manning, B., Charlet, L., & Choi, H. (2005). Removal of Arsenic (III) from Groundwater by Nanoscale Zero-Valent Iron. *Environmental Science & Technology*, *39*(5), 1291–1298.

Kim, J. Y., Lee, C., Love, D. C., Sedlak, D. L., Yoon, J., & Nelson, K. L. (2011). Inactivation of MS2 coliphage by ferrous ion and zero-valent iron nanoparticles. *Environmental Science and Technology*, *45*, 6978–6984.

Kim, J. Y., Park, H. J., Lee, C., Nelson, K. L., Sedlak, D. L., & Yoon, J. (2010). Inactivation of escherichia coli by nanoparticulate zerovalent iron and ferrous ion. *Applied and Environmental Microbiology*, *76*(22), 7668–7670.

Kim, M. J., & Nriagu, J. (2000). Oxidation of arsenite in groundwater using ozone and oxygen. *Science of the Total Environment*, *247*, 71–79.

Lantagne, D. S. (2001). *Investigation of the Potters for Peace Colloidal Silver Impregnated Ceramic Filter Report 1 : Intrinsic Effectiveness*. Allston.

Lee, C., Kim, J. Y., Lee, W. Il, Nelson, K. L., Yoon, J., & David, L. (2008). Bactericidal effect of zero-valent iron nanoparticles on Escherichia coli, *42*(13), 4927–4933.

Lee, C., Kim, J. Y., Lee, W. Il, Nelson, K. L., Yoon, J., & Sedlak, D. L. (2008). Bactericidal effect of zero-valent iron nanoparticles on Escherichia coli. *Environmental Science & Technology*, *42*(13), 4927–4933.

Li, X., Elliott, D. W., & Zhang, W. (2006). Zero-Valent Iron Nanoparticles for Abatement of Environmental Pollutants: Materials and Engineering Aspects. *Critical Reviews in Solid State and Materials Sciences*, *31*(March 2015), 111–122.

Lin, Y.S. E., Vidic, R. D., Stout, J. E., & Victor L. Y. (1996). Individual and combined effects of copper and silver ions on inactivation of Legionella Pneumophila. *Water Research, 30*(8), 1905–1913.

Lin, Z., & Puls, R. W. (2000). Adsorption, desorption and oxidation of arsenic affected by clay minerals and aging process. *Environmental Geology*, *39*(7), 753–759.

Lu, L., Sun, R., Chen, R., Hui, C., & Ho, C. (2008). Silver nanoparticles inhibit hepatitis B virus replication. *Antiviral …*, *13*, 253–262.

Mamindy-Pajany, Y., Hurel, C., Marmier, N., & Roméo, M. (2011). Arsenic (V) adsorption from aqueous solution onto goethite, hematite, magnetite and zero-valent iron: Effects of pH, concentration and reversibility. *Desalination*, *281*, 93–99.

Manning, B. a., Hunt, M. L., Amrhein, C., & Yarmoff, J. a. (2002). Arsenic(III) and arsenic(V) reactions with zerovalent iron corrosion products. *Environmental Science and Technology*, *36*(24), 5455–5461.

Mathews, S., Hans, M., Mücklich, F., & Solioz, M. (2013). Contact killing of bacteria on copper is suppressed if bacterial-metal contact is prevented and is induced on iron by copper ions. *Applied and Environmental Microbiology*, *79*(8), 2605–11.

Mittelman, A. M., Lantagne, D. S., Rayner, J., & Pennell, K. D. (2015). Silver Dissolution and Release from Ceramic Water Filters. *Environmental Science & Technology*,

Mohapatra, D., Mishra, D., Chaudhury, G. R., & Das, R. P. (2007). Arsenic adsorption mechanism on clay minerals and its dependence on temperature. *Korean Journal of Chemical Engineering*, *24*(3), 426–430.

Morones, J. R., Elechiguerra, J. L., Camacho, A., Holt, K., Kouri, J. B., Ramírez, J. T., & Yacaman, M. J. (2005). The bactericidal effect of silver nanoparticles. *Nanotechnology*, *16*(10), 2346–2353.

Mosaferi, M., Nemati, S., Khataee, A., Nasseri, S., & Hashemi, A. A. (2014). Removal of Arsenic (III, V) from aqueous solution by nanoscale zero-valent iron stabilized with starch and carboxymethyl cellulose. *Journal of Environmental Health Science & Engineering*, *12*(1), 74.

Murad, E., & Wagner, U. (1998). Clays and clay minerals : The firing process. *Hyperfine Interactions*, *117*, 337–356.

Neumann, A., Kaegi, R., Voegelin, A., Hussam, A., Munir, A. K. M., & Hug, S. J. (2013). Arsenic removal

with composite iron matrix filters in Bangladesh: A field and laboratory study. *Environmental Science and Technology*, *47*, 4544–4554.

Ngun, B. K., Mohamad, H., Sulaiman, S. K., Sulaiman, M. Y. M., Isobe, T., Okada, K., & Ahmad, Z. A. (2012). Changes in physical, chemical, and microstructures and strength relationships of some Cambodian clays. *Journal of Ceramic Processing Research*, *13*(5), 547–555.

Nurmi, J. T., Tratnyek, P. G., Sarathy, V., Baer, D. R., Amonette, J. E., Wang, C., … Driessen, M. D. (2005). Characterization and Properties of Metallic Iron Characterization and Properties of Metallic Iron Nanoparticles : Spectroscopy , Electrochemistry , and Kinetics, 1221–1230.

Oyanedel-Craver, V. a., & Smith, J. a. (2008). Sustainable Colloidal-Silver-Impregnated Ceramic Filter for Point-of-Use Water Treatment. *Environmental Science & Technology*, *42*(3), 927–933.

Park, H.-J., Kim, J. Y., Kim, J., Lee, J.-H., Hahn, J.-S., Gu, M. B., & Yoon, J. (2009). Silver-ion-mediated reactive oxygen species generation affecting bactericidal activity. *Water Research*, *43*(4), 1027–32.

Peckham, T. J., Schmeisser, J., Rodgers, M., & Holdcroft, S. (2007). Main-chain, statistically sulfonated proton exchange membranes: the relationships of acid concentration and proton mobility to water content and their effect upon proton conductivity. *Journal of Materials Chemistry*, *17*(30), 3255.

Plaza, R. C., Quirantes, A., & Delgado, A. V. (2002). Stability of Dispersions of Colloidal Hematite/Yttrium Oxide Core-Shell Particles. *Journal of Colloid and Interface Science*, *252*(1), 102–108.

Ramos, M. a V, Yan, W., Li, X., Koel, B. E., & Zhang, W. (2009). Simultaneous Oxidation and Reduction of Arsenic by Zero-Valent Iron Nanoparticles: Understanding the Signi cance of the Core-Shell Structure. *Society*, (Iii), 2–5.

Reed, J. S. (1995). *Principles of ceramics processing*. *Wiley* (2nd ed.). New York: Wiley.

Ren, D., & Smith, J. a. (2013). Retention and transport of silver nanoparticles in a ceramic porous medium used for point-of-use water treatment. *Environmental Science and Technology*, *47*, 3825–3832.

Robbins, E. (2011). Development of an Iron-Oxide Coated Ceramic Filter for Removal of As (III) and As (V) in Developing Nations.

Ryan, J. N., Harvey, R. W., Metge, D., Elimelech, M., Navigato, T., & Pieper, A. P. (2002). Field and laboratory investigations of inactivation of viruses (PRD1 and MS2) attached to iron oxide-coated quartz sand. *Environmental Science and Technology*, *36*(11), 2403–2413.

Sagripanti, J. L., Routson, L. B., & Lytle, C. D. (1993). Virus inactivation by copper or iron ions alone and in the presence of peroxide. *Applied and Environmental Microbiology*, *59*(12), 4374–4376.

Salsali, H., McBean, E., & Brunsting, J. (2011). Virus removal efficiency of Cambodian ceramic pot water purifiers. *Journal of Water and Health*, *9*, 306–311.

Scroth, B. K., Sposito, G., & Schroth, B. K. (1997). Surface charge properties of kaolinite. *Clays and Clay Minerals*, *45*(1), 85–91.

Shafiquzzam, M., Hasan, M. M., & Nakajima, J. (2013). Iron mixed ceramic pellet for arsenic removal from groundwater. *Environmental Engineering Research*, *18*(3), 163–168.

Shafiquzzaman, M., Azam, M. S., Nakajima, J., & Bari, Q. H. (2011). Investigation of arsenic removal performance by a simple iron removal ceramic filter in rural households of Bangladesh. *Desalination*, *265*, 60–66.

Sherman, D. M., & Randall, S. R. (2003). Surface complexation of arsenic(V) to iron(III) (hydr)oxides: Structural mechanism from ab initio molecular geometries and EXAFS spectroscopy. *Geochimica et Cosmochimica Acta*, *67*(22), 4223–4230.

Simonis, J. J., & Basson, A. K. (2011). Evaluation of a low-cost ceramic micro-porous filter for elimination of common disease microorganisms. *Physics and Chemistry of the Earth*, *36*(14-15), 1129–1134.

Smedley, P. L., & Kinniburgh, D. G. (2002). A review of the source, behaviour and distribution of arsenic in natural waters. *Applied Geochemistry*, *17*, 517–568.

Sondi, I., & Salopek-Sondi, B. (2004). Silver nanoparticles as antimicrobial agent: a case study on E. coli as a model for Gram-negative bacteria. *Journal of Colloid and Interface Science*, *275*(1), 177–82.

Stolboushkin, A. U., Zorya, V. N., & Stolboushkina, O. A. (2013). SEM Investigation of the Structure of Ceramic Matrix Composite Produced from Iron-Ore Waste. *Advanced Materials Research*, *831*, 36–39.

Su, C., & Puls, R. W. (2001). Arsenate and arsenite removal by zerovalent iron: Effects of phosphate, silicate, carbonate, borate, sulfate, chromate, molybdate, and nitrate, relative to chloride. *Environmental Science and Technology*, *35*(22), 4562–4568.

Sun, L., Singh, A. K., Vig, K., Pillai, S. R., & Singh, S. R. (2008). Silver nanoparticles inhibit replication of respiratory syncytial virus. *Journal of Biomedical Nanotechnology*, *4*(2), 149–158.

Temuujin, J., Jadambaa, T., & MacKenzie, K. J. D. (2000). Effect of water vapour atmospheres on thermal transformations and mechanical strength of montmorillonite clay compacts. *British Ceramics Transactions*, *99*(2), 63–66.

The Ceramics Manufacturing Group. (2011). *Best Practice Recommendations for Local Manufacturing of Ceramic Pot Filters for Household Water Treatment* (Vol. 1). Atlanta, GA, USA:CDC.

Tolaymat, T. M., El Badawy, A. M., Genaidy, A., Scheckel, K. G., Luxton, T. P., & Suidan, M. (2010). An evidence-based environmental perspective of manufactured silver nanoparticle in syntheses and applications: A systematic review and critical appraisal of peer-reviewed scientific papers. *Science of the Total Environment*, *408*(5), 999–1006.

Trevett, A. F., & Carter, R. C. (2008). Targeting appropriate interventions to minimize deterioration of drinking-water quality in developing countries. *Journal of Health, Population and Nutrition*, *26*(2), 125–138.

Van der Laan, H., van Halem, D., Smeets, P. W. M. H., Soppe, a. I. a, Kroesbergen, J., Wubbels, G., … Heijman, S. G. J. (2014). Bacteria and virus removal effectiveness of ceramic pot filters with different silver applications in a long term experiment. *Water Research*, *51*, 47–54.

Van Halem, D. (2006). *Ceramic silver impregnated pot filters for household drinking water treatment in developing countries*.

Van Halem, D., Heijman, S. G. J., Soppe, a. I. a., van Dijk, J. C., & Amy, G. L. (2007). Ceramic silver-impregnated pot filters for household drinking water treatment in developing countries: material characterization and performance study. *Water Science & Technology: Water Supply*, *7*(5-6), 9.

Van Halem, D., van der Laan, H., Heijman, S. G. J., van Dijk, J. C., & Amy, G. L. (2009). Assessing the sustainability of the silver-impregnated ceramic pot filter for low-cost household drinking water treatment. *Physics and Chemistry of the Earth, Parts A/B/C*, *34*(1-2), 36–42.

Van Halem, D. (2011). Subsurface iron and arsenic removal for drinking water treatment in

Bangladesh. *Water Management Academic Press, 7.*

Weaver, C. E., & Pollard, L. D. (1973). *The chemistry of clay minerals, TT* -. Amsterdam,: Elsevier Scientific Pub. Co.,

World Health Organisation. (2014). *Global Health Observatory*.

World Health Organisation. (2011a). Evaluating Houseold Water Treatment Options. Retrieved from http://www.who.int/water_sanitation_health/publications/2011/evaluating_water_treatment.pdf

World Health Organisation. (2011b). *Guidelines for Drinking-water Quality*. (W. H. Organisation, Ed.) (4th edition).

World Health Organisation, & Unicef. (2009). *Diarrhoea: Why children are still dying and what can be done*.

World Health Organisation, & Unicef. (2014). Progess on Drinking Water and Sanitation.

You, J., Zhang, Y., & Hu, Z. (2011). Bacteria and bacteriophage inactivation by silver and zinc oxide nanoparticles. *Colloids and Surfaces B: Biointerfaces*, *85*(2), 161–167.

Zhang, H., Oyanedel-craver, V., & Asce, A. M. (2012). Evaluation of the Disinfectant Performance of Silver Nanoparticles in Different Water Chemistry Conditions, (January), 58–66.

Zhu, H., Jia, Y., Wu, X., & Wang, H. (2009). Removal of arsenic from water by supported nano zero-valent iron on activated carbon. *Journal of Hazardous Materials*, *172*, 1591–1596.

List of figures

Figure 1–1|CPF system (van Halem et al., 2009). 2
Figure 1–2|Schematic illustration of the SONO filter (Van Halem, 2011[3]). 5
Figure 2–1|(a) Schematic picture of the core-shell structure of a ZVI particle. (b) High resolution transmission electron microscopy micrograph of a nZVI particle (Ramos et al., 2009). 7
Figure 2–2|Illustration of the different adsorption planes with the associated charge components (Essington, 2004). 9
Figure 2–3|Schematic illustration of the diffuse layer around a colloidal particle. 9
Figure 2–4|Eh-pH diagram for aqueous arsenic species in the system As-O_2-H_2O at 25°C and 1 bar total pressure ((Smedley & Kinniburgh, 2002) 10
Figure 2–5|Schematic representation of a (a) monodentate mononuclear, (b) bidentate mononuclear and (c) bidentate binuclear bindings (Eick et al., 1999). 11
Figure 2–6|Schematic picture of the core-shell structure of ZVI together with the As(III) removal processes by ZVI (Ramos et al., 2009). 12
Figure 2–7|The development of the ceramic structure during vitrification: (a) loose clay particles, (b) initial stage of vitrification and (c) intermediate stage of vitrification. 16
Figure 3–1|Process diagram for the manufacturing of CDFs. 20
Figure 3–2|Schematic drawing of a part of the experimental set-up of the filter experiment. 24
Figure 3–3|Schematic illustration of a CDF combined with a layer of CIM. 25
Figure 3–4|Illustration of a syringe filled with the resin, together with the As species. 25
Figure 4–1|(a) Silicon tetrahedron. (b) Silicon tetrahedral sheet (Weaver & Pollard, 1973). 28
Figure 4–2|(a) Aluminium octahedron. (b) Octahedral sheet (Weaver & Pollard, 1973). 28
Figure 4–3|Structure of kaolinite (Weaver & Pollard, 1973). 28
Figure 4–4|Structure of montmorillonite (Weaver & Pollard, 1973). 29
Figure 4–5|Mössbauer spectra obtained at 300 K for the samples from an unfired filter with 5% nZVI, a fired filter with 5% nZVi and a fired blank filter. 31
Figure 4–6|Microscope images of powdered samples of (a) fired blank CDF (b) fired CDF containing 5% nZVI, (c) fired CDF containing 5% CIM, (d) unfired CDF containing 5% nZVI and (e) unfired CDF containing 5% CIM. 33
Figure 4–7|(a) SEM image of the sample from a fired CDF with 5% CIM and the corresponding distributions of (b) iron and (c) oxygen, determined with SEM-EDX. 34
Figure 4–8|(a) SEM image of the sample from a blank CDF and (b) the corresponding distribution of iron determined with SEM-EDX. 35
Figure 4–9|In figure (a) and (c) SEM images of the sample from a fired CDF with 5% nZVI are shown (measurement one and two, respectively) and in figure (b) and (d) the corresponding distributions of iron, determined with SEM-EDX, are depicted. 35
Figure 4–10|Measured flow rates of the CDFs of the first hour after filling the water columns with 5 L test water. 36

Figure 4–11 | Calculated flow rates of a CPF, which are translated from the measured flow rates of the CDFs tested in this study with a water level at half the height of the pot filter. The flow rates are both averaged for difference between the duplicate disks and for the differences in time. The lower and upper dotted line indicates the minimum and maximum desired flow rate for a CPF, respectively. 38
Figure 5–1 | Schematic illustration of (a) the potential attraction in the adsorption experiment with pH7.2 between the negatively charged MS2 bacteriophages and positively charged nZVI particles and of (b) the potential repulsion during the first elution with pH 9.5 between the negatively charge MS2 bacteriophages and the negatively charged nZVI. 45
Figure 5–2 | The development of the ceramic structure during vitrification: (a) loose clay particles and loose metal particles, (b) initial stage of vitrification and (c) intermediate stage of vitrification. 48
Figure 5–3 | The adsorbed amount of arsenic in time with addition of 2.5 g/L nZVI, 0.06 g/L nZVI and 0.06 g/L CIM 50
Figure 5–4 | The adsorbed amount of arsenic in time by the addition of 0.06 g/L nZVI with As(III) as initial solution versus As(V) as initial solution. 51
Figure 5–5 | The adsorbed amount of arsenic in time with addition of 50 g/L ground material of a blank fired CDF, of a fired CDF containing 5% nZVI and of a fired CDF containing 5% CIM. 53
Figure 5–6 | The adsorbed amount of arsenic in time with addition of 50 g/L ground material of (a) a fired CDF containing 5% nZVI versus an unfired CDF containing 5% nZVI and of (b) a fired CDF containing 5% CIM versus a unfired CDF containing 5% CIM. 54
Figure 5–7 | The adsorbed amount arsenic in time with addition of 50 g/L ground material of an unfired CDF containing 5% nZVI versus an unfired CDF containing 0.05% nZVI. 55
Figure 5–8 | Average pH-values during the arsenic batch experiments with fired and unfired CDFs 56
Figure 5–9 | The adsorbed amount of total As in time with addition of 50 g/L ground material of an unfired filter containing 5% nZVI versus 0.06 g/L of solely nZVI. 56
Figure 6–1 | LRVs for *E. coli* of samples that were taken directly from the CDFs. The larger than signs (>) indicate the cases where there was a detection limit for both duplicates 60
Figure 6–2 | Illustration of the pores in ceramic filter material: (a) ceramic material with a low tortuosity and (b) ceramic material with a high tortuosity (adapted from: Peckham et al., 2007) 61
Figure 6–3 | LRVs for MS2 bacteriophages of samples that were taken directly from the CDFs. 62
Figure 6–4 | Schematic illustration of how the added metal particles might be located inside the CDFs. In the left figure an illustration is given of metal particles that are situated at the surface of the pores and in the right figure an illustration is given of metal particles that are hidden in the ceramic structure. 64
Figure 6–5 | Average iron and silver concentrations, which leached off from the different CDFs. 64
Figure 6–6 | LRVs for *E. coli* of samples that were taken directly from the CDFs (D) and of samples that were taken 16-18 h later form the receptacle (ON) 65
Figure 6–7 | LRVs for MS2 bacteriophages of samples that were taken directly from the CDFs (D) and of samples that were taken 16-18 h later form the receptacle (ON). 66
Figure 6–8 | Removal of arsenic by a blank CDF and two CDFs containing 5% nZVI. The initial arsenic concentration was 200 µg/L As(III). The dotted black line indicates the theoretical breakthrough of arsenic, based on the results of the batch experiments. 68
Figure 6–9 | Removal of arsenic by CDFs containing 5% nZVI with a layer of 1.5 cm CIM on top of the CDFs. The initial arsenic concentration was 200 µg/L As(III). 69
Figure 7–1 | Schematic illustration of concepts of potential alternatives for CPFs in combination with ZVI. (a) Represents an CPF with an iron coating, (b) illustrates CPFs with pre-treatment of with ZVI and (c) shows a CPF in combination with iron mixed ceramic pellets. 73

List of tables

Table 1-1 | Log_{10} reduction requirements for HWTS for the targets "interim", "protective" and "highly protective" established by the WHO (WHO, 2011a).....3
Table 2-1 | pH_{PZC} values for different clay minerals reported in literature.....10
Table 3-1 | Overview of the different ceramic disks that were manufactured and their metal composition as a percentage of the dry clay weight.....19
Table 4-1 | The minerals per type of filter that were identified by means of XRD, besides quartz and ordered albite, which are present in each sample.....27
Table 4-2 | The Mössbauer fitted parameters of the samples from an unfired filter with 5% nZVI, a fired filter with 5% nZVi and a fired blank filter. Experimental uncertainties: Isomer shift: I.S. ± 0.01 $mm \cdot s^{-1}$; Quadrupole splitting: Q.S. ± 0.01 $mm \cdot s^{-1}$; Line width: Γ ± 0.01 $mm \cdot s^{-1}$; Hyperfine field: ± 0.1 T; Spectral contribution: ± 3%. [a] Mean hyperfine field. 31
Table 4-3 | Iron percentages per filter, obtained from the SEM-EDX elemental analyses, performed with SEM-EDX at 1000x magnification.....34
Table 4-4 | The filter characterization parameters: linear velocity, porosity and dispersion coefficient per filter, which were determine by means of tracer breakthrough experiment.....39
Table 5-1 | Overview of the calculated LRVs for the initial adsorption of MS2 bacteriophages by the ceramic material, the LRVs and percentages for the recovered phages during the first and second elution and the LRVs for the eventual irreversible adsorption of MS2 bacteriophages.....44
Table 5-2 | Amount of metals that leached of from the ceramic material in the batch experiment with MS2 bacteriophages.....46
Table 5-3 | Kinetic parameters of the pseudo-first-order and the pseudo-second-order rate model for adsorption of As(III) and As(V) on nZVI.....52
Table 6-1 | Average, minimum and maximum LRVs per CDF type, established by combining all the influent E. coli concentrations and all the effluent E. coli concentrations, together with the standard deviations. 60
Table 6-2 | Average, minimum and maximum LRVs per CDF type, established by combining all the influent MS2 concentrations and all the effluent MS2 concentrations, together with the standard deviations. 63
Table 6-3 | Measured flow rates of the CDFs of the first hour after filling the water columns with 5 L test water.....68
Table 6-4 | Ratio of As(III) and As(V) concentration for the effluent samples of the blank CDF and the two CDFs with 5% nZVI after approximately 4 L of test water was passed through the CDFs. These values were determined by means of an chloride resin.....69

Appendix I: Materials and methods

I.1 Bicarbonate concentration in Nicaragua as reference for test water

The synthetic water for the arsenic experiment contained 4 mM sodium bicarbonate. This bicarbonate concentration was based on a small data collection of measuring points in Nicaragua where corresponding arsenic concentration were measured. These measured values are presented in Table I-1.

Table I-1| Measured concentrations of bicarbonate and arsenic at several locations in Nicaragua.

Location	Arsenic concentration [µg/L]	Bicarbonate concentration [mM/L]
Monasterio Trapense	70-200	5.09
Pozo Ocoton	180-240	3.96
Aguas Calientes	175	4.34
Paso Picado	250	5.24
La Cabecerita	210	4.92
Olocotón	325	4.18
La Unión	73	3.11
Mean		**4.41**

I.2 Calculation required nZVI content for CDF

With the use of previous studies the required amount of nZVI was calculated for a CDF. This was based on a minimum discharge of 12 L/day and a lifespan of the filter of one year. The calculation can be found in Table I-2.

Table I-2| Calculation of the required nZVI content of a CDF.

Assumption: number of people per household	6
Assumption: minimum required amount of water	2 L/day
Minimum amount water per day, filtered by CPF	6 · 2 = 12 L/day
Assumption: CDF is 1/10 of a CPF	
Minimum amount water per day, filtered by CDF	12 · 1/10 = 1.2 L/day
Assumption: minimum life span	365 days
Minimum amount of filtered water per CDP	1.2 · 365 = 438 L
Assumption: As(III) concentration	0.2 mg/L
Total As(III) that needs to be adsorbed	438 · 0.2 = 87.6 mg
Adsorption capacity q_e nZVI (Kanel et al., 2005)	3.5 mg As(III) /g nZVI
Required amount of nZVI	**87.6 / 3.5 = 25 g**

I.3 Photos of manufacturing process of CDFs

Below several pictures of the manufacturing process of CDFs at a local factory of the non-profit organisation FilterPure are shown.

Figure I-1| Pictures of the manufacturing proces of the CDFs. From left to right: the mixer with which the clay mixture was mixed, the addition of a metal solution to a dry clay mixture and a clay ball inside the mold.

Figure I-2| Pictures of the manufacturing proces of the CDFs. From left to right: the press to press the CDFs, the press together with the mold and a pressed CDF.

Figure I-3| Pictures of the manufacturing proces of the CDFs. From left to right: CDFs that are drying, CDFs inside the kiln and the kiln with which the CDFs were fired.

I.4 X-ray diffraction technique

XRD measurements are performed by a X-ray diffractometer[19]. An X-ray tube produces X-rays, which are passed through a filter to create monochromatic X-rays required for X-ray diffraction and are subsequently incident on the crystalline sample. The incident X-rays interact with the sample material and are reflected from crystal planes within the material. Due to destructive interference most scattered waves are cancelled out by each other. However, when the conditions meet Bragg's Law constructive interference takes place and hence a diffracted beam occurs (see Figure I-4). Bragg's Law is satisfied when the deviated X-rays reflect at an angle equal to the incidence angle and they differ in phase by an integral number of wavelengths (Cullity, 1956):

$$n\lambda = 2d\sin(\theta) \qquad (2.1)$$

[19] There are two types of configurations in which diffractometer can be operated, the transmission and the reflection configuration. Since the reflection configuration, also referred to as Bragg-Brentano configuration, was used in this study this configuration is further discussed.

n = integer

λ = wavelength of incident X-ray beam

d = distance between atomic layers in a crystalline material

θ = angle of the incidence

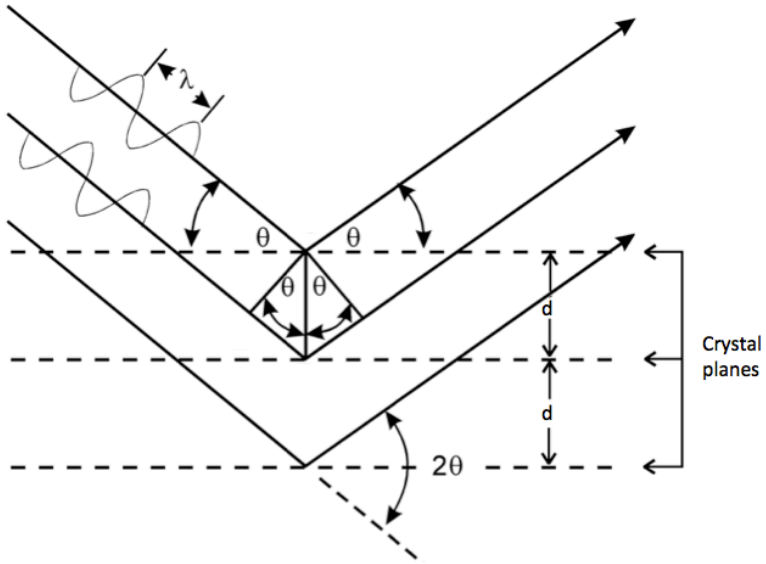

Figure I-4|Schematisation of Bragg's law conditions. The reflected X-rays are in phase, which results in constructive interference and a diffracted beam.

A detector rotates around the sample on an arm at twice the incidence angle θ of the X-ray beam in order to detect all possible diffracted X-rays of the random oriented crystals within the sample and records the intensities of the reflected X-rays. At specific detector angles certain crystal happen to be oriented in a way that the X-ray geometry satisfies Bragg's law. This causes that the X-ray undergoes constructive interference, which results in an X-ray peak signal.

The distances between the atomic layers of a certain crystal are calculated by means of converting the diffraction peaks with the Bragg equation. Each crystalline solid has an own set of exclusive d-spacings, which can be used as a 'fingerprint' to identified the crystal by comparing the obtained d-spacings to reference d-spacings. Usually the results are presented in the form of a graph with on the y-axis the intensity of the X-ray counts and on the x-axis the peak positions at 2θ.

Appendix II: CDF characterisation

II.1 XRD pattern

Figure II-1 shows the measured XRD pattern of a sample of an unfired CDF with 0.05% nZVI. The XRD pattern is depicted in black, after background subtraction and displacement correction. The coloured sticks give the peak positions and intensities of the possibly present phases, using the ICDD pdf4 database.

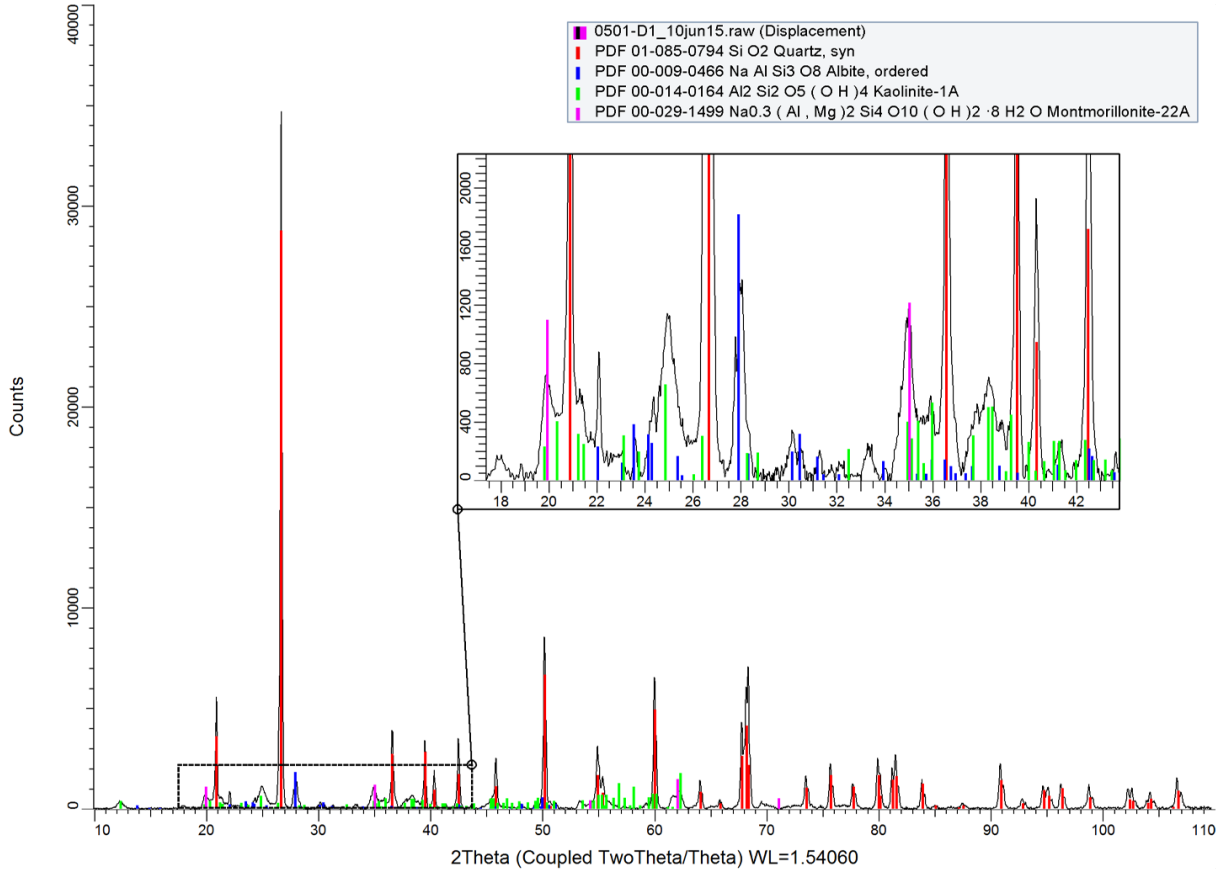

Figure II-1| XRD-pattern of a sample 1 of an unfired CDF with 0.05% nZVI.

II.2 SEM and SEM-EDX

In Figure II-2 the SEM and SEM-EDX images of the samples of the unfired CDFs are presented. The iron looks evenly spread.

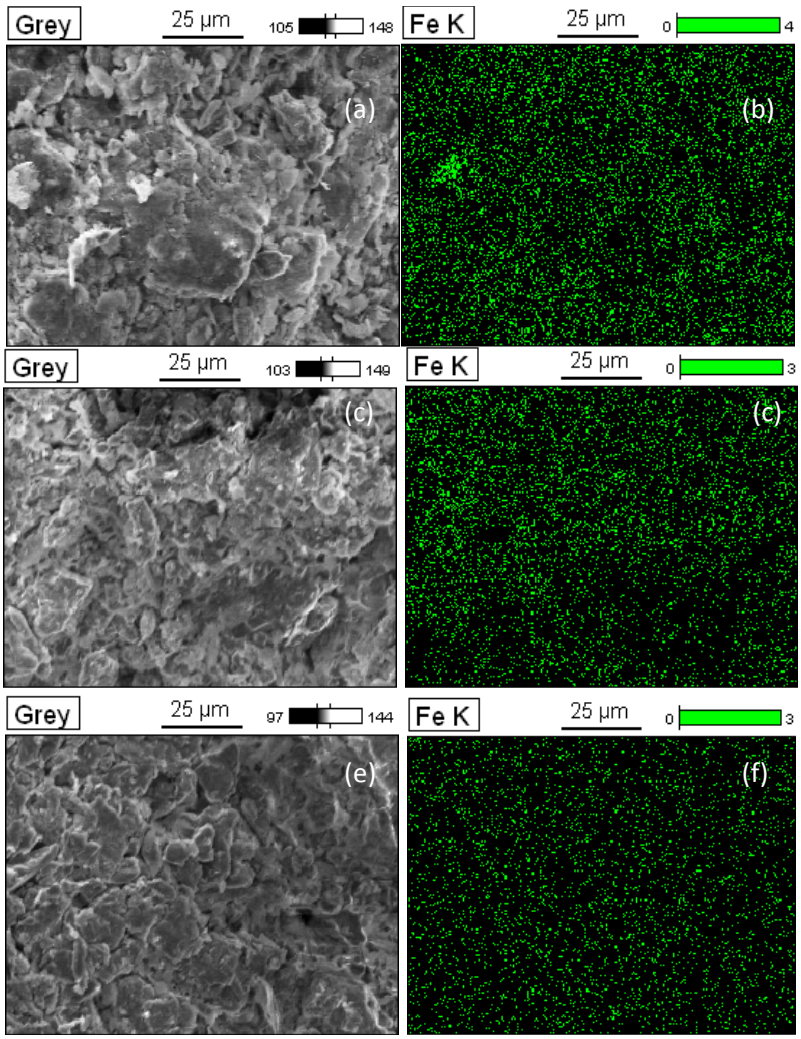

Figure II-2| In figure (a), (c) and (e) SEM images of the sample from an unfired CDF with 0.05% nZVI, 5% nZVI and 5% CIM, respectively, are shown and in figure (b), (d) and (f) the corresponding distributions of iron, determined with SEM-EDX, are depicted.

II.3 Dimensions of a CPF for translation flow rate

To translate the flow rate of the ceramic disk to the flow rate of a CPF, dimensions of the filter from Ghana from the study by Van Halem (2006) were used. These dimension are presented in Table II-1 and Figure II-3.

Table II-1| Dimension of a CPF from Ghana, obtained from a study by Van Halem (2006).

Dimensions CPF	
r_1 [cm]	27.0
r_2 [cm]	20.0
L [cm]	23.5
t_f [cm]	1.3
t_b [cm]	1.5

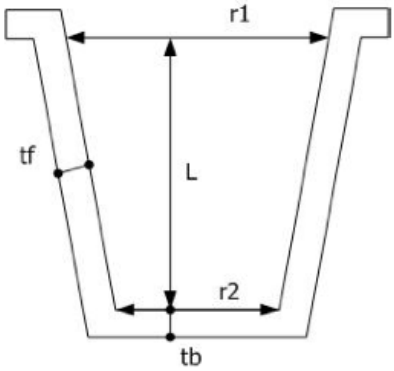

Figure II-3| Schematic illustrations of the dimensions of a CPF (Van Halem, 2006).

II.4 Breakthrough tracer

Below in Figure II-4 the breakthrough graphs of the tracer experiments with sodium chloride are presented.

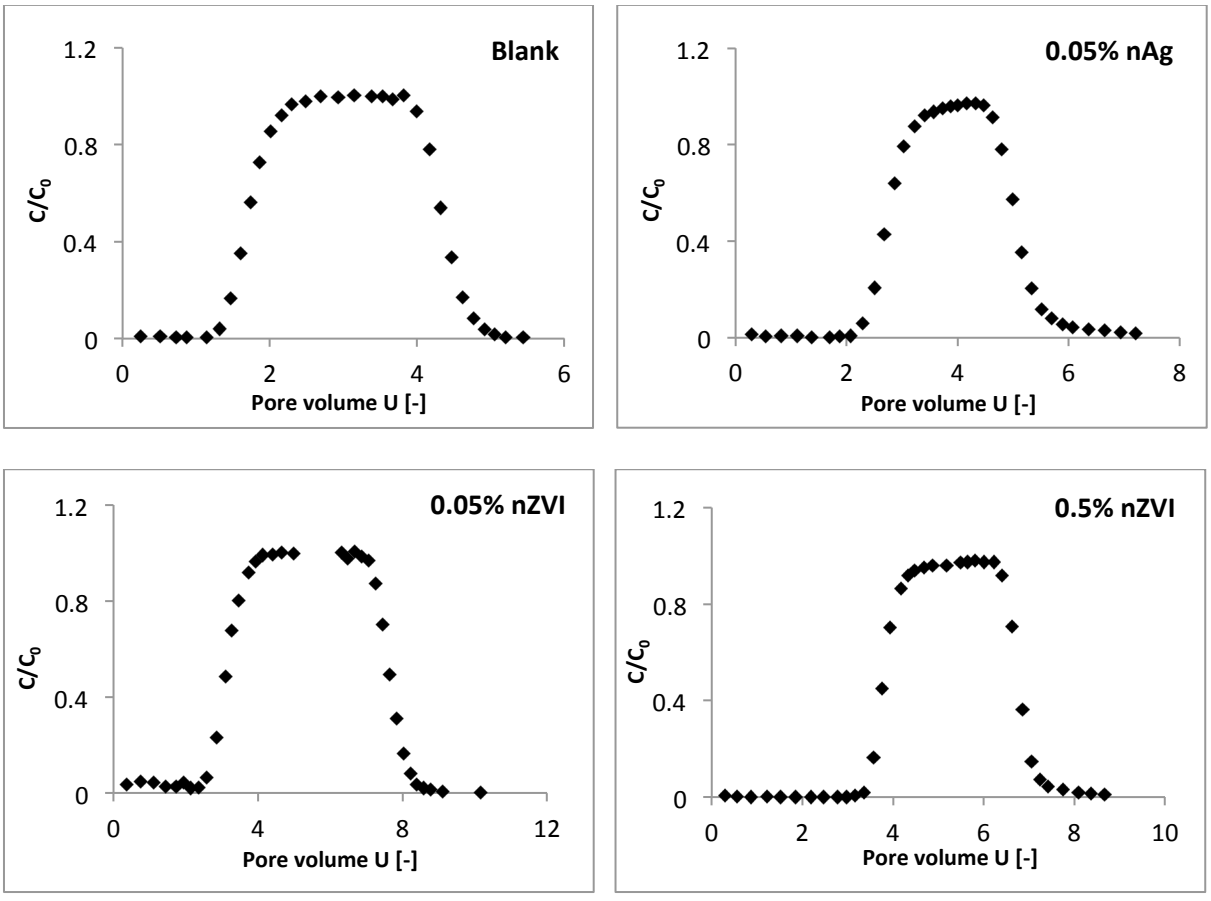

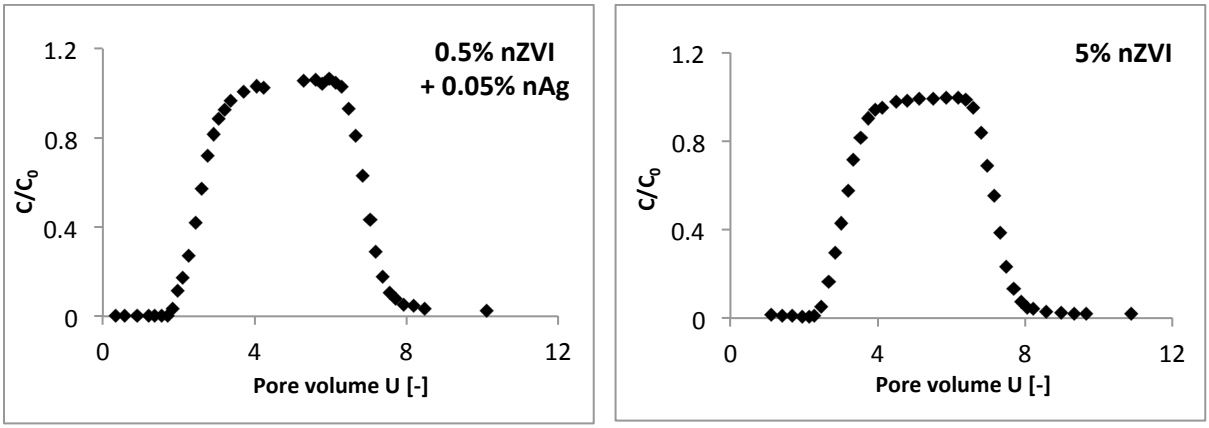

Figure II-4| Graphs of the breakthrough experiment with sodium chloride.

Appendix III: Batch experiments

III.1 pH during arsenic batch experiments

The pH was monitored at the beginning of the batch experiment, after 90 minutes, after 360 minutes and at the end of the experiment. This was done with a WTW pH Electrode SenTix 41-3 device. The measured pH values are presented in Table III-1. As can be seen in table III-1, in the experiments with solely ZVI and in the experiments with fired ceramic material the pH increased. In the experiments with the unfired material the pH increased only slightly.

Table III-1| Measured pH values during arsenic adsorption batch experiments.

Experiment		0 min [-]	90 min [-]	360 min [-]	1440 min [-]
Solely iron	nZVI As(III)	7.02	7.50	7.69	-
		7.02	7.41	7.60	-
	nZVI As(V)	7.02	7.53	7.72	-
		7.02	7.55	7.73	-
	CIM	7.01	7.43	7.62	-
		7.02	7.42	7.63	-
Fired CDFs	Blank	7.01	7.35	7.54	7.71
		7.00	7.39	7.56	7.73
	5% nZVI	6.99	7.25	7.45	7.64
		7.00	7.26	7.44	7.62
	5% CIM	7.02	7.43	7.58	7.78
		7.01	7.41	7.61	7.81
Unfired CDFs	0.05% nZVI	7.02	7.08	7.18	7.18
		7.03	7.06	7.10	7.14
	5% nZVI	6.97	7.02	7.08	7.11
		7.01	7.03	7.08	7.06
	5% CIM	7.04	7.12	7.17	7.15
		7.00	7.22	7.23	7.19

III.2 Temperature during arsenic batch experiments

The temperature was monitored at the beginning of the batch experiment, after 90 minutes, after 360 minutes and at the end of the experiment. This was done with a WTW pH Electrode SenTix 41-3 device. The measured temperature values are presented in Table III-2. The relatively high temperatures were due to the warm summer months when the experiments were performed.

Table III-2| Measured temperature values during arsenic adsorption batch experiments.

Experiment		0 min [°C]	90 min [°C]	360 min [°C]	1440 min [°C]
Solely iron	nZVI As(III)	23.2	27.8	27.9	-
		23.3	27.7	28.0	-
	nZVI As(V)	24.4	27.8	27.9	-
		24.2	27.7	27.9	-
	CIM	24.5	27.8	27.9	-
		24.5	27.8	27.9	-
Fired CDFs	Blank	26.1	29.1	29.4	29.4
		26.0	29.1	29.4	29.4
	5% nZVI	25.6	29.1	29.3	28.7
		25.6	29.1	29.4	28.8
	5% CIM	26.2	29.2	29.4	29.4
		26.3	29.0	29.4	29.4
Unfired CDFs	0.05% nZVI	25.2	27.8	27.9	27.8
		25.1	27.5	27.7	27.7
	5% nZVI	24.5	27.8	28.1	27.8
		25.1	27.6	28.0	27.9
	5% CIM	24.9	27.9	27.9	27.8
		24.5	28.0	28.0	28.0

Appendix IV: Filter experiments

IV.1 LRVs of *E. coli* for the direct and overnight samples

The *E. coli* removal by the CDFs was evaluated by means of LRVs. For the concentration calculations of the samples, the average of the duplicate plate counts was used. In case several dilutions were analysed the weighted average concentration of these dilutions was calculated. The calculated values are shown in Table IV-1. In some of the *E. coli* analyses a detection limit was reached, this is indicated in Table IV-1 with a larger than sign (>).

Table IV-1| LRVs for *E. coli* of the samples that were taken directly from the CDFs and the overnight samples that were taken after 16-18 h form the receptacle. The larger than signs (>) indicate the cases where there was a detection limit.

		Blank		0.05% nAg		0.05% nZVI		0.5% nZVI		0.5% nZVI + 0.05% nZVI	
Day 1	**D**	>4.27	>4.22	4.17	>4.22	1.91	0.23	5.27	>4.22	>5.27	>4.90
	ON	4.80	>4.22	>5.27	>4.22	3.43	1.03	>5.27	>4.22	>5.27	4.90
Day 2	**D**	4.07	4.30	>4.85	>4.90	1.75	0.06	4.07	>4.90	>4.85	>3.96
	ON	3.23	3.43	>4.85	>4.90	1.94	0.38	3.95	>4.06	>4.85	>3.96
Day 3	**D**	3.18	1.81	>4.61	>3.96	1.92	0.17	4.26	2.29	>4.61	>3.89
	ON	2.66	2.38	-	>3.96	2.54	0.96	3.50	2.38	>4.61	>3.89
Day 4	**D**	2.77	2.08	>4.48	>3.89	1.97	0.29	2.99	2.04	4.48	3.83
	ON	2.46	2.73	>4.48	>3.89	2.61	0.85	3.37	2.09	>4.48	>3.83
Day 9	**D**	1.91	2.51	>4.90	3.31	2.17	-0.24	3.04	2.06	4.43	2.28
	ON	1.35	2.36	>4.90	>3.31	2.25	0.20	2.65	1.84	>4.90	>3.31
Day 16	**D**	3.31	2.65	>3.31	3.58	2.51	2.96	2.13	3.05	2.62	3.10
	ON	3.05	2.85	3.31	3.58	2.31	3.05	3.31	3.05	>3.31	4.35

IV.2 pH values filter experiment

In Table IV-2 the pH values, which were measured overnight from the receptacle, are presented. The pH values of the effluent are close to pH values of the influent. In the batch experiment the fired ceramic material caused the pH to increase, this might be due to more intensive contact. Van Halem (2006) noticed an increase in alkalinity in the effluent from CPFs. This was explained by means of a diffusion model for concrete materials. The reason that in this study no increase of pH was observed might be because different clays were used for the manufacturing of the ceramic filters.

Moreover, there was no trend visible in the metal content of CDFs and the effluent pH value

Table IV-2| Average pH values, which were measured overnight from the receptacle, per CDF type and the corresponding standard deviations.

	pH [-]	σ [-]
Influent	7.19	0.01
Blank	7.10	0.16
0.05% nAg	7.12	0.16
0.05% nZVI	7.10	0.14
0.5% nZVI	7.09	0.18
0.5% nZVI + 0.05% nAg	7.06	0.20

IV.3 LRVs of MS2 bacteriophages for the direct and overnight samples

The MS2 bacteriophages removal by the CDFs was evaluated by means of LRVs. For the concentration calculations of the samples, the average of the duplicate plate counts was used. In case several dilutions were analysed the weighted average concentration of these dilutions was calculated. The calculated values are shown in Table IV-3.

Table IV-3| LRVs for MS2 bacteriophages of the samples that were taken directly from the CDFs and the overnight samples that were taken after 16-18 h form the receptacle.

		Blank		**0.05% nAg**		**0.05% nZVI**		**0.5% nZVI**		**0.5% nZVI + 0.05% nZVI**	
Day 1	**D**	0.38	0.02	0.05	0.13	0.09	0.12	0	0.06	-0.14	-0.03
	ON	-0.02	0.10	-0.20	0.20	0.24	0.22	-0.07	0.11	-0.05	0.03
Day 2	**D**	-0.07	-0.01	-0.03	0.05	0.42	0.07	0.04	-0.02	0.00	0.16
	ON	0.00	0.08	0.15	0.02	0.16	0.10	0.01	0.01	-0.12	0.16
Day 3	**D**	0.05	0.24	0.15	0.17	0.29	0.38	0.08	0.07	0.13	0.26
	ON	0.33	0.24	-	0.17	0.54	0.38	0.32	0.07	0.36	0.10
Day 4	**D**	0.12	0.21	0.24	0.32	0.38	0.32	0.22	0.19	0.09	0.04
	ON	0.07	0.18	0.24	0.25	0.42	0.17	0.14	0.02	0.15	0.07
Day 9	**D**	-0.06	0.19	-0.04	0.24	0.40	0.21	-0.08	0.14	-0.08	0.15
	ON	0.11	0.61	0.06	0.45	0.38	0.07	0.04	0.36	0.06	0.20
Day 16	**D**	0.58	0.05	0.37	0.14	0.37	0.13	0.35	0.01	0.18	0.07
	ON	0.77	0.05	0.34	0.14	0.79	0.17	0.37	0.04	0.30	0.08

IV.4 Leached silver and copper from blank CDF

In Figure IV-1 the concentrations of leached silver and copper from the blank CDF are presented.

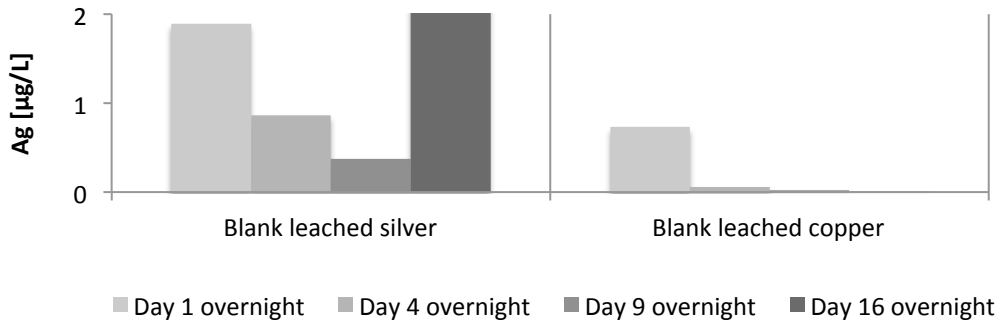

Figure IV-1| Concentrations of leached silver and copper of the blank CDF.

IV.5 Calculation arsenic breakthrough

The calculation of the theoretical arsenic breakthrough is presented in Table IV-5.

Table IV-5| Calculation to estimate the breakthrough of arsenic of a CDF wit 5% nZVI.

Estimated As equilibrium concentration	40	µg/L
Concentration crushed CDF material (5% nZVI)	50	µg/L
Equilibrium adsorption capacity	0.8	µg/g
Weight CDF	333	g
As adsorption with CDF	266	µg
As concentration test water	200	µg/L
Breakthrough As	**1.3**	**L**